

THE FINITE ELEMENT RESPONSE MATRIX METHOD FOR
COARSE MESH REACTOR ANALYSIS

by

Horacio Nakata

Orientador: William R. Martin

A dissertation submitted in partial fulfillment
of the requirements for the degree of
Doctor of Philosophy
(Nuclear Engineering)
in The University of Michigan
1981

Doctoral Committee:

Assistant Professor William R. Martin, Chairman
Professor James J. Duderstadt
Associate Professor John C. Lee
Professor Wei H. Yang

16612

AR 6

ABSTRACT

THE FINITE ELEMENT RESPONSE MATRIX METHOD FOR
COARSE MESH REACTOR ANALYSIS

by

Horacio Nakata

Chairman: William R. Martin

A new technique is developed with an alternative formulation of the response matrix method implemented with the finite element scheme. As in standard response matrix methods, the reactor core is partitioned into several coarse meshes and the global solution is obtained imposing continuity of partial currents across the boundaries of the coarse meshes.

The finite element method, with quadratic Serendipity elements, is applied in the local calculations (for each coarse mesh). The weak form of the inhomogeneous diffusion equation is then solved for prescribed partial currents on the boundary. The local calculation results are used to generate the response matrices which are then used in the global solution for the partial currents and fluxes. The partial currents and fluxes in the global calculations are independently expanded in quadratic or cubic Serendi-

pity finite element basis functions. The equations for the global expansion coefficients are solved using Gauss-Seidel iterations until a converged partial current distribution is obtained.

The response matrix method in the present formulation includes response matrices due to both incoming partial currents and sources (in-scatter+fission), thus decoupling the response matrix generation from the neutron multiplication factor.

To evaluate the performance of the finite element coarse mesh method the assembly averaged power distribution and detailed neutron flux distribution for two difficult and realistic problems, the 2D-IAEA benchmark problem (zone-loaded PWR) and a Biblis benchmark problem with checkerboard loading, have been obtained. The results indicate that the proposed method yields satisfactory accuracies with relatively large coarse mesh size. Furthermore, the use of the finite element method for the response matrix generation allows the consideration of different geometries (such as triangular geometry for fast reactors), the treatment of spatially dependent cross sections for burn-up calculations, and the treatment of local heterogeneities. Finally, the use of separate matrices for currents and sources eliminates the expensive regeneration of the response matrices for eigenvalue problems and has allowed conventional solution techniques for multigroup problems.

To My Wife

For Her Understanding, Patience and Love

ACKNOWLEDGEMENT

I wish to express my sincere gratitude to Dr. William R. Martin, Chairman of my doctoral committee, for his invaluable guidance and support throughout the course of this investigation.

The gratitude is also expressed to Dr. James J. Duderstadt, Dr. John C. Lee and Dr. Wei H. Yang for serving as members of my doctoral committee.

I wish also to acknowledge many valuable suggestions received from Dr. John C. Lee, Dr. Wei H. Yang, Dr. Noboru Kikuchi, Dr. William Anderson, Dr. Jeffrey Rauch, and my fellow students, during the course of this investigation.

The financial support which I received from Instituto de Pesquisas Energeticas e Nucleares and Comissao Nacional de Energia Nuclear is gratefully acknowledged.

Finally, special thanks to Mrs. Pam Derry for her excellent typing and accommodating schedule.

TABLE OF CONTENTS

| | Page |
|---|------|
| DEDICATION | ii |
| ACKNOWLEDGEMENTS | iii |
| LIST OF TABLES | vi |
| LIST OF FIGURES | vii |
| LIST OF APPENDICES | ix |
| CHAPTER | |
| 1 INTRODUCTION | 1 |
| 1.1 Coarse Mesh Methods | 3 |
| 1.2 Research Objectives | 10 |
| 1.3 Summary of Investigation | 11 |
| 2 RESPONSE MATRIX METHOD | 15 |
| 2.1 Theory | 15 |
| 2.2 Alternative Formulation | 20 |
| 2.3 Numerical Approximations | 24 |
| 2.4 Solution Algorithm | 31 |
| 3 FINITE ELEMENT RESPONSE MATRIX METHOD | 34 |
| 3.1 Galerkin Approximation | 35 |
| 3.2 Finite Element Solution | 38 |
| 3.3 Response Matrices Generation | 43 |
| 4 COMPUTER IMPLEMENTATION | 52 |
| 4.1 Basis Functions | 52 |
| 4.2 Inner Iterations Scheme | 64 |
| 4.3 Outer Iterations and Acceleration Schemes | 69 |

TABLE OF CONTENTS (cont.)

| | Page |
|---|------|
| 5 EVALUATION OF THE FINITE ELEMENT RESPONSE MATRIX METHOD | 76 |
| 5.1 Fixed Source Problem | 76 |
| 5.2 Eigenvalue Problem | 82 |
| 5.2.1 2D-IAEA Benchmark Calculation | 82 |
| 5.2.2 Biblis Benchmark Calculation | 96 |
| 6 CONCLUDING REMARKS | 107 |
| 6.1 Summary of Investigation | 107 |
| 6.2 Conclusions | 109 |
| 6.3 Recommendations for Further Study | 112 |
| APPENDICES | 114 |
| REFERENCES | 136 |

LIST OF TABLES

| TABLE | Page |
|---|------|
| 4.1 R_m^{σ} for 2D-IAEA benchmark problem. | 60 |
| 4.2 R_m^s for 2D-IAEA benchmark problem. | 61 |
| 5.1 Bare homogeneous core calculation (fixed source problem) with 20cm x 20cm coarse meshes. | 78 |
| 5.2 Bare homogeneous core calculation (fixed source problem) with 10cm x 10cm coarse meshes. | 79 |
| 5.3 Computational time required for VENTURE calculation (with IBM 360/91) for different mesh sizes. | 84 |
| 5.4 Computational time required for response matrix generation. | 86 |
| 5.5 Effect of convergence criterion $\epsilon\phi$. | 87 |
| 5.6 Summary of 2D-IAEA benchmark calculations. | 88 |
| 5.7 2D-IAEA benchmark problem solved by coarse mesh methods. | 97 |
| 5.8 Biblis benchmark problem solved by coarse mesh methods. | 99 |
| 5.9 Summary of Biblis benchmark calculations. | 100 |
| IV.1 One-group diffusion constants for bare homogeneous reactor. | 133 |
| IV-2 Two-group diffusion constants for 2D-IAEA benchmark problem. | 134 |
| IV.3 Two-group diffusion constants for Biblis benchmark problem. | 135 |

LIST OF FIGURES

| FIGURE | Page |
|--|------|
| 2.1 Illustration of domain Ω , subdomain Ω_i , and inward and outward partial currents. | 17 |
| 4.1 Nodes for Serendipity elements, $\Psi_s(\xi, \eta)$. | 55 |
| 4.2 Nodes for Lagrange polynomials, $\Psi_{sk}(\pi_s)$. | 55 |
| 4.3 Nodes for quadratic Serendipity elements, $\psi_{mi}^h(\Pi)$, and for piecewise polynomials, $\psi_{smi}^h(\pi_s)$, in the coarse mesh Ω_m subdivided in 4 subdomains Ω_{mm} , $m=1, \dots, 4$. | 58 |
| 4.4 Outward partial currents due to the constant inward partial current on the bottom. | 62 |
| 4.5 Outward partial currents due to the constant source within the coarse mesh. | 63 |
| 4.6 Coarse mesh ordering and outward partial currents, represented by arrows, for quadratic elements. | 65 |
| 4.7 Block-Jacobi matrix equation. | 68 |
| 4.8 Acceleration of outer iterations with asymptotic source extrapolation method. | 73 |
| 4.9 Acceleration of outer iterations with Chebyshev polynomial method. | 74 |
| 5.1 Neutron flux distribution in a bare homogeneous core calculated with quadratic partial currents. | 80 |
| 5.2 2D-IAEA benchmark problem. | 83 |
| 5.3 2D-IAEA assembly averaged power distribution calculated with corner mesh fine mesh (1cm) finite difference scheme (PDQ-7). | 85 |
| 5.4 2D-IAEA assembly averaged power distribution obtained with 9/1 quadratic calculation ($\epsilon_\phi = 10^{-5}$). | 90 |
| 5.5 2D-IAEA assembly averaged power distribution obtained with 9/1 cubic calculation ($\epsilon_\phi = 10^{-5}$). | 91 |

LIST OF FIGURES (cont.)

| FIGURE | Page |
|--|------|
| 5.6 2D-IAEA thermal neutron flux distribution obtained with 16/1 quadratic calculation ($\epsilon_{\phi} = 10^{-5}$). | 92 |
| 5.7 2D-IAEA thermal neutron flux distribution obtained with 16/1 cubic calculation ($\epsilon_{\phi} = 10^{-5}$). | 93 |
| 5.8 2D-IAEA thermal neutron flux distribution obtained with 16/4 quadratic calculation ($\epsilon_{\phi} = 2 \cdot 10^{-5}$). | 94 |
| 5.9 2D-IAEA thermal neutron flux distribution obtained with 16/4 cubic calculation ($\epsilon_{\phi} = 1.3 \cdot 10^{-5}$). | 95 |
| 5.10 Biblis benchmark problem. | 98 |
| 5.11 Biblis assembly averaged power distribution obtained with 16/4 quadratic calculation ($\epsilon_{\phi} = 3 \cdot 10^{-5}$). | 101 |
| 5.12 Biblis assembly averaged power distribution obtained with 16/4 cubic calculation ($\epsilon_{\phi} = 2 \cdot 10^{-5}$). | 102 |
| 5.13 Biblis assembly averaged power distribution obtained with 16/1 quadratic calculation ($\epsilon_{\phi} = 3 \cdot 10^{-5}$). | 103 |
| 5.14 Biblis assembly averaged power distribution obtained with 16/1 cubic calculation ($\epsilon_{\phi} = 2 \cdot 10^{-5}$). | 104 |
| 5.15 Biblis thermal neutron flux distribution obtained with 16/4 cubic calculation ($\epsilon_{\phi} = 2 \cdot 10^{-5}$). | 105 |

LIST OF APPENDICES

| APPENDIX | Page |
|--|------|
| I ACCELERATION SCHEMES | 115 |
| II VARIATIONAL FORMULATION OF DIFFUSION EQUATION | 123 |
| III INTERPRETATION OF THE BLOCK-JACOBI SPECTRAL NORM | 131 |
| IV DIFFUSION GROUP CONSTANTS | 133 |

CHAPTER 1
INTRODUCTION

The development of the nuclear industry during the past few decades has been accompanied with steadily increasing economic restrictions and safety requirements. These constraints place demands on nuclear analysts because one needs to know the neutron flux distribution within the reactor in order to perform the various safety and economic analyses. And in order to keep pace with these demands they have strived to improve the accuracy and computational efficiency of calculational methods for determining the neutron flux distribution in a reactor.

As the complexity and size of power reactors increase the well-known and reliable techniques become less practical to be used on a routine basis for neutronic analyses, whether used as part of an economic analysis to optimize a fuel management scheme or to determine detailed fuel pin power profiles for a safety analysis. Thus there is a need for more efficient yet sufficiently accurate techniques to substitute for the reliable but expensive fine mesh diffusion theory codes (e.g., PDQ-7⁽¹⁾) to determine the neutron flux distribution in the reactor core. Consequently, research in the area of neutronics methods

development has been an active area for many years and will continue to be an active area for many years.

The simplicity of the finite difference equations and the relative efficiency of the well-known methods⁽²⁻⁴⁾ to solve the associated linear algebraic equations have been the major advantages of the fine mesh finite difference method. In addition, detailed pin power distributions which agree very well with measured power profiles can be obtained because the mesh size is comparable to the fuel pin pitch. The spatial dependence of the neutron flux is approximated by a low-order Taylor series and the solution is obtained imposing neutron balance in the fine-mesh subject to interface continuity and external boundary conditions. However, since it is a low order approximation the computational time necessary to obtain the solution tends to become excessively long for mesh spacing typically used in a global (e.g., 1/4 core or full core) fine mesh calculation.

Thus fine mesh calculations are impractical for routine two-dimensional global calculations and out of the question for three-dimensional global calculations, and emphasis has been placed on developing computational methods to be used on a relatively coarse mesh, on the order of several diffusion lengths, compared to fine mesh. These methods are appropriately termed coarse mesh methods, and they cover a wide range of approximations, ranging from

empirical parameter fittings to sophisticated higher order finite element methods. In the past decade a number of coarse mesh methods have been developed and due to the lack of an unifying analysis of the existing methods, precise and unambiguous classification of these methods becomes difficult. But in the next section an attempt is made to define representative broad categories in which most of the present coarse mesh methods may be included.

1.1. Coarse Mesh Methods

Basically the coarse mesh methods which have been developed or are still under development can be divided in four broad groups: ⁽⁵⁾ coarse mesh finite difference methods, flux synthesis methods, nodal methods, and response matrix methods. But some of the recent coarse mesh methods defy precise characterization because they combine some ideas of these basic methods, e.g., nodal collision probability methods, coarse mesh synthesis method, nodal expansion method, coarse mesh expansion method, nodal Green's function method, etc. But the broad common goal of all these coarse mesh methods has been to satisfy the accuracy requirements for reactor design calculations, usually quoted as a few tenths of a percent for the neutron multiplication factor and within a few percent for the local power distribution, while avoiding the excessive computational expense characteristic of fine mesh methods.

The coarse mesh finite difference method⁽⁶⁾ is based on the fine mesh finite difference scheme, but the number of unknowns is reduced by using a coarse mesh with appropriate parameter corrections. The parameter corrections have been obtained by a wide range of techniques: empirical fittings, analytical calculations and finite difference solutions. Higher order approximations for the neutron flux expansion inside the coarse meshes have also been considered.^(7,8)

Flux synthesis methods, either single- or multi-channel⁽⁹⁻¹²⁾, have been developed in the attempt to reduce the computational time and still retain satisfactory accuracy. The procedure is to relax the spatial discretization in the direction parallel to the fuel elements, taking advantage of the fact that the flux is relatively smooth in this direction due to the lack of spatial heterogeneities. The spatial distribution of the neutron flux in the reactor is obtained by expanding the unknown solution in terms of a few local solutions of two-dimensional finite difference equations, where the expansion coefficients are determined by a variational principle.

Closely related to the coarse mesh finite difference methods are the nodal methods.^(6,13-18) The basic derivation of nodal methods is based on the concept of neutron balance, which is formulated in terms of integral quantities such as average neutron flux and average current.

Different approaches are used in order to determine the relationship between the neutron flux in the node and neutron current on its faces. Early methods⁽⁶⁾ were limited by the assumption of constant nodal fluxes, but later improvements have considered spatial dependence inside the nodes.⁽¹³⁻¹⁸⁾ In particular, the nodal expansion method⁽¹⁹⁾ and the nodal Green's function method⁽²⁰⁾ assume x-y-z separability of the flux distribution⁽¹⁵⁾ in the nodes and the nodal coupling coefficients are calculated by combining several one-dimensional calculations. The combining coefficients are determined by weighted residual techniques and continuity conditions. The coupling between directions is taken into account by expanding the transversal leakage in quadratic polynomials with coefficients dependent on the average transverse leakage in adjacent nodes.

The primary results computed in nodal methods are average fluxes and average currents for the nodes. However, higher order interpolation schemes⁽¹⁴⁾ have been developed to obtain the detailed spatial distribution of the flux inside the nodes from the information contained in the average quantities.

The finite element method^(21,22) widely used in structural analysis has been applied to reactor analysis.⁽²³⁻³¹⁾ Since high order approximations can easily be incorporated, the element volume can be relatively large,

resulting in a reduction of the number of unknowns. The flux is expanded in piecewise polynomials within each element and the system of equations to be solved for the expansion coefficients is obtained by an appropriate variational principle or integral law formulation. The flexibility in the choice of the finite element basis functions allows the method to be applied to quite irregular geometries including local mesh refinement within a large homogeneous region. Furthermore the theoretical foundations of the finite element method are well established^(21,27) and definite analytic error bounds can be predicted for most applications of interest. And since the polynomials are defined in a piecewise fashion, continuity or jump conditions may be readily incorporated at the interfaces between regions.

However, there are also some disadvantages with the finite element method. The irregularity of non-zero elements in the coefficient matrix may result in complicated storage and addressing schemes. For large problems the direct inversion may not be economical⁽¹⁸⁾ and iterative techniques may have to be used. Eigenvalue problems can be solved by the power method but some of the acceleration schemes regularly used in finite difference methods to accelerate outer iterations^(3,4) may not represent real advantages for finite element methods.⁽²⁹⁾

The response matrix method can be considered a particular class of nodal methods. Basically the procedure is to divide the reactor into several coarse meshes within which explicit solutions for the neutron flux distribution for a given incident current distribution is obtained. The neutron flux distribution can then be used to determine the response functions (e.g., outgoing current distributions) for these small domains. Thus the net result is a "response matrix" corresponding to the change in the outgoing current (the response) due to a change in the input current. It is expected to save in the global time by solving the reactor equation over several small domains rather than solving the problem at once over the entire domain. For reactors with only a few types of fuel elements the response matrix method can yield significant savings in computational time.

The response matrix method has evolved from the original study of reflection and transmission of light through a pile of plates by G. G. Stokes⁽³²⁾ in 1862, and subsequent applications of response functions were made in several fields.⁽³³⁾ The neutron transport equation was treated by a similar principle known as the principle of invariant imbedding⁽³⁴⁾, which quickly led to several additional studies⁽³⁵⁻⁴⁴⁾ in this area.

In the early stages of development⁽³⁶⁾ the response matrix was generated by analytical solutions of the diffusion equations. However the application of the response matrix method to lattice calculations necessitated the use of more elaborate transport methods for determining the response matrix, such as collision probability methods^(37,40-42), Monte Carlo method^(38,40) or discrete ordinates methods.⁽³⁹⁾ The generation of response functions by experiment has also been suggested.⁽³³⁾

The partial currents which are related by the response matrices and which connect the coarse meshes in the global calculation have been from the beginning been treated as spatially dependent.⁽³⁵⁾ Burns and Dorning^(45,46) used a local Green's function for the diffusion-removal operators to generate response matrices which incorporated high order approximations for homogeneous rectangular coarse meshes. The flux and the partial currents are expanded in polynomials and the expansion coefficients are determined by a weighted residual technique. The high computational cost of this method led Lawrence and Dorning⁽²⁰⁾ to develop the nodal Green's function method mentioned above. In the higher order response matrix method of Weiss and Lindahl⁽⁴³⁾, the diffusion equation with a given incident partial current distribution which is itself expanded in Legendre polynomials is solved over the node via Fourier series expansion. The response, the outgoing partial

current distribution, is then a separate Legendre expansion. Similar to the local Green's function method, the generation of the response matrix is limited to homogeneous rectangular coarse meshes. Thus the effect of heterogeneities (e.g., burnable poison) on the outgoing partial current cannot be simulated.

Each one of the above mentioned coarse mesh methods adopts a distinct methodological approach with associated advantages and disadvantages. Thus one might expect that a method which combines some of these basic methods, may benefit from the favorable characteristics of the contributing basic methods. Of course, an unfavorable result may occur by combining the different methods in that the theoretical foundations of the resulting method may be weakened or lost completely and some of the undesirable characteristics may be emphasized in the combined method.

Although it is difficult, if not impossible, to single out a particular coarse mesh method which clearly outperforms the other methods, some of the most efficient methods have been obtained through a combination of the basic methods discussed above. In particular, two successful combined methods are the nodal expansion methods and the nodal Green's function method which were described above as being nodal methods. They are basically nodal methods with some ideas of the finite element methods. The one-dimensional neutron fluxes are expanded in piecewise poly-

nomials and the coefficients are determined by a weighted residual technique.

The present investigation also considers a combined method. The finite element method is applied in the context of the response matrix method. In the next chapters the details of the adopted approach is presented.

1.2. Research Objectives

The development of a new coarse mesh method should take into account existing methods as well as the goals and objectives that any coarse mesh method should attempt to meet. The above literature survey has described the current status of coarse mesh methods and now a brief description of the outstanding problems in the area of coarse mesh analysis will be given. These problems, which may be considered as objectives and goals for future work in the coarse mesh area have been presented succinctly by Froehlich: (5)

- 1) Improve the ability to predict local quantities (e.g., spatial distribution of the neutron flux and power);
- 2) Allow efficient modelling of feedback effects (e.g., Doppler and void coefficients);
- 3) Account for the effect of depletion induced spatial cross section variations;

- 4) Allow for hexagonal or triangular geometry (e.g., fast reactor calculations);
- 5) Account for the effect of heterogeneities and improve the methods for homogenization (e.g., calculation of equivalent homogenized group constants).
- 6) Contribute to a unifying theoretical foundation for coarse mesh methods.

While the current research effort will not address all of the above concerns, the objectives of the present investigation are to contribute to the solution of several of the above mentioned problems presently encountered by the coarse mesh methods when used in standard reactor design analysis calculations. In particular, the current investigation can be readily extended to address: prediction of local quantities in the presence of heterogeneities, the capability to include the effect of depletion induced spatial cross section variations and treatment of triangular geometry for fast reactors.

1.3. Summary of Investigation

The present investigation starts from the diffusion theory approximation and applies the finite element method to an alternative formulation of the response matrix method. This alternative form has a significant advantage in that it eliminates the need for the expensive recal-

culations of the response matrices in the eigenvalue problems, as will be discussed in more detail in Chapter 2.

Briefly the reactor is partitioned into coarse meshes and the solution for the diffusion equation inside each coarse mesh is obtained by the finite element method and the response matrices are generated. As will be described in more detail later, there are two basic response matrices, one relating to the outgoing partial current due to an internal source (fixed source, fission source, or inscatter source) and the other giving the outgoing partial current due to diffusion of the incoming partial current. The response matrix of each coarse mesh is then projected on separate basis functions defined on the reactor core and the neutron flux is obtained by an iterative scheme.

With this approach some advantages inherent to the finite element method can be exploited. The geometry of the coarse meshes can be rectangular or triangular and even the extreme case of an irregular boundary can be accommodated. Particular regions can be treated with higher detail than the rest of the domain with local mesh refinement. Spatially dependent cross sections can also be considered in this approach with little increase in computational cost, a feature which is desirable for burn-up calculations⁽²³⁾ or for heterogeneous nodes. Local quantities such as the neutron flux and power distributions are explicitly defined over the entire reactor core in

terms of a function expansion, which is not the case for many of the coarse mesh methods. (18)

The inherent disadvantage of the finite element method in large reactor problems, the irregular large matrix and less highly developed schemes for matrix inversion, is avoided in the present investigation because the finite element matrix equations are solved only at the coarse mesh level, albeit several times.

A brief description of the body of the present investigation is presented below.

In Chapter 2 the theory and the alternative formulation of the response matrix method is presented.

The finite element solution for the diffusion equation in the coarse mesh and the scheme to generate the response matrices is described in Chapter 3. To implement the finite element response matrix method, the basis functions and the iteration schemes, for both inner iterations and outer iterations, are presented in Chapter 4.

Chapter 5 shows the results of the test calculations using the proposed method for two types of reactor problems: a fixed source problem in a simplified bare reactor and two two-dimensional benchmark eigenvalue problems. Conclusions and recommendations for further study are presented in Chapter 6.

The acceleration schemes, asymptotic source extrapolation and the Chebyshev polynomial method, applied to

the finite element response matrix method are presented in Appendix I.

A variational formulation for the diffusion equation solution is shown in Appendix II.

Appendix III gives an interpretation of the block-Jacobi spectral norm for the response matrix method, and the diffusion group constants for evaluation of the present investigation are presented in Appendix IV.

CHAPTER 2

RESPONSE MATRIX METHOD

In Sec. 2.1 the basic theoretical formulation of the response matrix method is presented following closely the work of Weiss and Lindahl⁽⁴⁾, and to illustrate the method, a simple 1-D slab reactor is examined. In Sec. 2.2 an alternative formulation of the response matrix method is presented.

2.1. Theory

Consider the domain Ω in which the solution to the neutron transport or diffusion equation is sought and divide Ω into N subdomains Ω_i , $i=1, \dots, N$, called coarse-meshes. Each coarse-mesh Ω_i is bounded by a piecewise smooth boundary $\partial\Omega_i$ with the outward directed normal vector $\underline{n}(\underline{r}_s)$, where \underline{r}_s is the position vector on the boundary.

Define compact or coupled system as a system in which the domain Ω is simply connected and bounded by a piecewise smooth boundary $\partial\Omega$, and the loose system a system in which none of the boundaries $\partial\Omega_i$ has points in common with any other boundary $\partial\Omega_k$. Accordingly most reactor calculations are concerned with coupled systems whereas loose systems may be encountered in criticality problems,

such as the analysis of fuel storage arrays. The derivation shown below, while applicable to a coupled system, is readily adapted to a loose system with only minor modifications.

It is assumed that an arbitrarily accurate solution for the neutron transport or diffusion equation can be found in coarse-mesh Ω_i subject to the boundary conditions on $\partial\Omega_i$, corresponding to the irradiation of $\partial\Omega_i$ by an arbitrary current $J_i^-(r_s)$. In transport theory $J_i^-(r_s)$ corresponds to the angular flux at the boundary in the direction $\hat{\Omega}$ such that $\hat{\Omega} \cdot \underline{n}(r_s) < 0$, and for diffusion theory $J_i^-(r_s)$ is the partial current directed against the normal vector to the boundary $\partial\Omega_i$ at r_s .

The emerging current $J_i^+(r_s)$ from the boundary $\partial\Omega_i$ due to the irradiation of current $J_i^-(r_s)$ on $\partial\Omega_i$ can be obtained from the above solution for the neutron flux. In the transport theory $J_i^+(r_s)$ is the angular flux at the boundary in directions $\hat{\Omega}$ such that $\hat{\Omega} \cdot \underline{n}(r_s) > 0$, and in diffusion theory $J_i^+(r_s)$ is the partial current in the direction of the normal to the boundary $\partial\Omega_i$ at r_s .

For the sake of simplicity $J_i^+(r_s)$ will be referred to as the outward partial current and $J_i^-(r_s)$ as the inward partial current regardless of the approximation utilized to obtain the neutron flux.

Because of the linearity of the transport and diffusion equations the relationship between $J_i^+(r_s)$ and $J_i^-(r_s)$ can be

concisely expressed by a linear transformation

$$J_i^+(r_s) = \int_{\Omega_i} K_i(r'_s \rightarrow r_s) \cdot J_i^-(r'_s) d\Omega'_s + J_{i0}^+(r_s) \quad (2.1)$$

where $J_{i0}^+(r_s)$ is the outward partial current due to the external source inside the coarse-mesh. The determination of the kernel $K_i(r'_s \rightarrow r_s)$ is one of the objectives of the response matrix method. This kernel depends only on the geometrical and material properties of the coarse-mesh Ω_i ; e.g., the diffusion coefficient and the absorption and production cross sections.

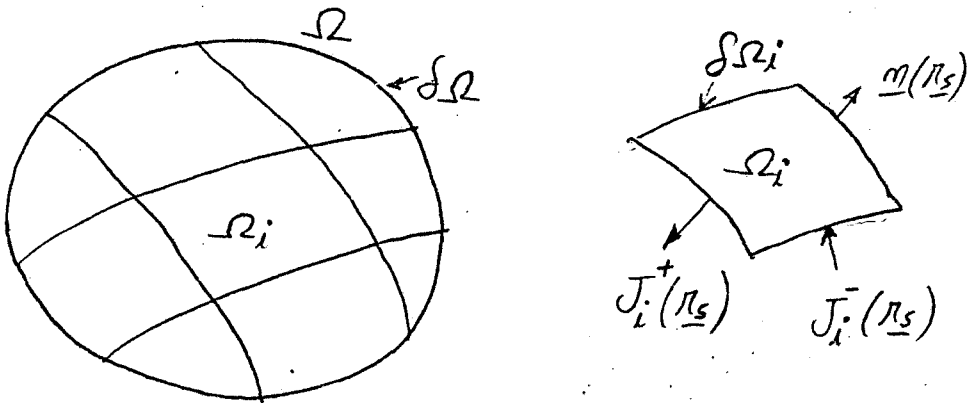


Fig. 2.1 Illustration of domain Ω , subdomain Ω_i , and inward and outward partial currents.

Define $H_{ik}(\underline{r}'_s \rightarrow \underline{r}_s)$, $i, k=1, \dots, N$, as the probability that a neutron leaving the surface $\oint \Omega_k$ at \underline{r}'_s reaches \underline{r}_s on the surface $\oint \Omega_i$. If the $H_{ik}(\underline{r}'_s \rightarrow \underline{r}_s)$ are known, the inward partial current $J_i^-(\underline{r}_s)$ for the coarse-mesh Ω_i can be related to the outward partial currents $J_k^+(\underline{r}'_s)$ from the coarse-meshes Ω_k , $k=1, \dots, N$, by the relationship

$$J_i^-(\underline{r}_s) = \sum_{\substack{k=1 \\ k \neq i}}^N \oint_{\Omega_k} H_{ik}(\underline{r}'_s \rightarrow \underline{r}_s) \cdot J_k^+(\underline{r}'_s) d\underline{r}'_s \quad (2.2)$$

For coupled systems $H_{ik}(\underline{r}'_s \rightarrow \underline{r}_s)$ is easily obtainable by imposing continuity of the partial currents across the boundaries, but for loose systems additional calculations are needed.

It was assumed that the solutions of the transport or diffusion equations for each coarse mesh Ω_i are known for an arbitrary inward partial current $J_i^-(\underline{r}_s)$. Then the neutron flux in the coarse mesh Ω_i can be expressed in terms of the kernel $M_i(\underline{r}_s \rightarrow \underline{r})$,

$$\Phi_i(\underline{r}) = \oint_{\Omega_i} M_i(\underline{r}_s \rightarrow \underline{r}) \cdot J_i^-(\underline{r}_s) d\underline{r}_s + \Phi_{i0}(\underline{r}) \quad (2.3)$$

where $\Phi_{i0}(\underline{r})$ is the neutron flux due to the external source inside Ω_i , and $M_i(\underline{r}_s \rightarrow \underline{r})$ is generated during the solution of transport or diffusion solution in the coarse mesh Ω_i .

Therefore the flux for the entire domain is obtained if either $J_i^-(\underline{r}_s)$ or $J_i^+(\underline{r}_s)$, $i=1, \dots, N$, are known.

Equations (2.1), (2.2), and (2.3) comprise the conventional formulation of the response matrix method for the solution to the proposed problem.

As an example of the response matrix method, the one-dimensional slab eigenvalue problem is presented. The external source is then zero and the diffusion equation is solved analytically, subject to unity inward partial current on a face of the slab of thickness h . From the neutron flux solution, the reflection and transmission functions are calculated by Weiss⁽⁵⁵⁾ as

$$r = \frac{\sin Bh}{\sin(Bh + \theta)}, \quad \theta = 2 \tan^{-1}(2DB), \quad B^2 = (k-1)/M^2 \gg 0$$

and $t = \frac{\sin \theta}{\sin(Bh + \theta)}$, respectively, or

$$r = \frac{\epsilon [1 - \exp(-2Kh)]}{1 - \epsilon^2 \exp(-2Kh)}, \quad \epsilon = \frac{1 - 2DK}{1 + 2DK}, \quad K^2 = (1-k)/M^2 \gg 0$$

and $t = \frac{(1 - \epsilon^2) \exp(-Kh)}{1 - \epsilon^2 \exp(-2Kh)}$, respectively,

where D is the diffusion coefficient,

M^2 is the migration area, and

k is the ratio of infinite multiplication factor and effective multiplication factor (eigenvalue).

The partial currents on the face of the slab can then be related by a response matrix as

$$\begin{bmatrix} J^+(h) \\ J^+(0) \end{bmatrix} = \begin{bmatrix} r & t \\ t & r \end{bmatrix} \cdot \begin{bmatrix} J^-(h) \\ J^-(0) \end{bmatrix}$$

2.2. Alternative Formulation

Unfortunately the response matrix method as formulated above is not in a convenient form for application to the eigenvalue problem (e.g., determination of the neutron multiplication factor, k_{eff}). The kernel $R_i(\underline{r}'_S \rightarrow \underline{r}_S)$ is dependent on the neutron multiplication within the coarse mesh Ω_i and since the fission source is scaled by the eigenvalue, the kernel $R_i(\underline{r}'_S \rightarrow \underline{r}_S)$ has to be generated several times during the course of the solution to the eigenvalue problem.

This investigation treats an alternative formulation of the response matrix method wherein the expensive recalculations of the kernel in the eigenvalue problems are eliminated by considering two kernels: $R_i^{J^-}(\underline{r}'_s \rightarrow \underline{r}_s)$ and $R_i^S(\underline{r} \rightarrow \underline{r}_s)$. They are dependent only on the diffusion coefficient and the absorption cross section of the coarse mesh Ω_i , and they are independent of the production cross section (fission + inscatter). This allows the non-linearity of the outward partial current caused by the fission source and the inscattering source to be transferred to the iterative scheme used to solve the eigenvalue problem or the fixed source problem as shown in the next section.

As a result of the linearity of transport and diffusion equations the outward partial current $J_i^+(\underline{r}_s)$ can be given by the following linear transformation

$$J_i^+(\underline{r}_s) = \int_{\Omega_i} R_i^{J^-}(\underline{r}'_s \rightarrow \underline{r}_s) J_i^-(\underline{r}'_s) d\underline{r}'_s + \int_{\Omega_i} R_i^S(\underline{r} \rightarrow \underline{r}_s) S_i(\underline{r}) d\underline{r}, \quad (2.4)$$

$$i = 1, \dots, N,$$

$$\underline{r}_s \in \partial\Omega_i,$$

$$\underline{r} \in \Omega_i.$$

where $S_i(\underline{r})$ is the neutron source within the coarse mesh $\underline{\Omega}_i$ due to the fission source, the inscatter source, and the external source. For eigenvalue problems the external source is absent and the fission source is scaled by the inverse of the multiplication factor, k_{eff} .

The kernel $R_i^{J^-}(\underline{r}'_s \rightarrow \underline{r}_s)$ gives the outward partial current response due to the diffusion of an inward partial current in the coarse mesh $\underline{\Omega}_i$, while the kernel $R_i^S(\underline{r} \rightarrow \underline{r}_s)$ gives the outward partial current response due to diffusion of neutrons generated in all kinds of sources within the coarse mesh $\underline{\Omega}_i$.

In this alternative formulation of the response matrix method the definition of the kernels $H_{ik}(\underline{r}'_s \rightarrow \underline{r}_s)$; $i, k=1, \dots, N$, is maintained and the relationship given by equation (2.2) remains unchanged.

The neutron flux in the coarse mesh $\underline{\Omega}_i$ will then be given by

$$\begin{aligned} \Phi_i(\underline{r}) = & \int_{\underline{\Omega}_i} M_i^{J^-}(\underline{r}_s \rightarrow \underline{r}) J_i^-(\underline{r}_s) d\underline{r}_s \\ & + \int_{\underline{\Omega}_i} M_i^S(\underline{r}' \rightarrow \underline{r}) S_i(\underline{r}') d\underline{r}' \end{aligned} \quad (2.5)$$

where the kernels $M_i^{J^-}(\underline{r}_s \rightarrow \underline{r})$ and $M_i^S(\underline{r}' \rightarrow \underline{r})$ are generated as byproducts during the generation of the kernels $R_i^{J^-}(\underline{r}'_s \rightarrow \underline{r}_s)$ and $R_i^S(\underline{r} \rightarrow \underline{r}_s)$.

The formal solution of the response matrix method is represented by the equations (2.2), (2.4) and (2.5) in the alternative formulation versus equations (2.1) and (2.2) for the conventional formulation described earlier.

The response matrix method is applicable whenever the kernels are computable, especially $R_i^{J^-}(\underline{r}'_S \rightarrow \underline{r}_S)$ and $R_i^S(\underline{r} \rightarrow \underline{r}_S)$. The kernel $H_{i\ell}(\underline{r}'_S \rightarrow \underline{r}_S)$ may impose some difficulties for loose systems but for coupled systems which comprise most of the practical problems in reactor calculations only interface continuity conditions across the boundaries of the coarse meshes may suffice and the kernel can be generated without any difficulty. The generation of the kernels $M_i^{J^-}(\underline{r}_S \rightarrow \underline{r})$ and $M_i^S(\underline{r}' \rightarrow \underline{r})$ is solely dependent on the computational scheme used to generate the kernels $R_i^{J^-}(\underline{r}'_S \rightarrow \underline{r}_S)$ and $R_i^S(\underline{r} \rightarrow \underline{r}_S)$ and as such does not represent an additional computational burden.

The present investigation is developed on the basis of this formulation of the response matrix method because it is in a form suitable for use in the eigenvalue problem and can also be used for the fixed source problem.

The multigroup eigenvalue problem can be treated as being composed of multiple fixed source problems, where the source includes any type of neutron production, including the fission source scaled by the multiplication factor. Since the kernels depend only on the diffusion coefficients

and the absorption cross section the response matrices need be generated only once.

2.3. Numerical Approximation

The formal solution for the alternative formulation of the response matrix method may be obtained by solving equations (2.2), (2.4) and (2.5). However, the implementation of the response matrix method on a digital computer requires various approximations to allow the equations to be numerically manipulated.

One approach which is utilized in the present investigation is to use a weighted residual method to approximate the response matrix equations in a form which is amenable to numerical computation.

Let a coarse mesh Ω_i contain L nodes conveniently located within its volume Ω_i , and define the polynomials $\Psi_l(r)$, $l=1, \dots, L$, with unitary value at the node l and zero at the remaining nodes. Also let a coarse mesh Ω_i contain K nodes on its boundary $\partial\Omega_i$ and define the polynomials $\Psi_{sk}(r_s)$, $k=1, \dots, K$, with unitary value at the node k and zero at the remaining nodes. It should be noted that in the present discussion the term "node" corresponds to a point, not a region of the problem domain.

The partial currents, the neutron flux and the neutron source can be approximated for each coarse mesh Ω_i , by an expansion in the appropriate basis polynomials

(i.e., boundary polynomials or volume polynomials)

$$J^{\pm}(\underline{r}_s) = \sum_{k=1}^K J_{ik}^{\pm} \Psi_{sk}(\underline{r}_s) , \quad \underline{r}_s \in \partial\Omega_i , \quad (2.6)$$

$$\Phi_i(\underline{\pi}) = \sum_{l=1}^L \Phi_{il} \Psi_l(\underline{\pi}) , \quad \underline{\pi} \in \Omega_i , \quad (2.7)$$

$$S_i(\underline{\pi}) = \sum_{l=1}^L S_{il} \Psi_l(\underline{\pi}) , \quad \underline{\pi} \in \Omega_i , \quad (2.8)$$

where J_{ik}^{\pm} , Φ_{il} and S_{il} are the partial currents on the boundary node k , the neutron flux value and the neutron source value at the volume node l , respectively.

However, the partial currents $J_{\underline{I}}^{\pm}(\underline{r}_s)$ are defined according to the orientation of the normal $\underline{n}(\underline{r}_s)$ on the boundary. Since $\underline{n}(\underline{r}_s)$ is discontinuous along the edges or on the corners, let the boundary polynomials $\Psi_{sk}(\underline{r}_s)$, $k=1, \dots, K$, $\underline{r}_s \in \partial\Omega_i$, $i=1, \dots, N$, be defined piecewisely such that the discontinuity of $J_{\underline{I}}^{\pm}(\underline{r}_s)$ on the corner or along the edges are explicitly accounted for.

The expansion coefficients $J_{ik}^{\pm}(\underline{r}_s)$, $i=1, \dots, N$; $k=1, \dots, K$, can be determined by requiring the residuals of the approximation of equation (2.4) and equation (2.2) to be orthogonal to the set of surface polynomials $\Psi_{sk'}(\underline{r}_s)$, $k'=1, \dots, K$.

From equation (2.4) the residuals can be defined as

$$\begin{aligned}
 g_i(\underline{r}_s) &= \sum_{k=1}^K \underline{\Psi}_{sk}(\underline{r}_s) J_{ik}^+ \\
 &\quad - \int_{\Omega_i} \underline{R}_i^J(\underline{r}'_s \rightarrow \underline{r}_s) \left[\sum_{k=1}^K \underline{\Psi}_{sk}(\underline{r}'_s) J_{ik}^- \right] d\underline{r}'_s \\
 &\quad - \int_{\Omega_i} \underline{R}_i^S(\underline{r} \rightarrow \underline{r}_s) \left[\sum_{l=1}^L \underline{\Psi}_l(\underline{r}) S_{il} \right] d\underline{r},
 \end{aligned} \tag{2.9}$$

$$i=1, \dots, N; \underline{r}_s \in \Omega_i; \underline{r} \in \Omega_i,$$

and requiring the residual to be orthogonal to

$$\underline{\Psi}_{sk'}(\underline{r}'_s), k'=1, \dots, K, \text{ one obtains}$$

$$\underline{T}_{\underline{\Psi}_s \underline{\Psi}_s} \cdot \underline{J}_i^+ = \underline{R}_i^J \cdot \underline{J}_i^- + \underline{R}_i^S \cdot \underline{S}_i \tag{2.10}$$

where

$$\underline{\underline{T}}_{\Psi_s \Psi_s} = \left(\int_{\Omega_i} \int_{\Omega_j} \Psi_{sk'}(\underline{n}_s) \Psi_{sk}(\underline{n}_s) d\underline{n}_s \right)_{k'k},$$

$k', k=1, \dots, K$, is a $K \times K$ matrix,

$$\underline{\underline{R}}_i^J = \left(\int_{\Omega_j} \int_{\Omega_i} \Psi_{sk'}(\underline{n}_s) R_i^J(\underline{n}_s \rightarrow \underline{n}_s') \Psi_{sk}(\underline{n}_s') d\underline{n}_s' d\underline{n}_s \right)_{k'k},$$

$k', k=1, \dots, K$, is a $K \times K$ matrix,

$$\underline{\underline{R}}_i^S = \left(\int_{\Omega_j} \int_{\Omega_i} \Psi_{sk'}(\underline{n}_s) R_i^S(\underline{n} \rightarrow \underline{n}_s) \Psi_{sl}(\underline{n}) d\underline{n} d\underline{n}_s \right)_{k'l},$$

$k'=1, \dots, K; l=1, \dots, L$, is a $K \times L$ matrix,

$$\underline{\underline{S}}_i = \text{col}(S_{i1}, S_{i2}, \dots, S_{iL})$$

$$\underline{\underline{J}}_i^\pm = \text{col}(J_{i1}^\pm, J_{i2}^\pm, \dots, J_{iK}^\pm) .$$

If $\underline{R}_i^{J^-}$ and \underline{R}_i^S are redefined in order to incorporate $\underline{T}_{\Psi_s \Psi_s}^{-1}$, equation (2.10) can be written as

$$\underline{J}_i^+ = \underline{R}_i^{J^-} \cdot \underline{J}_i^- + \underline{R}_i^S \cdot \underline{S}_i \quad (2.11)$$

Similarly from the equation (2.2), defining the residuals and requiring them to be orthogonal to $\underline{\Psi}_{ik'}(\underline{r}_s)$, $k'=1, \dots, K$, one gets

$$\underline{T}_{\Psi_s \Psi_s} \cdot \underline{J}_i^- = \sum_{\substack{j=1 \\ j \neq i}}^N \underline{H}_{ij} \cdot \underline{J}_j^+ \quad (2.12)$$

where

$$\underline{H}_{ij} = \left(\int_{\Omega_i} \int_{\Omega_j} \underline{\Psi}_i(\underline{r}_s) \underline{H}_{ij}(\underline{r}'_s \rightarrow \underline{r}_s) \underline{\Psi}_j(\underline{r}'_s) d\underline{r}'_s d\underline{r}_s \right)_{ij} ;$$

$i, j=1, \dots, K; \underline{r}_s \in \Omega_i; \underline{r}'_s \in \Omega_j$; is a $K \times K$ matrix, and redefining \underline{H}_{ij} in order to incorporate $\underline{T}_{\Psi_s \Psi_s}^{-1}$,

$$\underline{J}_i^- = \sum_{j=1}^N \underline{H}_{ij} \cdot \underline{J}_j^+ \quad (2.13)$$

For the coupled systems, however, the matrix \underline{H}_{ij} can be easily incorporated in the computational scheme simply by reindexing the outward partial currents, and no weighted residual calculation is needed.

The neutron flux expansion coefficients $\underline{\Phi}_{il}$, $l=1, \dots, L$, can be determined by requiring the residuals of the approximation of equation (2.5) to be orthogonal to all

the functions $\underline{\Psi}_{l'}(\underline{\pi})$, $l'=1, \dots, L, \underline{\pi} \in \Omega_i$,

$$\underline{T}_{\Psi\Psi} \cdot \underline{\Phi}_i = \underline{M}_i^{\underline{J}} \cdot \underline{J}_i^- + \underline{M}_i^{\underline{S}} \cdot \underline{S}_i \quad (2.14)$$

where $\underline{T}_{\Psi\Psi} = \left(\int_{\Omega_i} \underline{\Psi}_{l'}(\underline{\pi}) \underline{\Psi}_l(\underline{\pi}) d\underline{\pi} \right)_{l'l}$; $l', l = 1, \dots, L$,

is a $L \times L$ matrix,

$$\underline{M}_i^{\underline{J}} = \left(\int_{\Omega_i} \int_{\Omega_i} \underline{\Psi}_{l'}(\underline{\pi}) M_i^{\underline{J}}(\underline{\pi}_s \rightarrow \underline{\pi}) \underline{\Psi}_{sk}(\underline{\pi}_s) d\underline{\pi}_s d\underline{\pi} \right)_{l'k}$$

$l' = 1, \dots, L$; $k = 1, \dots, K$, is a $L \times K$ matrix,

$$\underline{M}_i^{\underline{S}} = \left(\int_{\Omega_i} \int_{\Omega_i} \underline{\Psi}_{l'}(\underline{\pi}) M_i^{\underline{S}}(\underline{\pi}' \rightarrow \underline{\pi}) \underline{\Psi}_l(\underline{\pi}') d\underline{\pi}' d\underline{\pi} \right)_{l'l}$$

$l', l = 1, \dots, L$, is a $L \times L$ matrix, and

$$\underline{\Phi}_i = \text{col}(\Phi_{i1}, \Phi_{i2}, \dots, \Phi_{iL}) ,$$

and redefining $\underline{M}_i^{\underline{J}}$ and $\underline{M}_i^{\underline{S}}$ in order to incorporate $\underline{T}_{\Psi\Psi}^{-1}$ one gets

$$\underline{\Phi}_i = \underline{M}_i^{\underline{J}} \cdot \underline{J}_i^- + \underline{M}_i^{\underline{S}} \cdot \underline{S}_i \quad (2.15)$$

The compact representation of the equations (2.11), (2.13), and (2.15) can be obtained by defining

$$\underline{J}^{\pm} = \text{col}(\underline{J}_1^{\pm}, \underline{J}_2^{\pm}, \dots, \underline{J}_N^{\pm}) , \text{ a } (K \times N) \text{ vector,}$$

$$\underline{\Phi} = \text{col}(\underline{\Phi}_1, \underline{\Phi}_2, \dots, \underline{\Phi}_N) , \text{ a } (L \times N) \text{ vector,}$$

$$\underline{\mathcal{S}} = \text{col}(\underline{s}_1, \underline{s}_2, \dots, \underline{s}_N)$$

, a $(L \times N)$ vector,

and rewriting the equations as

$$\underline{J}^+ = \underline{R}^J \cdot \underline{J}^- + \underline{R}^S \cdot \underline{\mathcal{S}}$$

(2.16) (2.2)

$$\underline{J}^- = \underline{H} \cdot \underline{J}^+$$

(2.17) (2.4)

$$\underline{\Phi} = \underline{M}^J \cdot \underline{J}^- + \underline{M}^S \cdot \underline{\mathcal{S}}$$

(2.18) (2.5)

where

$$\underline{R}^J = \text{diag}(\underline{R}_1^J, \underline{R}_2^J, \dots, \underline{R}_N^J) \quad , \text{ is a } (N \times K) \times (N \times K) \text{ matrix,}$$

$$\underline{R}^S = \text{diag}(\underline{R}_1^S, \underline{R}_2^S, \dots, \underline{R}_N^S) \quad , \text{ is a } (N \times K) \times (N \times L) \text{ matrix,}$$

$$\underline{M}^J = \text{diag}(\underline{M}_1^J, \underline{M}_2^J, \dots, \underline{M}_N^J) \quad , \text{ is a } (N \times L) \times (N \times K) \text{ matrix,}$$

$$\underline{M}^S = \text{diag}(\underline{M}_1^S, \underline{M}_2^S, \dots, \underline{M}_N^S) \quad , \text{ is a } (N \times L) \times (N \times L) \text{ matrix,}$$

and \underline{H} is a $(K \times N) \times (K \times N)$ matrix, which for coupled systems is a matrix composed of block permutation matrices of dimension $K \times K$, and also incorporates the boundary conditions of the domain Ω .

Equations (2.16), (2.17), and (2.18) are then the weighted residual formulations of the original response matrix equations (2.4), (2.2), and (2.5), respectively, and are in a form suitable for numerical solution, as will be described in the next section.

2.4. Solution Algorithms

The solution of the response matrix method represented by the equations (2.16), (2.17) and (2.18) requires only one type of partial current, either \underline{J}^+ or \underline{J}^- , to be determined. By inserting the equation (2.17) into the equations (2.16) and (2.18) the problem is given as

$$\underline{J}^+ = \underline{R}^{\underline{J}^-} \cdot \underline{H} \cdot \underline{J}^+ + \underline{R}^{\underline{S}} \cdot \underline{S} \quad \underline{J}^+ \cdot (\underline{I} - \underline{R}^{\underline{J}^-} \cdot \underline{H}) = \underline{R}^{\underline{S}} \cdot \underline{S} \quad (2.19)$$

$$\underline{\Phi} = \underline{M}^{\underline{J}^+} \cdot \underline{J}^+ + \underline{M}^{\underline{S}} \cdot \underline{S} \quad (2.20)$$

and if $(\underline{I} - \underline{R}^{\underline{J}^-} \cdot \underline{H})$ is invertible, where \underline{I} is the $(N \times K) \times (N \times K)$ identity matrix, the solution can be directly obtained as

$$\underline{J}^+ = (\underline{I} - \underline{R}^{\underline{J}^-} \cdot \underline{H})^{-1} \cdot \underline{R}^{\underline{S}} \cdot \underline{S}$$

For practical problems the dimension and the complexity of the $\underline{R}^{\underline{J}^-} \cdot \underline{H}$ matrix imply that direct inversion is impractical. The alternative is the use of iterative

methods, such as the Jacobi method, the Gauss-Seidel method, or the Successive Over-relaxation method. (2-4)

The convergence of the iterative methods can be guaranteed if the spectral radius of the iteration matrix

$$\rho(\underline{R}^{\underline{J}^-} \cdot \underline{H}) < 1.$$

In terms of more accessible quantities, the infinite norms, the sufficient condition is

$$\| \underline{R}^{\underline{J}^-} \cdot \underline{H} \|_{\infty} < 1,$$

and for a compact system with no incident current on its boundaries, $\| \underline{H} \|_{\infty} = 1$, the sufficient condition is

$$\| \underline{R}^{\underline{J}^-} \|_{\infty} < 1.$$

Recalling the definition of $\underline{R}^{\underline{J}^-}$, the sufficient condition now is

$$\| \underline{R}_i^{\underline{J}^-} \|_{\infty} < 1, \quad \text{for all } i=1, \dots, N.$$

The general solution algorithm can be given as

- Step 0 - Guess arbitrary non-negative $\underline{J}^{-(0)}$ and $\underline{S}^{(0)}$.
- Step 1 - $\underline{J}^{+(t)} = \underline{R}^{\underline{J}^-} \cdot \underline{J}^{-(t-1)} + \underline{R}^{\underline{S}} \cdot \underline{S}^{(n-1)}$
- Step 2 - $\underline{J}^{-(t)} = \underline{H} \cdot \underline{J}^{+(t)}$
- Step 3 - $\underline{\Phi}^{(n)} = \underline{M}^{\underline{J}^-} \cdot \underline{J}^{-(t)} + \underline{M}^{\underline{S}} \cdot \underline{S}^{(n-1)}$
- Step 4 - Update $\underline{S}^{(x)}$ from $\underline{\Phi}^{(n)}$
- } $t=1, 2, \dots$
- } $n=1, 2, \dots$

It should be noted that the above algorithm does not depend on the construction of the basis functions, except that they have unitary value at the nodes they are associated with. In addition, the above formulation is formal in the sense that the response matrices \underline{R}_i^J and \underline{R}_i^S were given in terms of the response kernels $\mathcal{R}_i^J(\pi_3' \rightarrow \pi_3)$ and $\mathcal{R}_i^S(\pi \rightarrow \pi_3)$, which have been defined in only a formal sense via equation (2.4). As will be seen in the next chapter, the finite element method is employed at the local(assembly) level to generate the response matrices used in the global solution algorithm outlined above.

CHAPTER 3

FINITE ELEMENT RESPONSE MATRIX METHOD

The previous chapter presented the general formulation of the response matrix method and a description of a weighted residual approach to cast the resultant response matrix equations in a form suitable for numerical approximation. The discussion was quite general and did not depend on the exact form of the approximation polynomials. In this chapter the specific method utilized in the present investigation to determine the response matrices is described. In particular, the finite element method is employed to solve the one-group diffusion equation in the coarse meshes, thereby generating the response matrices. Therefore, the coarse meshes are assumed to be composed of materials with properties compatible with the assumptions of diffusion theory: the absorption cross sections are expected to be relatively small compared to the scattering cross sections. This assumption is easily satisfied in most reactor problems since the coarse meshes are usually defined over an entire assembly or part of an assembly, where heterogeneities are homogenized and the assembly (or partial assembly) is treated as one material with equivalent homogenized cross sections.

3.1. Galerkin Formulation

The one-group diffusion equation is to be solved in each of the coarse meshes Ω_m , $n=1, \dots, N$, (the assembly level calculations)

$$-\nabla_{\underline{r}} D_m(\underline{r}) \nabla \phi_m(\underline{r}) + \Sigma_{a_m}(\underline{r}) \phi_m(\underline{r}) = S_m(\underline{r}), \quad (3.1)$$

$$m=1, \dots, N, \quad \underline{r} \in \Omega_m,$$

where $D_n(\underline{r})$ is the diffusion coefficient,

$\Sigma_{a_n}(\underline{r})$ is the total absorption cross section,

$s_n(\underline{r})$ is the source term,

subject to the irradiation of inward partial current

$j_n^-(\underline{r}_s)$ on the boundary $\partial\Omega_m$,

(3.2)

$$j_m^-(\underline{r}_s) = \frac{1}{4} \phi_m(\underline{r}_s) + \frac{1}{2} D_m(\underline{r}_s) \nabla \phi_m(\underline{r}) \Big|_{\underline{r}=\underline{r}_s} \cdot \underline{n}(\underline{r}_s), \quad \underline{r}_s \in \partial\Omega_m,$$

where $\underline{n}(\underline{r}_s)$ is the vector normal to the surface $\partial\Omega_m$,

and to interface conditions of continuity of current

and flux.

In order to formulate the Galerkin approximation, or weak form, of the problem the space of trial functions is defined as

$$H_2^1 = \left\{ \psi(\underline{r}) \in C^0 \mid \int_{\Omega_m} [\nabla \psi(\underline{r}) \nabla \psi(\underline{r}) + \psi(\underline{r}) \psi(\underline{r})] d\underline{r} < \infty \right\},$$

and for $f(\underline{r}), g(\underline{r}) \in H_2^1$ the inner product is defined as

$$(f, g) = \int_{\Omega_m} f(\underline{r}) g(\underline{r}) d\underline{r} ,$$

and the boundary inner product as

$$\langle f, g \rangle = \oint_{\partial\Omega_m} f(\underline{r}_s) g(\underline{r}_s) d\underline{r}_s .$$

Multiplying the equation (3.1) by an arbitrary element of the trial function space H_2^1 , $\psi_m(\underline{r})$, and integrating over Ω_m , one obtains

$$-\int_{\Omega_m} \nabla D_m(\underline{r}) \nabla \phi_m(\underline{r}) \psi_m(\underline{r}) d\underline{r} + \int_{\Omega_m} \Sigma_m(\underline{r}) \phi_m(\underline{r}) \psi_m(\underline{r}) d\underline{r} = \int_{\Omega_m} S_m(\underline{r}) \psi_m(\underline{r}) d\underline{r} . \quad (3.3)$$

By Green's theorem the first term of equation (3.3) can be written as (details in Appendix II)

$$-\int_{\Omega_m} \nabla \bar{D}_m(\underline{r}) \nabla \phi_m(\underline{r}) \psi_m(\underline{r}) d\underline{r} = \int_{\Omega_m} [D_m(\underline{r}) \nabla \phi_m(\underline{r})] \nabla \psi_m(\underline{r}) d\underline{r} - \oint_{\partial\Omega_m} D_m(\underline{r}_s) \nabla \phi_m(\underline{r}) \Big|_{\underline{r}=\underline{r}_s} \cdot \underline{m}(\underline{r}_s) d\underline{r}_s . \quad (3.4)$$

Now use the boundary condition (3.2)

$$D_m(\underline{r}_s) \nabla \phi_m(\underline{r}) \Big|_{\underline{r}=\underline{r}_s} \cdot \underline{m}(\underline{r}_s) = 2 j_m^-(\underline{r}_s) - \frac{1}{2} \phi_m(\underline{r}_s)$$

and insert it into the last term of equation (3.4) to obtain

$$-\int_{\Omega_m} \nabla D_m(\underline{x}) \nabla \phi_m(\underline{x}) \psi_m(\underline{x}) d\underline{x} = \int_{\Omega_m} D_m(\underline{x}) \nabla \phi_m(\underline{x}) \nabla \psi_m(\underline{x}) d\underline{x} \quad (3.5)$$

$$+ \frac{1}{2} \oint_{\partial \Omega_m} \phi_m(\underline{x}_s) \psi_m(\underline{x}_s) d\underline{x}_s - 2 \oint_{\partial \Omega_m} j_m^-(\underline{x}_s) \psi_m(\underline{x}_s) d\underline{x}_s .$$

Now combine equation (3.5) and equation (3.3) to obtain the final result, $a(\phi_n, \psi_n)$

$$\int_{\Omega_m} D_m(\underline{x}) \nabla \phi_m(\underline{x}) \nabla \psi_m(\underline{x}) d\underline{x} + \int_{\Omega_m} \Sigma_{am}(\underline{x}) \phi_m(\underline{x}) \psi_m(\underline{x}) d\underline{x}$$

$$+ \frac{1}{2} \oint_{\partial \Omega_m} \phi_m(\underline{x}_s) \psi_m(\underline{x}_s) d\underline{x}_s = \int_{\Omega_m} S_m(\underline{x}) \psi_m(\underline{x}) d\underline{x} \quad (3.6)$$

$$+ 2 \oint_{\partial \Omega_m} j_m^-(\underline{x}_s) \psi_m(\underline{x}_s) d\underline{x}_s$$

The solution $\phi_n(\underline{x})$ to equation (3.6) which is valid for all $\psi_m(\underline{x}) \in H_2^1$ is the weak solution to the original diffusion equation. Note that the original boundary condition, equation (3.2), is incorporated directly into the weak form and hence is a natural boundary condition. That is, the space H_2^1 does not need to obey the boundary condition in order for the weak solution to satisfy (in a weak sense) the boundary condition.

Defining the bilinear functional

$$a(\phi_m, \psi_m) = \int_{\Omega_m} D_m(\underline{\Omega}) \nabla \phi_m(\underline{\Omega}) \nabla \psi_m(\underline{\Omega}) d\underline{\Omega} \\ + \int_{\Omega_m} \sum_{a_m}(\underline{\Omega}) \phi_m(\underline{\Omega}) \psi_m(\underline{\Omega}) d\underline{\Omega} + \frac{1}{2} \oint_{\partial\Omega_m} \phi_m(\underline{\pi}_s) \psi_m(\underline{\pi}_s) d\underline{\pi}_s$$

the Galerkin approximation can be succinctly written

$$a(\phi_m, \psi_m) = (s_m, \psi_m) + 2 \langle j_m^-, \psi_m \rangle \quad , \psi_m \in H_2^1 \quad (3.7)$$

The same result could be obtained by minimizing the quadratic functional

$$F(\psi_m) = \int_{\Omega_m} [D_m(\underline{\Omega}) \nabla \psi_m(\underline{\Omega}) \nabla \psi_m(\underline{\Omega}) + \sum_{a_m}(\underline{\Omega}) \psi_m(\underline{\Omega}) \psi_m(\underline{\Omega}) - 2 s_m(\underline{\Omega}) \psi_m(\underline{\Omega})] d\underline{\Omega} \\ + \frac{1}{2} \oint_{\partial\Omega_m} [4 j_m^-(\underline{\pi}_s) - \psi_m(\underline{\pi}_s)]^2 d\underline{\pi}_s \quad , \psi_m \in H_2^1$$

The proof is presented in Appendix II.

3.2. Finite Element Solution

The weak form, Eq. (3.7), of the diffusion equation is in a form suitable for solution by the finite element method. Specifically, the Ritz approximation is utilized,

in which the trial functions ψ_m^h belong to a particular finite-dimensional subspace S^h contained in H_2^1 ,

$$\psi_m^h \in S^h \subset H_2^1.$$

In order to construct the finite element subspace S^h , the coarse mesh domain Ω_m is partitioned into M subdomains, Ω_{mm} , $m=1, \dots, M$, and the elements of S^h are polynomials defined over the subdomains Ω_{mm} , $m=1, \dots, M$, which are continuous across the subdomain boundaries. Also let the domain contain N_e nodes, and define $\psi_{mi}^h(\underline{x})$, $i=1, \dots, N_e$, $\psi_{mi}^h \in S^h$, functions with unitary value at the node i and zero at the remaining nodes. The Lagrangian finite element method is characterized by choosing as $\psi_{mi}^h(\underline{x})$, the continuous piecewise polynomials. These polynomials are the basis functions for the subspace S^h , since every member of S^h can be given as a combination of the $\psi_{mi}^h(\underline{x})$.

If the solution $\phi_m^h(\underline{x})$ is then sought within the space S^h , $\phi_m^h(\underline{x})$ can be expanded in the basis functions for S^h as

$$\phi_m^h(\underline{x}) = \sum_{i=1}^{N_e} \phi_{mi} \psi_{mi}^h(\underline{x}) \quad (3.8)$$

The Ritz-Galerkin approximation is obtained by inserting the approximation (3.8) into the weak form (3.7) and requiring (3.7) to be true for all basis functions

$$\psi_{mj}^h(\underline{r}), j=1, \dots, N_e:$$

$$a \left(\sum_{i=1}^{N_e} \phi_{mi} \psi_{mi}^h(\underline{r}), \psi_{mj}^h(\underline{r}) \right) = (s_m, \psi_{mj}^h(\underline{r})) + 2 \langle j^-, \psi_{mj}^h(\underline{r}) \rangle,$$

for all $j=1, \dots, N_e$, or

$$\sum_{i=1}^{N_e} \phi_{mi} a(\psi_{mi}^h, \psi_{mj}^h) = (s_m, \psi_{mj}^h) + 2 \langle j^-, \psi_{mj}^h \rangle, \quad (3.9)$$

for all $j=1, \dots, N_e$.

An identical result may be obtained from the variational principle, as shown in Appendix II, by searching for the stationary point in the space S^h ,

$$\frac{\partial}{\partial \phi_j} F(\phi_m^h(\underline{r})) = 0, \quad j=1, \dots, N_e.$$

which is equivalent to minimizing the quadratic functional discussed above.

Defining the vectors $\underline{\phi}_m$ and $\underline{\psi}_m^h(\underline{r})$ as

$$\underline{\phi}_m = \text{col}(\phi_{m1}, \phi_{m2}, \dots, \phi_{mN_e})$$

$$\underline{\psi}_m^h(\underline{r}) = \text{col}(\psi_{m1}^h(\underline{r}), \psi_{m2}^h(\underline{r}), \dots, \psi_{mN_e}^h(\underline{r}))$$

Equation (3.9) can be rewritten as a matrix equation

$$\underline{\underline{A}}_m \cdot \underline{\underline{\phi}}_m = \underline{\underline{s}}_m^\psi + \underline{\underline{j}}_m^{\psi^-} \quad (3.10)$$

where $\underline{\underline{A}}_m = (a(\psi_{mj}^h, \psi_{mi}^h))_{ij}$, $i, j=1, \dots, N_e$,

$$\underline{\underline{s}}_m^\psi = (s_m, \underline{\underline{\psi}}_m^h(\underline{\underline{\Omega}})) ,$$

$$\underline{\underline{j}}_m^{\psi^-} = 2 \langle \underline{\underline{j}}_m^-, \underline{\underline{\psi}}_m^h(\underline{\underline{\Omega}}) \rangle .$$

The linear matrix equation (3.10) can be solved either by direct inversion or by iterative methods as long as $\underline{\underline{A}}_m$ is invertible.

If $\underline{\underline{A}}_m$ is positive definite, $\underline{\underline{x}} \cdot \underline{\underline{A}}_m \cdot \underline{\underline{x}} > 0$, for $\underline{\underline{x}} \neq 0$ then $\underline{\underline{A}}_m$ is invertible and equation (3.10) can be solved. $\underline{\underline{A}}_m$ can be shown to be positive definite as follows.

Assume an arbitrary $\alpha^h(\underline{\underline{\Omega}}) \in S^h$ and expand

$$\alpha^h(\underline{\underline{\Omega}}) = \sum_{i=1}^{N_e} \alpha_i \psi_{mi}^h(\underline{\underline{\Omega}}) .$$

Now from the definition of the bilinear functional

$$a(\psi_{mi}^h, \psi_{mj}^h) \text{ from Eq. (3.7),}$$

$$a(\alpha^h(\underline{\underline{\Omega}}), \alpha^h(\underline{\underline{\Omega}})) > 0 \text{ if } D_m(\underline{\underline{\Omega}}) > 0, \sum a_m(\underline{\underline{\Omega}}) \geq 0 .$$

But

$$\begin{aligned}
 a(\alpha^h(\Omega), \alpha^h(\Omega)) &= a\left(\sum_{i=1}^{Ne} \alpha_i \psi_{mi}^h, \sum_{j=1}^{Ne} \alpha_j \psi_{mj}^h\right) \\
 &= \sum_{i=1}^{Ne} \sum_{j=1}^{Ne} a(\alpha_i \psi_{mi}^h, \alpha_j \psi_{mj}^h) \\
 &= \sum_{i=1}^{Ne} \sum_{j=1}^{Ne} \alpha_i a(\psi_{mi}^h, \psi_{mj}^h) \alpha_j \\
 &= \underline{\alpha} \cdot \underline{A}_m \cdot \underline{\alpha},
 \end{aligned}$$

and

$$\underline{\alpha} \cdot \underline{A}_m \cdot \underline{\alpha} > 0$$

if

$$\underline{\alpha} = \text{col}(\alpha_1, \alpha_2, \dots, \alpha_{Ne}) \neq \underline{0}$$

which is the desired result. Therefore \underline{A}_m is positive definite, thus invertible.

Since \underline{A}_m is invertible, the solution can be expressed as

$$\underline{\phi}_m = \underline{A}_m^{-1} \cdot \underline{S}_m \psi + \underline{A}_m^{-1} \cdot \underline{j} \cdot \underline{\psi}_m \quad (3.11)$$

and the flux in the coarse-mesh Ω_m is from (3.8),

$$\phi_m^h(\underline{\Omega}) = \left[\underline{\psi}_m^h(\underline{\Omega}) \right]^T \cdot \underline{A}_m^{-1} \cdot \underline{s}_m^\psi + \left[\underline{\psi}_m^h(\underline{\Omega}) \right]^T \cdot \underline{A}_m^{-1} \cdot \underline{j}_m^\psi$$

3.3. Response Matrices Generation

In order to generate the response matrices from the solution (3.11) it is necessary to expand the response current, which is the outward partial current $\underline{j}_n^+(\underline{r}_s)$ in an appropriate set of basis functions. In addition, it is necessary to determine the source term $\underline{s}_n(\underline{r})$ and the inward partial current $\underline{j}_n^-(\underline{r}_s)$.

The outward partial current $\underline{j}_n^+(\underline{r}_s)$ is expanded in piecewise polynomials defined on the boundary of the coarse mesh $\partial\Omega_m$. Since $\underline{j}_n^+(\underline{r}_s)$ is defined as the partial current in the direction of the vector $\underline{n}(\underline{r}_s)$ normal to the boundary $\partial\Omega_m$, it is necessary to exclude corners or edges of $\partial\Omega_m$, where $\underline{n}(\underline{r}_s)$ is discontinuous, and allow $\underline{j}_n^+(\underline{r}_s)$ to be discontinuous at these points. Then the polynomials are continuous only along each side of $\partial\Omega_m$ for two-dimensional problems, or continuous on each face of $\partial\Omega_m$ for three-dimensional problems.

Let the boundary $\partial\Omega_m$ contain N_s nodes and define $\underline{\psi}_{s_{mi}}^h(\underline{r}_s)$, $i=1, \dots, N_s$, $\underline{\psi}_{s_{mi}}^h \in S^h$, functions with unitary value at node i and zero at the remaining nodes. For convenience the $\underline{\psi}_{s_{mi}}^h(\underline{r}_s)$ are chosen to be piecewise polynomials, continuous between corners or between edges.

Therefore the outward partial current can be expanded in the boundary basis functions,

$$\underline{j}_m^{+}(\underline{r}_s) = \left[\underline{\Psi}_{S_m}^{+}(\underline{r}_s) \right]^T \cdot \underline{j}_m^{+} \quad (3.12)$$

where

$$\underline{\Psi}_{S_m}^{+}(\underline{r}_s) = \text{col} \left(\Psi_{S_{m1}}^{+}(\underline{r}_s), \Psi_{S_{m2}}^{+}(\underline{r}_s), \dots, \Psi_{S_{mN_s}}^{+}(\underline{r}_s) \right),$$

$$\underline{j}_m^{+} = \text{col} \left(j_{m1}^{+}, j_{m2}^{+}, \dots, j_{mN_s}^{+} \right).$$

The source term $s_n(\underline{r})$ and the inward partial current $j_n^{-}(\underline{r}_s)$ from the assembly calculation can be equated to the source $S_n(\underline{r})$ and inward partial current $J_n^{-}(\underline{r}_s)$ in the global calculation as follows :

$$s_m(\underline{r}) = \left[\underline{\Psi}(\underline{r}) \right]^T \cdot \underline{S}_m \quad (3.13)$$

and

$$j_m^{-}(\underline{r}_s) = \left[\underline{\Psi}_s^{-}(\underline{r}_s) \right]^T \cdot \underline{J}_m^{-} \quad (3.14)$$

where $\underline{\Psi}(\underline{r}) = \text{col} \left(\Psi_1(\underline{r}), \Psi_2(\underline{r}), \dots, \Psi_L(\underline{r}) \right),$

and $\underline{\Psi}_s^{-}(\underline{r}_s) = \text{col} \left(\Psi_{s1}^{-}(\underline{r}_s), \Psi_{s2}^{-}(\underline{r}_s), \dots, \Psi_{sK}^{-}(\underline{r}_s) \right),$

are the global volumetric and boundary basis functions, respectively, and \underline{S}_n and \underline{J}_n^{-} are defined in (2.10).

Inserting the expression (3.13) into the definition of \underline{S}_m^ψ in (3.10) one obtains

$$\underline{S}_m^\psi = \left(\underline{\Psi}_m^h(\underline{r}), [\underline{\Psi}(\underline{r})]^T \cdot \underline{S}_m \right)$$

or

$$\underline{S}_m^\psi = \left[\underline{T}_{\Psi\Phi} \right] \cdot \underline{S}_m + \left[\quad \right] S \quad (3.15)$$

where

$$\underline{T}_{\Psi\Phi} = \left(\underline{\Psi}_m^h(\underline{r}), [\underline{\Psi}(\underline{r})]^T \right)$$

is a $N_e \times L$ matrix.

Similarly, inserting expression (3.14) into the definition of $\underline{J}_m^{j\psi^-}$ in (3.10) one gets

$$\underline{J}_m^{j\psi^-} = 2 \left\langle \underline{\Psi}_m^h(\underline{r}_s), [\underline{\Psi}_s(\underline{r}_s)]^T \cdot \underline{J}_m^- \right\rangle$$

or

$$\underline{J}_m^{j\psi^-} = 2 \underline{T}_{\Psi\Phi_s} \cdot \underline{J}_m^- \quad (3.16)$$

where

$$\underline{T}_{\Psi\Phi_s} = \left\langle \underline{\Psi}_m^h(\underline{r}_s), [\underline{\Psi}_s(\underline{r}_s)]^T \right\rangle$$

is a $N_e \times K$ matrix.

Finally, inserting expressions (3.15) and (3.16) into equation (3.11), the flux can be expressed as

$$\underline{\phi}_m = \underline{A}_m^{-1} \cdot \underline{T}_{\Psi} \underline{\Psi} \cdot \underline{S}_m + \underline{A}_m^{-1} \cdot \underline{T}_{\Psi} \underline{\Psi}_S \cdot \underline{J}_m^- \quad (3.17)$$

Since the desired quantity is the outward partial current $\underline{j}_n^+(\underline{r}_S)$ on the coarse mesh boundary, one uses the diffusion approximation for the partial current,

$$\underline{j}_m^+(\underline{r}_S) = \frac{1}{4} \phi(\underline{r}_S) - \frac{1}{2} D(\underline{r}_S) \nabla \phi(\underline{r}) \Big|_{\underline{r}=\underline{r}_S} \cdot \underline{n}(\underline{r}_S) \quad (3.18)$$

Approximating $\underline{j}_n^+(\underline{r}_S)$ and $\phi(\underline{r})$ by expansion expressions (3.12) and (3.8), respectively, and defining the residual $\rho(\underline{r}_S)$ as

$$\rho(\underline{r}_S) = \left[\underline{\psi}_{S_m}^h(\underline{r}_S) \right]^T \cdot \underline{j}_m^+ - \frac{1}{4} \left[\underline{\psi}_m^h(\underline{r}_S) \right]^T \cdot \underline{\phi} + \frac{1}{2} D(\underline{r}_S) \nabla \left[\underline{\psi}_m^h(\underline{r}) \right]^T \Big|_{\underline{r}=\underline{r}_S} \cdot \underline{n}(\underline{r}_S) \cdot \underline{\phi} \quad (3.19)$$

the outward partial current coefficients \underline{j}_n^+ can be obtained by requiring the residual $\rho(\underline{r}_S)$ to be orthogonal to the $\underline{\psi}_{S_{mi}}^h(\underline{r}_S)$, $i=1, \dots, N_S$,

$$\begin{aligned} \left\langle \underline{\psi}_{S_m}^h(\underline{r}_S), \left[\underline{\psi}_{S_m}^h(\underline{r}_S) \right]^T \right\rangle \cdot \underline{j}_m^+ &= \frac{1}{4} \left\langle \underline{\psi}_{S_m}^h(\underline{r}_S), \left[\underline{\psi}_m^h(\underline{r}_S) \right]^T \right\rangle \cdot \underline{\phi} \\ &- \frac{1}{2} \left\langle \underline{\psi}_{S_m}^h(\underline{r}_S), D(\underline{r}_S) \nabla \left[\underline{\psi}_m^h(\underline{r}) \right]^T \Big|_{\underline{r}=\underline{r}_S} \cdot \underline{n}(\underline{r}_S) \right\rangle \cdot \underline{\phi} \end{aligned} \quad (3.20)$$

Defining the $N_s \times N_s$ matrix

$$\underline{T}_{\psi_s \psi_s} = \left\langle \underline{\psi}_{s_m}^A(\underline{n}_s), \left[\underline{\psi}_{s_m}^h(\underline{n}_s) \right]^T \right\rangle,$$

and the $N_s \times N_e$ matrix

$$\underline{T}_{D\psi_s \nabla \psi} = \left\langle \underline{\psi}_{s_m}^A(\underline{n}_s), D(\underline{n}_s) \left[\underline{\psi}_m^h(\underline{n}) \right]^T \Big|_{\underline{n}=\underline{n}_s} \cdot \underline{m}(\underline{n}_s) \right\rangle,$$

equation (3.20) can be concisely given as

$$\underline{T}_{\psi_s \psi_s} \cdot \underline{j}_m^+ = \left\{ \frac{1}{4} \underline{T}_{\psi_s \psi_s}^T - \frac{1}{2} \underline{T}_{D\psi_s \nabla \psi} \right\} \cdot \underline{\phi} \quad (3.21)$$

Inverting the positive definite matrix $\underline{T}_{\psi_s \psi_s}$ and substituting $\underline{\phi}$ from equation (3.17)

$$\begin{aligned} \underline{j}_m^+ &= \underline{T}_{\psi_s \psi_s}^{-1} \left\{ \frac{1}{4} \underline{T}_{\psi_s \psi_s}^T - \frac{1}{2} \underline{T}_{D\psi_s \nabla \psi} \right\} \cdot \underline{A}_m^{-1} \cdot \underline{T}_{\psi_s \psi_s} \cdot \underline{s}_m^+ \\ &+ \underline{T}_{\psi_s \psi_s}^{-1} \left\{ \frac{1}{2} \underline{T}_{\psi_s \psi_s}^T - \underline{T}_{D\psi_s \nabla \psi} \right\} \cdot \underline{A}_m^{-1} \cdot \underline{T}_{\psi_s \psi_s} \cdot \underline{j}_m^- \end{aligned} \quad (3.22)$$

or

$$\underline{j}_m^+ = \underline{R}_m^s \cdot \underline{s}_m^+ + \underline{R}_m^j \cdot \underline{j}_m^- \quad (3.23)$$

where

$$\underline{R}_m^s = \underline{T}_{\psi_s \psi_s}^{-1} \cdot \left\{ \frac{1}{4} \underline{T}_{\psi_s \psi_s}^T - \frac{1}{2} \underline{T}_{D\psi_s \nabla \psi} \right\} \cdot \underline{A}_m^{-1} \cdot \underline{T}_{\psi_s \psi_s}$$

is a $N_s \times L$ matrix,

and

$$\underline{\underline{R}}_m^{\underline{J}^-} = \underline{\underline{T}}_{\psi_s \psi_s}^{-1} \cdot \left\{ \frac{1}{2} \underline{\underline{T}}_{\psi_s \psi_s}^T - \underline{\underline{T}}_{D\psi_s V\psi} \right\} \cdot \underline{\underline{A}}_m^{-1} \cdot \underline{\underline{T}}_{\psi \psi_s}$$

is a $N_s \times K$ matrix.

The response matrices $\underline{\underline{R}}_n^S$ and $\underline{\underline{R}}_n^{\underline{J}^-}$ connect the assembly level outward partial current $j_n^+(\underline{r}_s)$ to the global neutron source $S_n(\underline{r})$ and global inward partial current $J_n^-(\underline{r}_s)$, respectively. However, what is desired are global response matrices $\underline{\underline{R}}_n^S$ and $\underline{\underline{R}}_n^{\underline{J}^-}$ which connect the global outward partial currents $J_n^+(\underline{r}_s)$ to the global neutron source and inward partial current. These can be obtained by expanding the assembly level outward partial current $j_n^+(\underline{r}_s)$ in the global basis functions $\underline{\underline{\Psi}}_{sk}(\underline{r}_s)$, $k=1, \dots, K$; $\underline{r}_s \in \Omega_m$, as

$$j_m^+(\underline{r}_s) = \sum_{k=1}^K \underline{\underline{\Psi}}_{sk}(\underline{r}_s) J_{mk}^+ \quad (3.24)$$

But equation (3.24) does not have a unique solution J_n^+ , $k=1, \dots, K$, because $j_n^+(\underline{r}_s)$ is expanded in a more refined set of basis functions (the assembly level basis functions versus the global basis functions $\underline{\underline{\Psi}}_{sk}(\underline{r}_s)$). Therefore, equation (3.24) will be satisfied in a weak sense by applying the weighted residual method.

Recalling the expansion expression (3.12) for $j_n^+(\underline{r}_s)$ and defining the residual $\beta(\underline{r}_s)$ as

$$\beta(\underline{r}_s) = \left[\underline{\Psi}_{sm}^h(\underline{r}_s) \right]^T \cdot \underline{j}_m^+ - \left[\underline{\Psi}_s(\underline{r}_s) \right]^T \cdot \underline{J}_m^+,$$

the global expansion coefficient \underline{J}_n^+ can be obtained by requiring the residual $\beta(\underline{r}_s)$ to be orthogonal to the $\underline{\Psi}_{sk}(\underline{r}_s)$, $k=1, \dots, K$; $\underline{r}_s \in \mathcal{S}\Omega_m$:

$$\underline{T}_{\underline{\Psi}_s \underline{\Psi}_s} \cdot \underline{J}_m^+ = \underline{T}_{\underline{\Psi}_s \underline{\Psi}_s} \cdot \left(\underline{j}_m^+ = \underline{R}_m^s \cdot \underline{S}_m + \underline{R}_m^{\sigma^-} \cdot \underline{J}_m^- \right) \quad (3.25)$$

where

$$\underline{T}_{\underline{\Psi}_s \underline{\Psi}_s} = \left(\int_{\mathcal{S}\Omega_m} \underline{\Psi}_{sk}(\underline{r}_s) \underline{\Psi}_{sk'}(\underline{r}_s) d\underline{r}_s \right)_{kk'}, \quad k, k'=1, \dots, K,$$

is a $K \times K$ matrix,

$$\underline{T}_{\underline{\Psi}_s \underline{\Psi}_s} = \left(\int_{\mathcal{S}\Omega_m} \underline{\Psi}_{sk}(\underline{r}_s) \underline{\Psi}_{smj}(\underline{r}_s) d\underline{r}_s \right)_{kj}, \quad k=1, \dots, K; \\ j=1, \dots, N_s,$$

is a $K \times N_s$ matrix.

Substituting \underline{j}_n^+ from expression (3.23) and inverting the positive definite matrix $\underline{T}_{\underline{\Psi}_s \underline{\Psi}_s}$, one gets

$$\underline{J}_m^+ = \underline{R}_m^s \cdot \underline{S}_m + \underline{R}_m^{\sigma^-} \cdot \underline{J}_m^- \quad (3.26)$$

where

$$\underline{R}_m^s = \underline{T}_{\underline{\Psi}_s \underline{\Psi}_s}^{-1} \cdot \underline{T}_{\underline{\Psi}_s \underline{\Psi}_s} \cdot \underline{R}_m^s$$

and

$$\underline{\underline{R}}_m^{J^-} = \underline{\underline{T}}_{\underline{\Psi}_s \underline{\Psi}_s}^{-1} \cdot \underline{\underline{T}}_{\underline{\Psi}_s \underline{\Psi}_s} \cdot \underline{\underline{R}}_m^{J^-}$$

are the desired response matrices for the global partial current calculations.

The construction of the response matrices $\underline{\underline{M}}^S$ and $\underline{\underline{M}}^{J^-}$ for the global flux $\underline{\underline{\Phi}}_m$ can be obtained from equation (3.17) by expanding the local neutron flux $\phi_n(\underline{r})$ in the global basis functions $\underline{\underline{\Psi}}_l(\underline{r})$, $l=1, \dots, L$; $\underline{r} \in \Omega_m$,

$$\phi(\underline{r}) = [\underline{\underline{\Psi}}(\underline{r})]^T \cdot \underline{\underline{\Phi}}_m$$

Again the expansion coefficients $\underline{\underline{\Phi}}_m$ must be obtained by the weighted residual technique, and since $\phi_n(\underline{r})$ is given in terms of the basis functions $\underline{\underline{\Psi}}_l^h(\underline{r})$, one obtains in a similar manner,

$$\underline{\underline{\Phi}}_m = \underline{\underline{T}}_{\underline{\Psi} \underline{\Psi}}^{-1} \cdot \underline{\underline{T}}_{\underline{\Psi} \underline{\Psi}} \cdot \underline{\underline{\Phi}}_m \quad (3.27)$$

where $\underline{\underline{T}}_{\underline{\Psi} \underline{\Psi}} = \underline{\underline{T}}_{\underline{\Psi} \underline{\Psi}}^T$, defined in the equation (3.15),

and $\underline{\underline{T}}_{\underline{\Psi} \underline{\Psi}} = \left(\int_{\Omega_m} \underline{\underline{\Psi}}_l(\underline{r}) \underline{\underline{\Psi}}_{l'}(\underline{r}) d\underline{r} \right)_{ll'}$, $l, l'=1, \dots, L$.

Substituting the equation (3.17) into the equation

(3.27)

$$\underline{\Phi}_m = \underline{M}_m^s \cdot \underline{S}_m + \underline{M}_m^{j^-} \cdot \underline{J}_m \quad (3.28)$$

where

$$\underline{M}_m^{j^-} = 2 \underline{T}_{\Psi\Psi}^{-1} \cdot \underline{T}_{\Psi\psi} \cdot \underline{A}_m^{-1} \cdot \underline{T}_{\psi\Psi_s}$$

and

$$\underline{M}_m^s = \underline{T}_{\Psi\Psi}^{-1} \cdot \underline{T}_{\Psi\psi} \cdot \underline{A}_m^{-1} \cdot \underline{T}_{\psi\Psi}$$

are the desired response matrices for the global flux calculations.

CHAPTER 4
COMPUTER IMPLEMENTATION

4.1. Basis Functions

The global basis functions for the neutron flux expansion and for the partial currents expansion in the reactor problem were defined in Chapter 2 for coarse meshes Ω_m , $n=1, \dots, N$ as

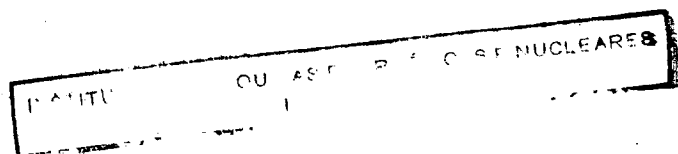
$$\Psi_l(\underline{r}) \quad , l=1, \dots, L; \underline{r} \in \Omega_m,$$

and

$$\Psi_{sk}(\underline{r}_s) \quad , k=1, \dots, K; \underline{r}_s \in \partial\Omega_m \quad , \text{ respectively,}$$

where L is the number of indexed nodes on the coarse mesh Ω_m , K is the number of indexed nodes on the coarse mesh boundary $\partial\Omega_m$, and the number of nodes, L and K , is dependent on the degree of the polynomials desired in the coarse mesh and on its boundary, respectively.

In the present investigation the geometry of the coarse mesh was chosen as a rectangle, since most of the practical problems in the reactor calculations can be solved with this geometry, but extension to the triangular geometry



does not impose any conceptual difficulties.

In a rectangular coarse mesh a simple scheme to generate the polynomial elements, $\Psi_l(x,y)$, $l=1,\dots,L$, of any degree is to form a direct product of univariate Lagrange polynomials, e.g., a $(m+n)$ th degree element

$$\Psi_l(x,y) = L_i^m(x) L_j^n(y)$$

where

$$L_i^m(x) = \frac{\prod_{\substack{m'=1 \\ m' \neq i}}^m (x - x_{m'})}{\prod_{\substack{m'=1 \\ m' \neq i}}^m (x_i - x_{m'})}, \quad L_j^n(y) = \frac{\prod_{\substack{m'=1 \\ m' \neq j}}^n (y - y_{m'})}{\prod_{\substack{m'=1 \\ m' \neq j}}^n (y_j - y_{m'})},$$

and (x_i, y_j) are the coordinates of the node l .

However the product of high order Lagrange polynomials results in a large number of internal nodes and tends to preserve very high order terms while neglecting some lower order terms. (49)

A polynomial generation scheme which preserves the low order terms in the high degree elements generates the Serendipity elements. (48, 49) Figure 4.1 illustrates the number and the location of nodes for quadratic and cubic Serendipity elements.

It is convenient to define a local coordinate system for the polynomials and simplify the calculation of

integrals which are transformed from the physical coordinate system to the local coordinate system. A convenient local coordinate system for rectangular elements may be defined by the following transformation,

$$\xi = (x - x_0)/a, \quad \eta = (y - y_0)/b,$$

where (x_0, y_0) are the coordinates of the center of an arbitrary rectangle, and a and b are the dimensions of the rectangle.

In the local coordinate system the quadratic Serendipity elements are

$$\Psi_i(\xi, \eta) = \frac{1}{4}(1 + \xi\xi_i)(1 + \eta\eta_i)(\xi\xi_i + \eta\eta_i - 1),$$

$$i=1, 3, 6, 8;$$

$$\Psi_i(\xi, \eta) = \frac{1}{2}(1 - \xi^2)(1 + \eta\eta_i),$$

$$i=2, 7;$$

$$\Psi_i(\xi, \eta) = \frac{1}{2}(1 + \xi\xi_i)(1 - \eta^2),$$

$$i=4, 5;$$

where (ξ_i, η_i) are the local coordinates of the node i .

Similarly, the cubic Serendipity elements are

$$\Psi_i(\xi, \eta) = \frac{1}{32}(1 + \xi\xi_i)(1 + \eta\eta_i)[-10 + 9(\xi^2 + \eta^2)],$$

$$i=1, 4, 9, 12;$$

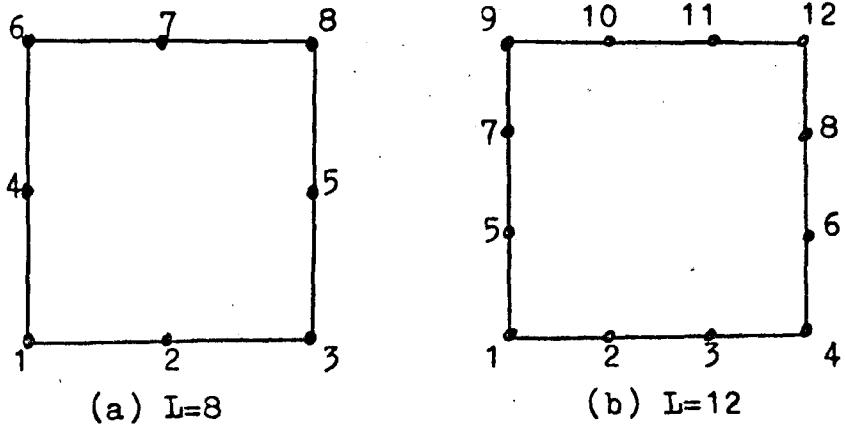


Fig. 4.1 Nodes for Serendipity elements, $\Psi_L(\xi, \eta)$,
 (a)quadratic, (b)cubic.

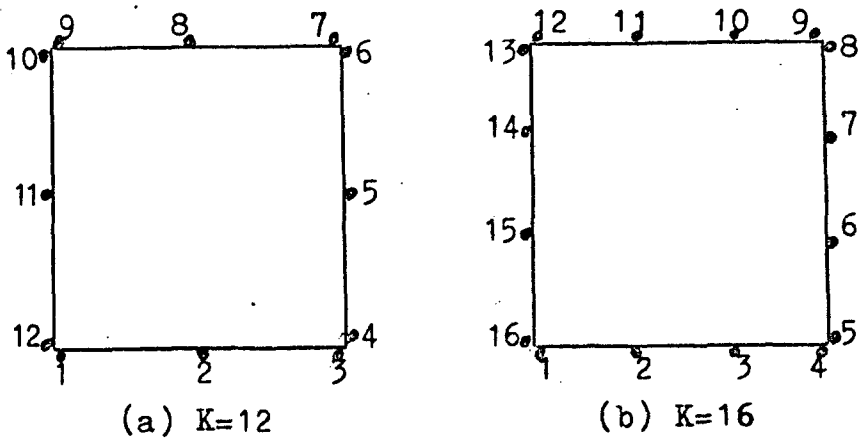


Fig. 4.2 Nodes for Lagrange polynomials, $\Psi_{Lsk}(\underline{\pi}_s)$,
 (a)quadratic, (b)cubic.

$$\Psi_i(\xi, \eta) = \frac{9}{32} (1 + \xi \xi_i) (1 - \eta^2) (1 + 9 \eta \eta_i),$$

i=5,6,7,8;

$$\Psi_i(\xi, \eta) = \frac{9}{32} (1 + 9 \xi \xi_i) (1 - \xi^2) (1 + \eta \eta_i),$$

i=2,3,10,11 .

The basis functions $\Psi_{sk}(r_s)$, $k=1, \dots, K$, for the partial currents expansion on the coarse mesh boundary ∂R_m , is defined on each side of the rectangle as Lagrange polynomials. The corners are not included in the definition because partial currents are defined according to the normal vector orientation, and the normal vector is not defined on the corners.

Figure 4.2 illustrates the nodes on the boundary of a coarse mesh for quadratic and cubic Lagrange polynomials.

The quadratic Lagrange polynomials in the local coordinates system are

$$\Psi_{si}(\xi) = \frac{1}{2} \xi \xi_i (1 + \xi \xi_i), \quad i=1,3,7,9,$$

where ξ_i is the abscissa of node i on the faces $(\xi, \pm 1)$,

$$\Psi_{si}(\xi) = (1 - \xi^2), \quad i=2,8,$$

$$\Psi_{si}(\eta) = \frac{1}{2} \eta \eta_i (1 + \eta \eta_i), \quad i=4,6,10,12,$$

where η_i is the ordinate of node i on the faces $(\pm 1, \eta)$

$$\Psi_{S_i}^-(\eta) = (1 - \eta^2) \quad , \quad i=5, 11 \quad ,$$

The cubic Lagrange polynomials are

$$\Psi_{S_i}^-(\xi) = \frac{1}{16} (1 + 3\xi\xi_i) (9\xi^2 - 1) \quad , \quad i=1, 4, 9, 12,$$

$$\Psi_{S_i}^-(\xi) = \frac{9}{16} (1 + 9\xi\xi_i) (1 - \xi^2) \quad , \quad i=2, 3, 10, 11,$$

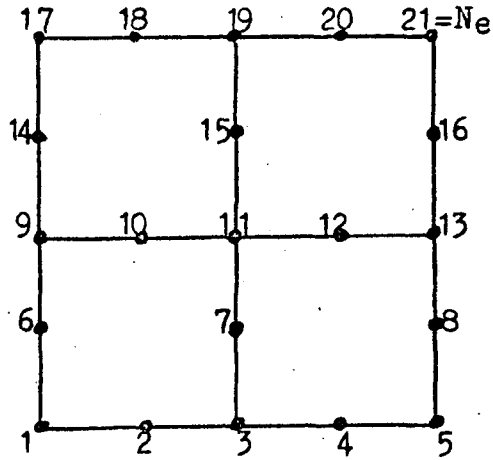
$$\Psi_{S_i}^-(\eta) = \frac{1}{16} (1 + \eta\eta_i) (9\eta^2 - 1) \quad , \quad i=5, 8, 13, 16,$$

$$\Psi_{S_i}^-(\eta) = \frac{9}{16} (1 + 9\eta\eta_i) (1 - \eta^2) \quad , \quad i=6, 7, 14, 15.$$

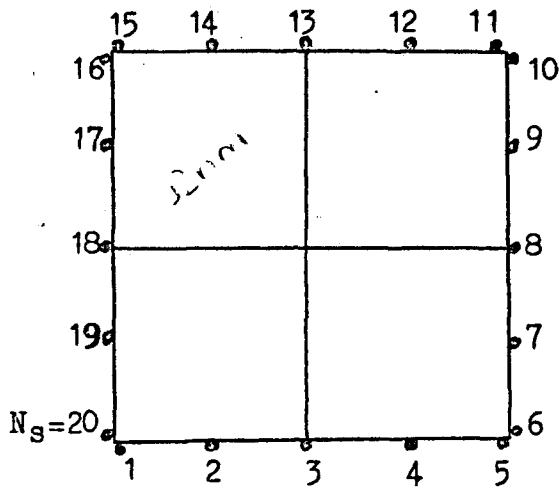
The basis functions to be used in the generation of the response matrices were defined for coarse meshes Ω_m , $n=1, \dots, N$, in Chapter 3, as

$$\psi_{m_i}^h(\underline{r}) \quad , \quad i=1, \dots, N_e, \underline{r} \in \Omega_m,$$

and $\psi_{S_{m_i}}^h(\underline{r}_S)$, $i=1, \dots, N_S$, $\underline{r}_S \in \partial\Omega_m$, where N_e and N_S are the number of volume nodes and boundary nodes, respectively, of Ω_m . The $\psi_{m_i}^h(\underline{r})$ and $\psi_{S_{m_i}}^h(\underline{r}_S)$ basis functions are used for the neutron flux expansion and for the partial current expansions, respectively, in the assembly level calculation.



(a) nodes for $\psi_{mi}^h(\underline{r}), i=1, \dots, N_e$



(b) nodes for $\psi_{smi}^h(\underline{r}_s), i=1, \dots, N_s$

Fig. 4.3. Nodes for quadratic Serendipity elements,

$\psi_{mi}^h(\underline{r})$, and for piecewise polynomials,

$\psi_{smi}^h(\underline{r}_s)$, in the coarse mesh Ω_m

subdivided in 4 subdomains Ω_{mm} ,

$m=1, \dots, 4$.

To illustrate, Fig. 4.3 shows a coarse mesh divided in M subdomains, Ω_{mm} , $m=1, \dots, M$, together with the volume nodes for quadratic Serendipity elements (flux expansion) and boundary nodes for quadratic Lagrange polynomials (current expansion).

The basis functions $\psi_{mi}^h(\underline{r})$ have the value unity at node i and the value zero at the remaining nodes, and $\psi_{mi}^h(\underline{r})$ is defined on the subdomains over which the common node i is defined. Within each subdomain the basis function $\psi_{mi}^h(\underline{r})$ is a Serendipity polynomial as defined above.

The basis functions $\psi_{smi}^h(\underline{r}_s)$ are each defined on only one side of the coarse mesh, with the corners representing double nodes, one for each side. This is consistent with the behavior of the partial currents at a corner, where a discontinuous change in the outward normal $\underline{n}(\underline{r}_s)$ occurs. For convenience $\psi_{smi}^h(\underline{r}_s)$ are defined as piecewise Lagrange polynomials.

For illustrative purposes the response matrices defined in equation (3.31) were generated for a typical light water reactor⁽⁴⁷⁾ using the basis functions defined above. Table 4.1 and Table 4.2 contain the response matrices $\underline{R}_m^{\sigma^-}$ and $\underline{R}_m^{\sigma^+}$, respectively. Figure 4.4 illustrates the outward partial currents due to a flat inward partial current incident on one face of the coarse mesh. Figure 4.5 shows the outward partial currents due to a constant neutron source within the coarse mesh. The

Table 4.1 - R_m^j for 2D-IAEA benchmark problem (47) (zone 1, group 1) in quadratic basis functions $\psi_{jk}(r_B)$, $k=1, \dots, 12$.

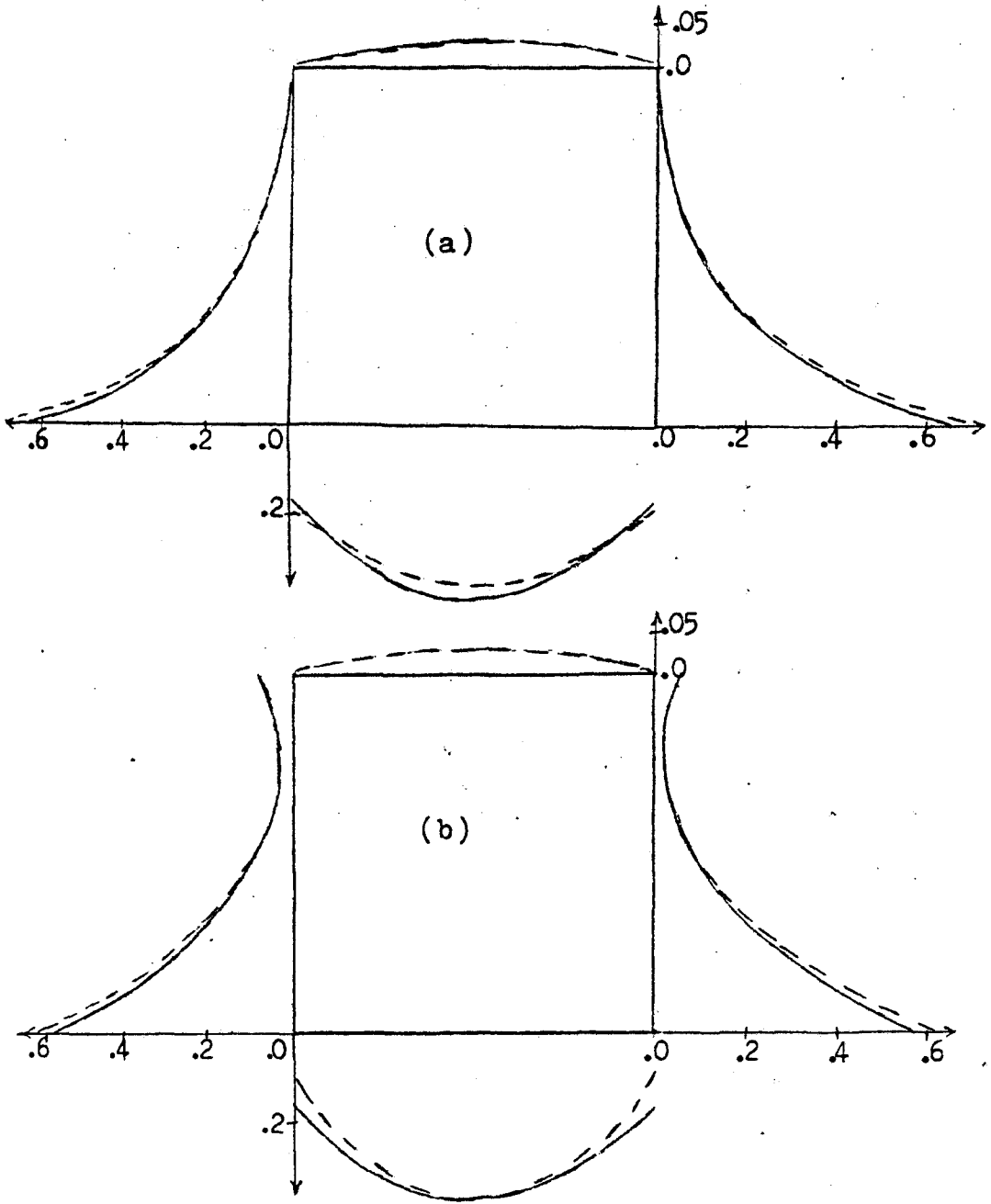
| | J = 1 | 2 | 3 | 4 | 5 | 6 |
|-----|-------------|------------|-------------|-------------|------------|-------------|
| I=1 | 4.3352E-02 | 1.0101E-01 | -4.8625E-02 | 4.8690E-02 | 2.3907E-02 | -6.5671E-03 |
| 2 | 5.2577E-02 | 2.6463E-01 | 5.2577E-02 | 1.7200E-02 | 5.9121E-02 | 9.2671E-04 |
| 3 | -4.8625E-02 | 1.0101E-01 | 4.3352E-02 | 3.6101E-01 | 3.0302E-01 | -4.9940E-02 |
| 4 | -4.9940E-02 | 3.0302E-01 | 3.6101E-01 | 4.3351E-02 | 1.0101E-01 | -4.8624E-02 |
| 5 | 9.2669E-04 | 5.9121E-02 | 1.7200E-02 | 5.2576E-02 | 2.6463E-01 | 5.2577E-02 |
| 6 | -6.5670E-03 | 2.3907E-02 | 4.8690E-02 | -4.8624E-02 | 1.0101E-01 | 4.3351E-02 |
| 7 | -8.0094E-05 | 6.1030E-03 | 2.3023E-03 | -4.9940E-02 | 3.0303E-01 | 3.6101E-01 |
| 8 | 3.2142E-03 | 1.8764E-02 | 3.2142E-03 | 9.2667E-04 | 5.9122E-02 | 1.7200E-02 |
| 9 | 2.3023E-03 | 6.1031E-03 | -8.0087E-05 | -6.5671E-03 | 2.3907E-02 | 4.8690E-02 |
| 10 | 4.8690E-02 | 2.3907E-02 | -6.5670E-03 | -8.0100E-05 | 6.1031E-03 | 2.3023E-03 |
| 11 | 1.7200E-02 | 5.9121E-02 | 9.2669E-04 | 3.2142E-03 | 1.8764E-02 | 3.2142E-03 |
| 12 | 3.6101E-01 | 3.0302E-01 | -4.9940E-02 | 2.3023E-03 | 6.1030E-03 | -8.0084E-05 |

| | 7 | 8 | 9 | 10 | 11 | 12 |
|-----|-------------|------------|-------------|-------------|------------|-------------|
| I=1 | -8.0089E-05 | 6.1029E-03 | 2.3022E-03 | -4.9940E-02 | 3.0302E-01 | 3.6101E-01 |
| 2 | 3.2142E-03 | 1.8764E-02 | 3.2142E-03 | 9.2669E-04 | 5.9121E-02 | 1.7200E-02 |
| 3 | 2.3023E-03 | 6.1030E-03 | -8.0073E-05 | -6.5670E-03 | 2.3907E-02 | 4.8690E-02 |
| 4 | 4.8690E-02 | 2.3907E-02 | -6.5671E-03 | -8.0094E-05 | 6.1030E-03 | 2.3023E-03 |
| 5 | 1.7200E-02 | 5.9122E-02 | 9.2672E-04 | 3.2142E-03 | 1.8764E-02 | 3.2142E-03 |
| 6 | 3.6101E-01 | 3.0303E-01 | -4.9940E-02 | 2.3023E-03 | 6.1031E-03 | -8.0092E-05 |
| 7 | 4.3351E-02 | 1.0101E-01 | -4.8624E-02 | 4.8690E-02 | 2.3907E-02 | -6.5671E-03 |
| 8 | 5.2577E-02 | 2.6463E-01 | 5.2577E-02 | 1.7200E-02 | 5.9122E-02 | 9.2668E-04 |
| 9 | -4.8624E-02 | 1.0101E-01 | 4.3351E-02 | 3.6101E-01 | 3.0303E-01 | -4.9940E-02 |
| 10 | -4.9940E-02 | 3.0303E-01 | 3.6101E-01 | 4.3351E-02 | 1.0101E-01 | -4.8625E-02 |
| 11 | 9.2672E-04 | 5.9122E-02 | 1.7200E-02 | 5.2576E-02 | 2.6463E-01 | 5.2577E-02 |
| 12 | -6.5671E-03 | 2.3907E-02 | 4.8690E-02 | -4.8624E-02 | 1.0101E-01 | 4.3351E-02 |

UNIT OF THE RESEARCH AND DEVELOPMENT DEPARTMENT OF THE IAEA

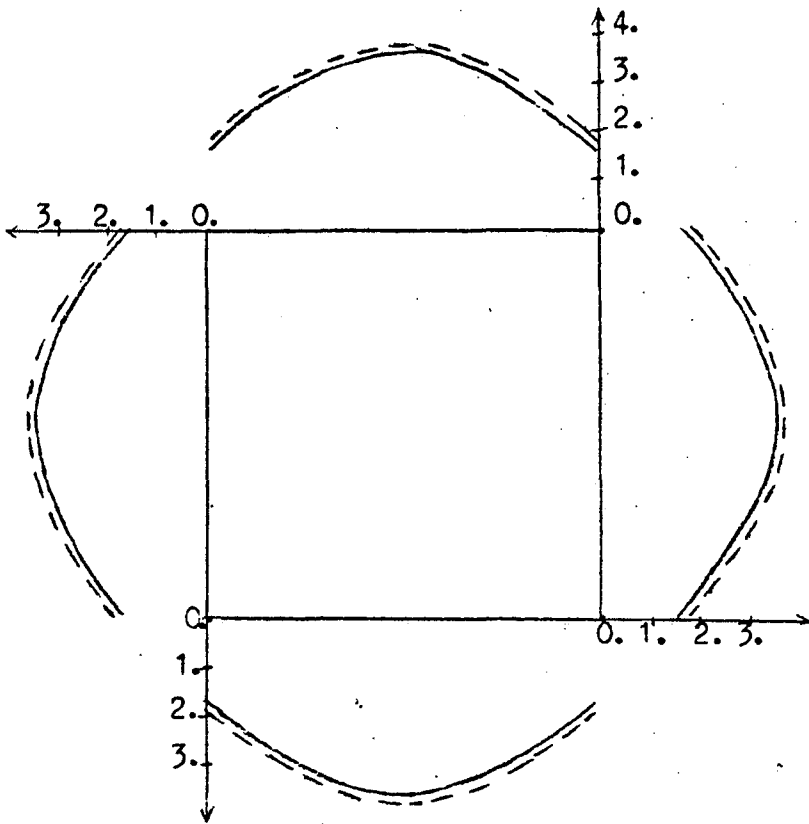
Table 4.2 - R_n^s for 2D-IAEA benchmark problem⁽⁴⁷⁾ (zone 1, group 1) in quadratic basis functions $\Psi_k(\underline{r}_g)$, $k=1, \dots, 12$, and $\Psi_l(\underline{r}), l=1, \dots, 8$.

| | J = 1 | 2 | 3 | 4 | 5 | 6 | 7 | 8 |
|-----|-------------|------------|-------------|------------|------------|-------------|------------|-------------|
| I=1 | 6.3409E-01 | 5.0921E-01 | -2.4938E-01 | 9.2104E-01 | 7.9575E-02 | -2.1498E-01 | 2.0479E-01 | -9.3158E-02 |
| 2 | -2.9444E-01 | 2.2488E+00 | -2.9444E-01 | 1.1206E+00 | 1.1206E+00 | -4.5290E-01 | 7.4402E-01 | -4.5290E-01 |
| 3 | -2.4938E-01 | 5.0922E-01 | 6.3409E-01 | 7.9579E-02 | 9.2105E-01 | -9.3160E-02 | 2.0479E-01 | -2.1499E-01 |
| 4 | -2.1498E-01 | 9.2104E-01 | 6.3409E-01 | 2.0479E-01 | 5.0921E-01 | -9.3158E-02 | 7.9575E-02 | -2.4938E-01 |
| 5 | -4.5290E-01 | 1.1206E+00 | -2.9444E-01 | 7.4403E-01 | 2.2488E+00 | -4.5290E-01 | 1.1206E+00 | -2.9444E-01 |
| 6 | -9.3160E-02 | 7.9579E-02 | -2.4938E-01 | 2.0479E-01 | 5.0922E-01 | -2.1499E-01 | 9.2105E-01 | 6.3409E-01 |
| 7 | -9.3158E-02 | 2.0479E-01 | -2.1498E-01 | 7.9574E-02 | 9.2104E-01 | -2.4938E-01 | 5.0921E-01 | 6.3409E-01 |
| 8 | -4.5291E-01 | 7.4403E-01 | -4.5291E-01 | 1.1206E+00 | 1.1206E+00 | -2.9444E-01 | 2.2488E+00 | -2.9444E-01 |
| 9 | -2.1499E-01 | 2.0479E-01 | -9.3159E-02 | 9.2105E-01 | 7.9576E-02 | 6.3409E-01 | 5.0922E-01 | -2.4938E-01 |
| 10 | -2.4938E-01 | 7.9578E-02 | -9.3160E-02 | 5.0921E-01 | 2.0479E-01 | 6.3409E-01 | 9.2104E-01 | -2.1499E-01 |
| 11 | -2.9444E-01 | 1.1206E+00 | -4.5290E-01 | 2.2488E+00 | 7.4403E-01 | -2.9444E-01 | 1.1206E+00 | -4.5290E-01 |
| 12 | 6.3410E-01 | 9.2105E-01 | -2.1499E-01 | 5.0921E-01 | 2.0479E-01 | -2.4938E-01 | 7.9576E-02 | -9.3159E-02 |



— coarse mesh with 4 subdomains(2x2)
 ---- coarse mesh with 16 subdomains(4x4)

Fig. 4.4 Outward partial currents due to the constant inward partial current on the bottom.(a)cubic elements,(b)quadratic elements.(arbitrary units)



——— coarse mesh with 4 subdomains(2x2)
 - - - - coarse mesh with 16 subdomains(4x4)

Fig. 4.5 Outward partial currents(arbitrary units) due to the constant source within the coarse mesh.(both quadratic and cubic elements yield almost same results)

results using quadratic and cubic elements are almost coincident, because the outward partial current due to an isotropic uniform source is not expected to be a sensitive function of spatial position.

The basis functions $\psi_m^h(\Omega)$ and $\psi_{sm_i}^h(\Omega)$ are chosen as quadratic elements, and the degree of approximation is varied by changing the number of subdomains in the coarse mesh Ω_m .

4.2. Inner Iterations Scheme

The one-group global response matrix equations for the reactor problem were given by equations (2.16), (2.17), and (2.18), which for convenience are rewritten below as

$$\underline{J}^+ = \underline{R}^{\underline{J}^-} \cdot \underline{J}^- + \underline{R}^{\underline{S}} \cdot \underline{S} \quad (4.1)$$

$$\underline{J}^- = \underline{H} \cdot \underline{J}^+ \quad (4.2)$$

$$\underline{\Phi} = \underline{M}^{\underline{J}^-} \cdot \underline{J}^- + \underline{M}^{\underline{S}} \cdot \underline{S} \quad (4.3)$$

For a given source \underline{S} , an iterative scheme used to determine either \underline{J}^+ or \underline{J}^- is termed an inner iterations scheme. A convenient form for the inner iterations scheme is obtained by inserting equation (4.2) into (4.1), yielding

$$\underline{J}^+ = \underline{R}^{\underline{J}^-} \cdot \underline{H} \cdot \underline{J}^+ + \underline{R}^{\underline{S}} \cdot \underline{S} \quad (4.4)$$

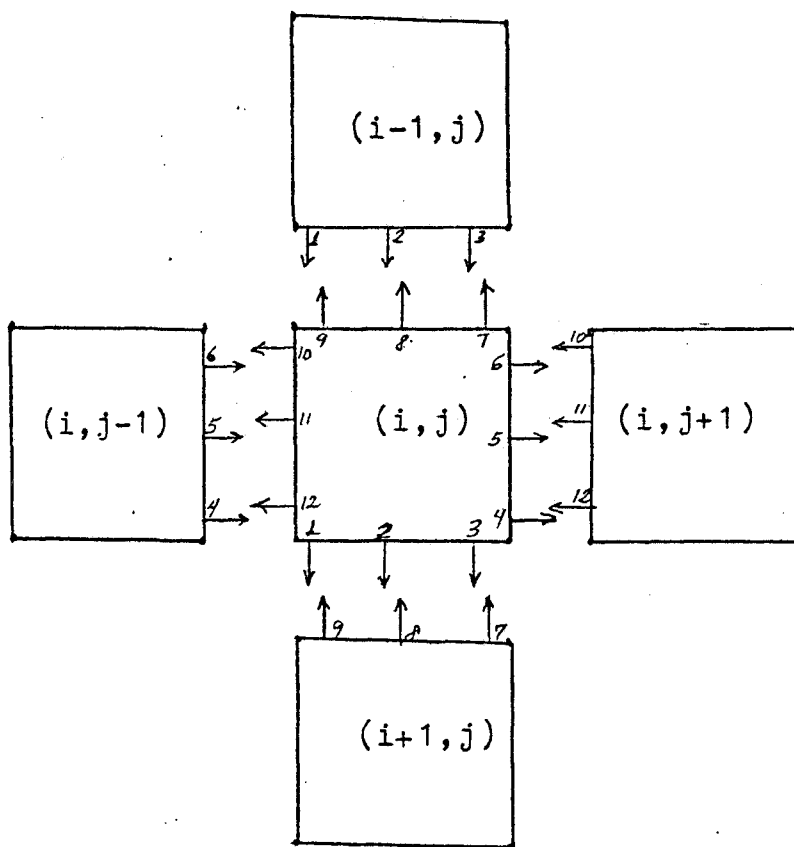


Fig. 4.6 - Coarse mesh ordering and outward partial currents, represented by arrows, for quadratic elements.

In rectangular geometry it is convenient to change the subscripts of the coarse meshes Ω_m , $n=1, \dots, N$, to (i, j) , $i=1, \dots, i_{\max}$; $j=1, \dots, j_{\max}$, such that a coarse mesh $\Omega(i, j)$ and its neighbors $\Omega(i \pm 1, j \pm 1)$ can be ordered as illustrated in Figure 4.6.

With this transformation the permutation matrix $\underline{\underline{H}}$ can be represented by the following algorithm,

$$\begin{aligned} \underline{\underline{J}}(i, j) = & \underline{\underline{T}}_1 \cdot \underline{\underline{J}}^+(i+1, j) + \underline{\underline{T}}_2 \cdot \underline{\underline{J}}^+(i, j+1) \\ & + \underline{\underline{T}}_3 \cdot \underline{\underline{J}}^+(i-1, j) + \underline{\underline{T}}_4 \cdot \underline{\underline{J}}^+(i, j-1) \end{aligned} \quad (4.5)$$

, $i=1, \dots, i_{\max}$; $j=1, \dots, j_{\max}$,

where $\underline{\underline{J}}^+(i, j) = \text{col}(\underline{\underline{J}}_1^+(i, j), \underline{\underline{J}}_2^+(i, j), \dots, \underline{\underline{J}}_{i_2}^+(i, j))$,

$$\underline{\underline{T}}_1 = \begin{bmatrix} 0 & 0 & \underline{\underline{P}} & 0 \\ 0 & 0 & 0 & 0 \\ 0 & 0 & 0 & 0 \\ 0 & 0 & 0 & 0 \end{bmatrix}$$

$$\underline{\underline{T}}_2 = \begin{bmatrix} 0 & 0 & 0 & 0 \\ 0 & 0 & 0 & \underline{\underline{P}} \\ 0 & 0 & 0 & 0 \\ 0 & 0 & 0 & 0 \end{bmatrix}$$

$$\underline{\underline{T}}_3 = \begin{bmatrix} 0 & 0 & 0 & 0 \\ 0 & 0 & 0 & 0 \\ \underline{\underline{P}} & 0 & 0 & 0 \\ 0 & 0 & 0 & 0 \end{bmatrix}$$

$$\underline{\underline{T}}_4 = \begin{bmatrix} 0 & 0 & 0 & 0 \\ 0 & 0 & 0 & 0 \\ 0 & 0 & 0 & 0 \\ 0 & \underline{\underline{P}} & 0 & 0 \end{bmatrix}$$

$$\underline{\underline{P}} = \begin{pmatrix} 0 & 0 & 1 \\ 0 & 1 & 0 \\ 1 & 0 & 0 \end{pmatrix} \quad \text{for quadratic elements,}$$

and for boundary coarse mesh $\Omega(i,j)$ the boundary conditions are explicitly included in the calculational scheme by assessing values for some of the elements of the inward partial current $\underline{J}^-(i,j)$ (e.g., $J_k^-(i,j)=0$ for vacuum boundary conditions, where k is a node on the boundary of the reactor).

The inner iterations scheme represented by the equation (4.4) can be given by the algorithm

$$\underline{J}^+(i,j) = \underline{\underline{R}}^{\bar{J}}(i,j) \cdot \left[\underline{\underline{T}}_1 \cdot \underline{J}^+(i+1,j) + \underline{\underline{T}}_2 \cdot \underline{J}^+(i,j+1) \right. \quad (4.6)$$

$$\left. + \underline{\underline{T}}_3 \cdot \underline{J}^+(i-1,j) + \underline{\underline{T}}_4 \cdot \underline{J}^+(i,j-1) \right] + \underline{\underline{R}}^S(i,j) \cdot \underline{S}(i,j),$$

$$i=1, \dots, i_{\max}; j=1, \dots, j_{\max}.$$

Explicit representation of the Jacobi matrix equation is shown in Figure 4.7. From the graph theory⁽²⁾, the matrix can be seen to be a consistently ordered 2-cyclic block-Jacobi matrix; hence Gauss-Seidel iteration will converge twice as fast as block-Jacobi iteration.⁽²⁾

Therefore the iterative scheme adopted in the present investigation is the Gauss-Seidel method which may be represented by the following algorithm

$$\begin{aligned}
 \underline{J}^+(i,j)^{(t)} &= \underline{R}^{\underline{J}^-}(i,j) \cdot \left[\underline{T}_1 \cdot \underline{J}^+(i+1,j)^{(t-1)} + \underline{T}_2 \cdot \underline{J}^+(i,j+1)^{(t-1)} \right. \\
 &\quad \left. + \underline{T}_3 \cdot \underline{J}^+(i-1,j)^{(t)} + \underline{T}_4 \cdot \underline{J}^+(i,j-1)^{(t)} \right] \\
 &\quad + \underline{R}^s(i,j) \cdot \underline{S}(i,j) \quad , t=1,2,3,\dots
 \end{aligned} \tag{4.7}$$

where it is assumed that the progression through the mesh is to the right and down (see Fig. 4.6). Other progressions are readily treated.

4.3. Outer Iterations and Acceleration Schemes

The specific application of the finite element response matrix method is the solution of the two-group diffusion equation, assuming a fission source only in group 1,

$$\left\{ \begin{aligned}
 -\nabla D^1(\underline{r}) \nabla \Phi^1(\underline{r}) + (\Sigma_a^1(\underline{r}) + \Sigma_{s1}(\underline{r})) \Phi^1(\underline{r}) &= \\
 \frac{1}{k} (\nu^1 \Sigma_f^1(\underline{r}) \Phi^1(\underline{r}) + \nu^2 \Sigma_f^2(\underline{r}) \Phi^2(\underline{r})) &= s_1(\underline{r}) \\
 -\nabla D^2(\underline{r}) \nabla \Phi^2(\underline{r}) + \Sigma_a^2(\underline{r}) \Phi^2(\underline{r}) &= \Sigma_{s1}(\underline{r}) \Phi^1(\underline{r}) - s_2(\underline{r})
 \end{aligned} \right. \tag{4.8}$$

where $\Sigma_{s1}(\underline{r})$ is the down-scattering cross section,
 $\Sigma_f^g(\underline{r})$ is the fission cross section for group g ,
 ν^g is the number of neutrons generated per fission event in group g ,

and k_{eff} is the eigenvalue to be determined.

The formulation of the response matrix method used in the present investigation is based on the assumption that the source term comprises all types of neutron sources. Therefore the response matrices are generated by considering

$$S^1(\underline{r}) = \frac{1}{k_{eff}} \left(\nu \Sigma_f^1(\underline{r}) \Phi^1(\underline{r}) + \nu^2 \Sigma_f^2(\underline{r}) \Phi^2(\underline{r}) \right)$$

as the source for group 1, and

$$S^2(\underline{r}) = \Sigma_{21}(\underline{r}) \Phi^1(\underline{r})$$

as the source for group 2, such that the coupled equation (4.8) can be considered as being composed of two fixed source problems connected to each other by source terms.

The solution for a fixed source problem has already been obtained in equation (4.7), where the outward partial currents \underline{J}^+ due to a specified source distribution \underline{S} are obtained with inner iterations. The neutron flux is obtained by the equation (2.18) as

$$\underline{\Phi}^g = \underline{M}_g^J \cdot \underline{J}^{g+} + \underline{M}_g^S \cdot \underline{S}^g, \quad g=1,2,$$

where $\underline{\Phi}^g$ is the expansion coefficients for the global flux $\Phi^g(\underline{r})$.

The eigenvalue problem (4.8) can then be solved by the power method⁽²⁻⁴⁾ with an iterative scheme known as outer iterations or source iterations⁽⁵⁰⁾, which is given by the algorithm (the outer iteration)

Step 1 - Guess $k_{eff}^{(0)}$, $\Phi^{1(0)}(\Omega)$ and $\Phi^{2(0)}(\Omega)$ and compute

$$S^{1(0)}(\Omega) = \frac{1}{k_{eff}^{(0)}} \left(\nu^1 \sum_j^1(\Omega) \Phi^{1(0)}(\Omega) + \nu^2 \sum_j^2(\Omega) \Phi^{2(0)}(\Omega) \right),$$

Step 2 - Solve the fixed source problem for group 1,
(the inner iteration)

$$-\nabla D^1(\Omega) \nabla \Phi^{1(t)}(\Omega) + \left(\Sigma_a^1(\Omega) + \Sigma_{21}(\Omega) \right) \Phi^{1(t)}(\Omega) = S^{1(t-1)}(\Omega),$$

Step 3 - Calculate the source for group 2,

$$S^{2(t)}(\Omega) = \Sigma_{21}(\Omega) \Phi^{1(t)}(\Omega),$$

Step 4 - Solve the fixed source problem for group 2,
(inner iterations)

$$-\nabla D^2(\Omega) \nabla \Phi^{2(t)}(\Omega) + \Sigma_a^2(\Omega) \Phi^{2(t)}(\Omega) = S^{2(t)}(\Omega)$$

Step 5 - Estimate the new eigenvalue,

$$k_{eff}^{(t)} = k_{eff}^{(t-1)} \frac{\int_{\Omega} [\nu^1 \Sigma_f^1(\Omega) \Phi^1(\Omega) + \nu^2 \Sigma_f^2(\Omega) \Phi^2(\Omega)] d\Omega}{\int_{\Omega} [\nu^1 \Sigma_f^1(\Omega) \Phi^1(\Omega) + \nu^2 \Sigma_f^2(\Omega) \Phi^2(\Omega)] d\Omega}$$

Step 6 - Estimate the new source for group 1,

$$S^1(\Omega) = \frac{1}{k_{eff}^{(t)}} [\nu^1 \Sigma_f^1(\Omega) \Phi^1(\Omega) + \nu^2 \Sigma_f^2(\Omega) \Phi^2(\Omega)]$$

and iterate, $t=1,2,3,\dots$, from step 1 through step 6 until the solutions $\Phi^1(\Omega), \Phi^2(\Omega)$ and $k^{(t)}$ satisfy the required convergence criteria.

The matrix representation of the algorithm is presented in Appendix I.

In order to accelerate the convergence rate of outer iterations two acceleration schemes were considered: the asymptotic source extrapolation method⁽⁵¹⁾ and the Chebyshev polynomial method.^(52,53) Both methods are described in Appendix I. To test the relative merits of these methods, a two-dimensional 2D-IAEA benchmark problem⁽⁴⁷⁾ was solved applying the acceleration schemes to the finite element response matrix method.

Plotted in Figure 4.8 are the results obtained with the asymptotic source extrapolation method along with the results obtained without accelerating the outer iterations. The number of outer iterations is decreased, but

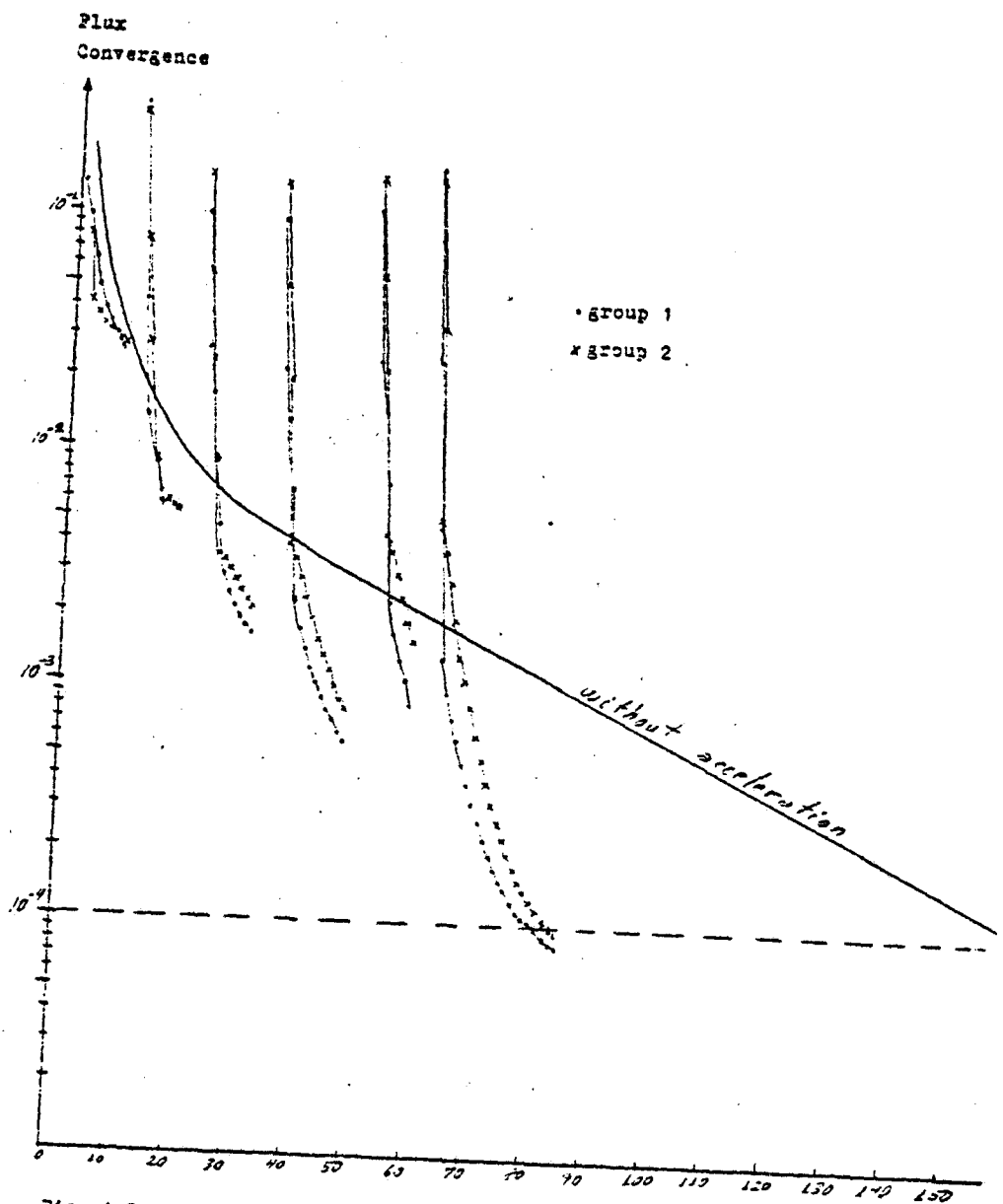


Fig. 4.3 -Acceleration of outer iterations with asymptotic source extrapolation method.

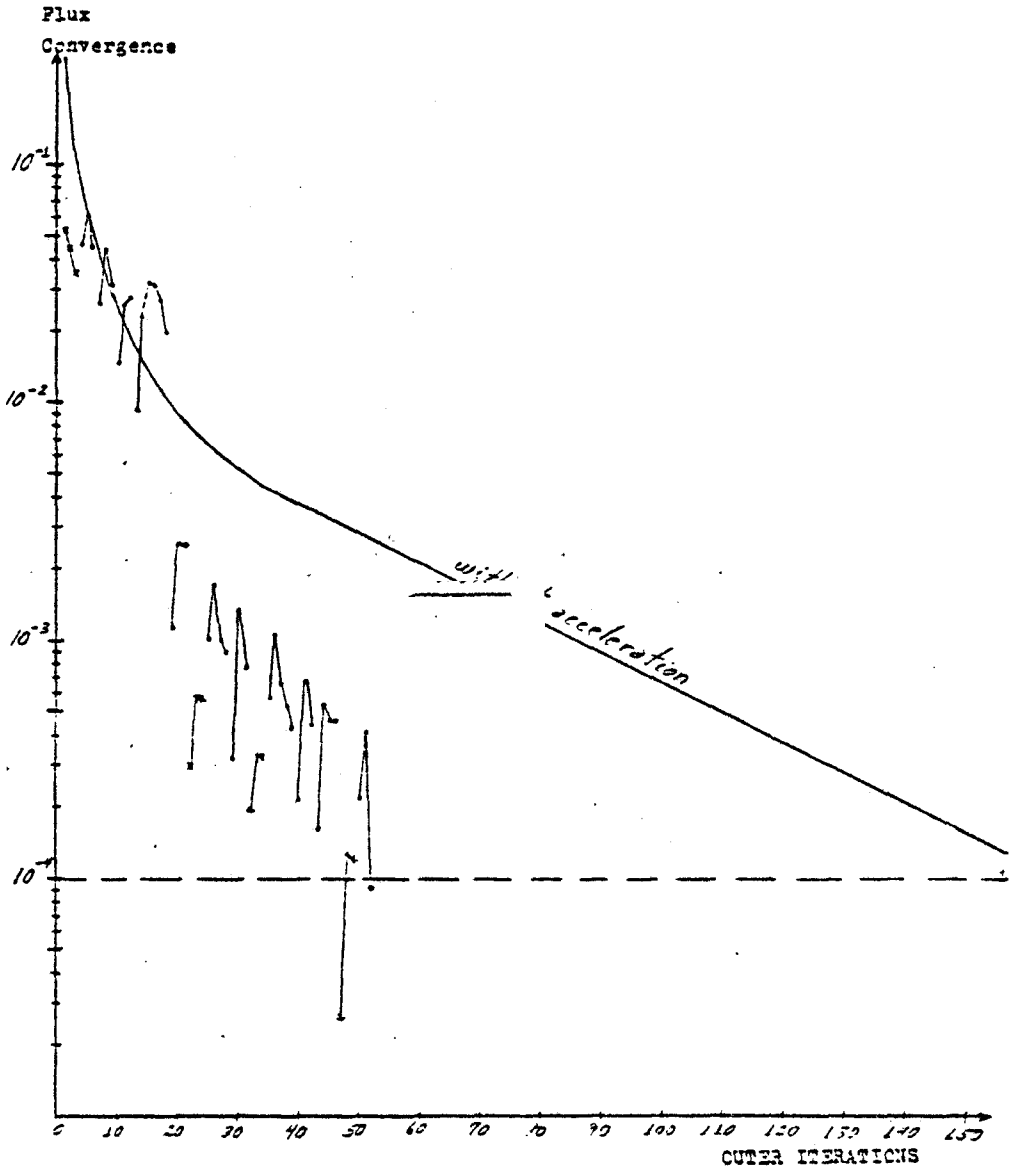


Fig. 4.9 - Acceleration of outer iterations with Chebyshev polynomial method.

the number of inner iterations per outer iteration increases due to the extra inner iterations needed in order to reach the asymptotic convergence behavior, and the total computational time is increased.

A similar comparison of the Chebyshev polynomial method results with the results obtained without acceleration is shown in Figure 4.9. In this case the number of outer iterations in the accelerated calculations is decreased without the increase in the number of inner iterations per outer iteration observed with the asymptotic source extrapolation method. The net result is that the overall computational time is effectively shortened by about a factor of 2.

Therefore, the Chebyshev polynomial method was chosen to accelerate the outer iterations in the finite element response matrix method.

CHAPTER 5

EVALUATION OF THE FINITE ELEMENT RESPONSE MATRIX METHOD

The evaluation of the finite element response matrix method was performed by application to two types of reactor problems: a fixed source problem and two eigenvalue problems.

The fixed source problem consists of an idealized bare homogeneous core, and the eigenvalue problems are two benchmark problems that have been used for testing various coarse mesh methods.

The computations were performed with the Amdahl-470/V8 computer at the Computing Center at The University of Michigan.

5.1 Fixed Source Program

The simplified reactor used for the fixed source calculations is a 200cm x 200cm bare uniform core composed of materials typical of a light water reactor.⁽⁵⁰⁾ A constant neutron source was imposed and only one energy group was utilized. (The one-group constants are shown in Appendix IV).

It is recognized that a bare uniform reactor is only of academic interest and should not be used in a test of

a coarse mesh method; however, the main objective of this effort is to investigate the effects of varying several of the computational parameters, such as the convergence criteria for the inner iterations, the maximum number of inner iterations, the degree of polynomial approximations for the partial currents, and the number of subdomains in a coarse mesh. Experience gained from these parameter variations may then be utilized in the more practical benchmark problem calculations. The exact analytical solution for the bare uniform reactor obtained by Fourier series expansion is taken as the reference solution for the comparison of the results.

The partial currents in the reactor (global) calculation were approximated by quadratic and cubic polynomials and the basis functions used to generate the response matrices in the assembly (local) calculations for the coarse meshes are chosen to be quadratic polynomials. Various degrees of approximations are obtained by varying the number of subdomains in a coarse mesh. Two coarse mesh dimensions were considered, 20cm x 20cm and 10cm x 10cm, and summaries of the calculations are succinctly presented in Table 5.1 and Table 5.2, respectively.

The neutron flux distribution, illustrated in Figure 5.1, displays a noticeable discontinuity at $x=80\text{cm}$, although in the rest of the core the neutron flux calculated by the present method agrees very well with the

Table 5.1 - Bare homogeneous core calculation (fixed source problem) with 20cmx20cm coarse meshes.

 ϕ^- = neutron flux at X=80cm in the right coarse mesh. ϕ^+ = neutron flux at X=80cm in the left coarse mesh.

| partial current | ξ_j | number of subdomains | inner iterations | CPU (sec) | | Y = 0 | | | Y = X | | |
|---------------------|---------|----------------------|------------------|------------------|-------|----------|----------|-----------------|----------|----------|-----------------|
| | | | | inner iterations | total | ϕ^- | ϕ^+ | ϕ^-/ϕ^+ | ϕ^- | ϕ^+ | ϕ^-/ϕ^+ |
| | | | | | | | | | | | |
| QUADRATIC | .05 | 1x1 | 4 | .034 | .110 | .946 | .935 | 1.012 | .901 | .864 | 1.043 |
| | .05 | 2x2 | 3 | .025 | .152 | .940 | .920 | 1.022 | .883 | .823 | 1.073 |
| | .05 | 3x3 | 3 | .025 | .296 | .936 | .916 | 1.022 | .875 | .815 | 1.074 |
| | .05 | 4x4 | 3 | .025 | .658 | .934 | .914 | 1.022 | .872 | .812 | 1.075 |
| CUBIC | .05 | 1x1 | 4 | .057 | .171 | .946 | .935 | 1.012 | .901 | .864 | 1.043 |
| | .05 | 2x2 | 4 | .054 | .257 | .921 | .925 | .996 | .852 | .852 | 1.000 |
| | .05 | 3x3 | 3 | .042 | .456 | .932 | .936 | .996 | .867 | .864 | 1.003 |
| | .05 | 4x4 | 3 | .042 | .903 | .931 | .935 | .996 | .866 | .863 | 1.003 |
| QUADRATIC | .01 | 1x1 | 6 | .048 | .122 | .932 | .920 | 1.013 | .879 | .842 | 1.043 |
| | .01 | 2x2 | 6 | .048 | .176 | .914 | .892 | 1.025 | .844 | .783 | 1.077 |
| | .01 | 3x3 | 6 | .047 | .321 | .910 | .888 | 1.025 | .838 | .777 | 1.079 |
| | .01 | 4x4 | 6 | .048 | .667 | .909 | .887 | 1.025 | .835 | .775 | 1.077 |
| CUBIC | .01 | 1x1 | 6 | .079 | .189 | .932 | .920 | 1.013 | .879 | .843 | 1.043 |
| | .01 | 2x2 | 6 | .080 | .284 | .908 | .912 | .996 | .834 | .833 | 1.001 |
| | .01 | 3x3 | 6 | .081 | .497 | .906 | .909 | .997 | .830 | .825 | 1.006 |
| | .01 | 4x4 | 6 | .080 | .938 | .905 | .908 | .997 | .829 | .824 | 1.006 |
| QUADRATIC | .001 | 1x1 | 10 | .079 | .156 | .924 | .913 | 1.012 | .869 | .832 | 1.044 |
| | .001 | 2x2 | 10 | .078 | .205 | .907 | .885 | 1.025 | .836 | .775 | 1.079 |
| | .001 | 3x3 | 10 | .077 | .348 | .904 | .882 | 1.025 | .830 | .769 | 1.079 |
| | .001 | 4x4 | 10 | .079 | .711 | .903 | .881 | 1.025 | .828 | .768 | 1.078 |
| CUBIC | .001 | 1x1 | 10 | .131 | .244 | .924 | .913 | 1.012 | .869 | .832 | 1.044 |
| | .001 | 2x2 | 10 | .129 | .331 | .902 | .905 | .997 | .826 | .824 | 1.002 |
| | .001 | 3x3 | 10 | .129 | .541 | .900 | .902 | .998 | .822 | .818 | 1.005 |
| | .001 | 4x4 | 10 | .132 | 1.008 | .899 | .902 | .997 | .822 | .817 | 1.006 |
| Analytical Solution | | | | | | .9004 | .9004 | | .8217 | .8217 | |

Table 5.2 - Bare homogeneous core calculation (fixed source problem) with 10cmx10cm coarse meshes.

 ϕ^- = neutron flux at X=80cm in the right coarse mesh. ϕ^+ = neutron flux at X=80cm in the left coarse mesh.

| partial current | ϵ_j | number of subdomains | inner iterations | CPU(sec) | | Y = 0 | | | Y = X | | |
|---------------------|--------------|----------------------|------------------|-----------------|-------|----------|----------|-----------------|----------|----------|-----------------|
| | | | | inner iteration | total | ϕ^- | ϕ^+ | ϕ^-/ϕ^+ | ϕ^- | ϕ^+ | ϕ^-/ϕ^+ |
| | | | | | | | | | | | |
| QUADRATIC | .05 | 1x1 | 5 | .149 | .259 | .936 | .935 | 1.001 | .878 | .876 | 1.002 |
| | .05 | 2x2 | 4 | .120 | .284 | .942 | .940 | 1.002 | .883 | .882 | 1.001 |
| | .05 | 3x3 | 4 | .121 | .434 | .940 | .939 | 1.001 | .880 | .879 | 1.001 |
| | .05 | 4x4 | 4 | .120 | .775 | .939 | .939 | 1.000 | .878 | .878 | 1.000 |
| CUBIC | .05 | 1x1 | 5 | .249 | .412 | .936 | .935 | 1.001 | .878 | .876 | 1.002 |
| | .05 | 2x2 | 4 | .204 | .461 | .941 | .941 | 1.000 | .882 | .884 | .998 |
| | .05 | 3x3 | 4 | .205 | .667 | .939 | .940 | .999 | .879 | .881 | .998 |
| | .05 | 4x4 | 4 | .204 | 1.127 | .938 | .940 | .998 | .879 | .881 | .998 |
| QUADRATIC | .01 | 1x1 | 8 | .233 | .341 | .916 | .914 | 1.002 | .847 | .843 | 1.005 |
| | .01 | 2x2 | 7 | .204 | .367 | .915 | .913 | 1.002 | .841 | .838 | 1.004 |
| | .01 | 3x3 | 7 | .204 | .512 | .913 | .911 | 1.002 | .839 | .836 | 1.004 |
| | .01 | 4x4 | 7 | .204 | .860 | .912 | .911 | 1.001 | .838 | .835 | 1.004 |
| CUBIC | .01 | 1x1 | 8 | .388 | .552 | .916 | .914 | 1.002 | .847 | .843 | 1.005 |
| | .01 | 2x2 | 7 | .341 | .599 | .914 | .914 | 1.000 | .840 | .841 | .999 |
| | .01 | 3x3 | 7 | .343 | .813 | .912 | .913 | .999 | .838 | .839 | .999 |
| | .01 | 4x4 | 7 | .343 | 1.264 | .912 | .912 | 1.000 | .837 | .838 | .999 |
| QUADRATIC | .001 | 1x1 | 14 | .401 | .509 | .906 | .904 | 1.002 | .834 | .830 | 1.005 |
| | .001 | 2x2 | 13 | .373 | .537 | .902 | .899 | 1.003 | .825 | .820 | 1.006 |
| | .001 | 3x3 | 13 | .373 | .686 | .901 | .898 | 1.002 | .824 | .819 | 1.006 |
| | .001 | 4x4 | 13 | .373 | 1.037 | .901 | .898 | 1.002 | .823 | .819 | 1.005 |
| CUBIC | .001 | 1x1 | 14 | .669 | .835 | .906 | .904 | 1.002 | .834 | .830 | 1.005 |
| | .001 | 2x2 | 13 | .622 | .881 | .901 | .901 | 1.000 | .824 | .823 | 1.001 |
| | .001 | 3x3 | 13 | .622 | 1.095 | .900 | .900 | 1.000 | .823 | .822 | 1.001 |
| | .001 | 4x4 | 13 | .622 | 1.545 | .900 | .900 | 1.000 | .822 | .822 | 1.000 |
| Analytical Solution | | | | | | .9004 | .9004 | | .8217 | .8217 | |

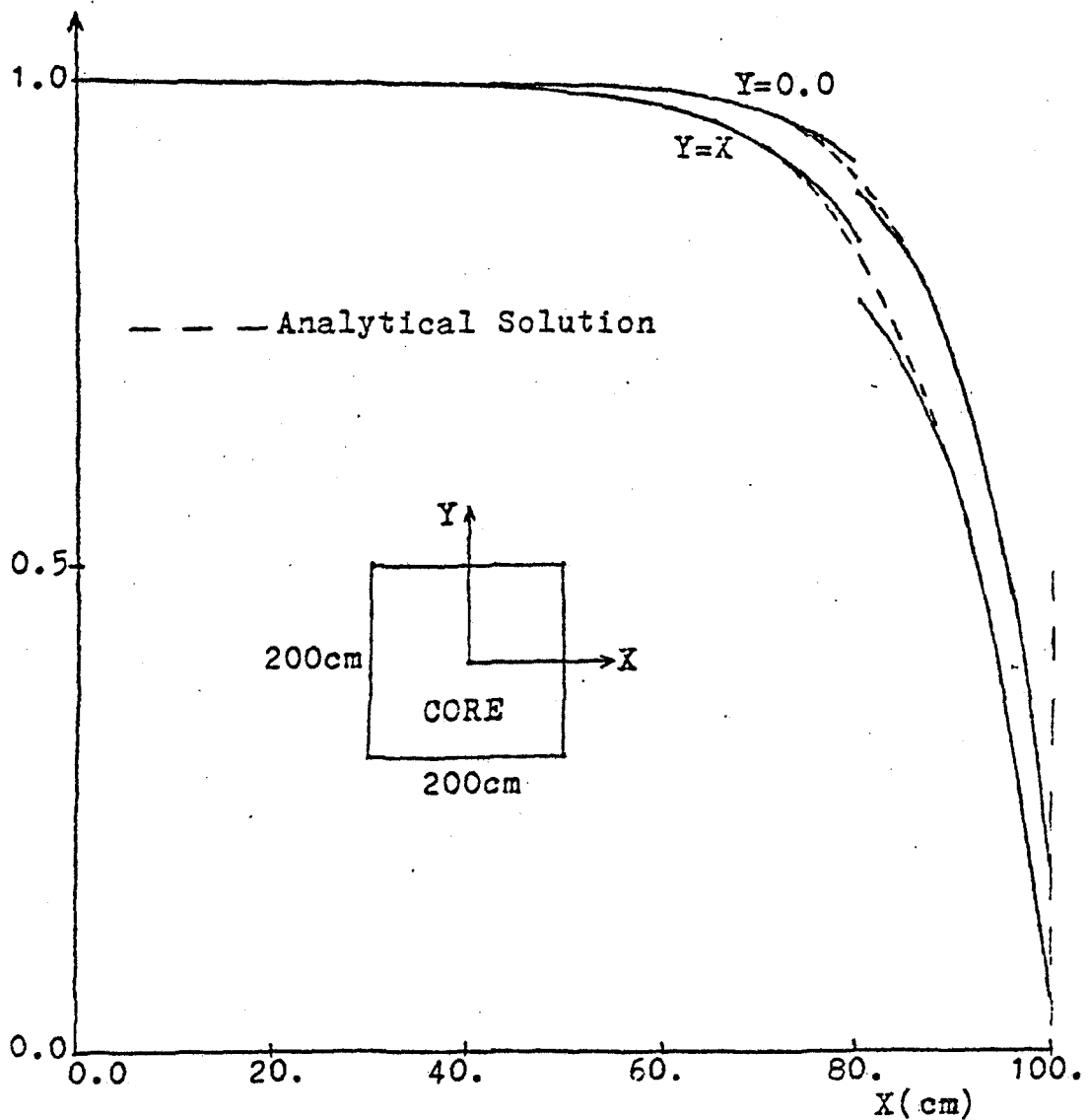


Fig. 5.1 - Neutron flux distribution in a bare homogeneous core calculated with quadratic partial currents. (20cmx20cm coarse mesh, $\epsilon_J = .01$, 3x3 subdomains).

analytic solutions. One of the factors contributing to this discontinuity is the assumption of the response matrix method itself, which is based on the continuity of the partial currents across the coarse meshes but not on the continuity of the neutron fluxes.

When cubic polynomials are used for the partial currents the discontinuity is less pronounced than that with quadratic polynomials, and for both approximations the discontinuity decreases by increasing the number of subdomains in the coarse mesh. From the results observed in Table 5.1 and Table 5.2 the division of the coarse mesh in 9 subdomains (3x3) can be considered sufficiently fine since it yields results almost coincident to the results obtained with division in 16 subdomains (4x4).

The convergence criterion for the partial currents, $\mathcal{E}_J = .01$, yields results comparable to the results obtained with $\mathcal{E}_J = .001$, such that after approximately 6 inner iterations the results are almost converged to the results obtained with 10 inner iterations, in the calculations with 20cm x 20cm coarse meshes.

From the above results, the inner iterations parameters to be used in the eigenvalue problems (with outer and inner iterations) can be estimated as:

- a) the initial (first outer iteration) limit for the number of inner iterations should be approximately 5,

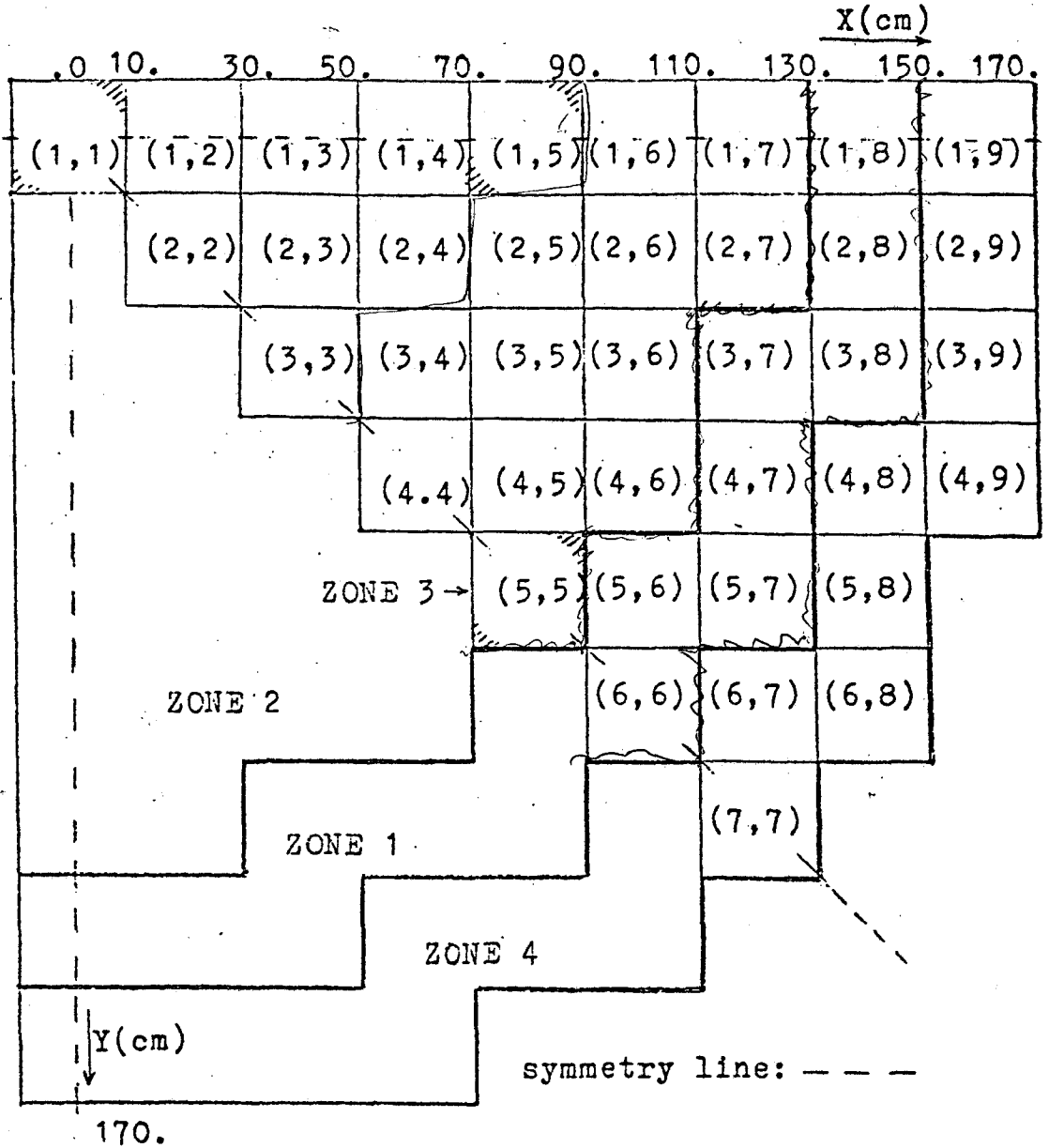
- b) the initial (first outer iterations) limit for the convergence criterion for partial currents should be approximately $\epsilon_J = .01$,
- c) at least two inner iterations (in opposite sweeping directions) should be performed for each outer iteration ,
- d) the number of subdomains for each coarse mesh should be about 9 (3x3).

5.2 Eigenvalue Problem

The evaluation of the finite element response matrix method for more realistic configurations was performed by applying the method to two benchmark problems: the 2D-IAEA benchmark problem⁽⁴⁷⁾ and a Biblis benchmark problem.⁽⁵⁶⁾

5.2.1 2D-IAEA Benchmark Calculation

The 2D-IAEA benchmark problem⁽⁴⁷⁾ is an idealized pressurized water reactor (PWR) problem with zone loading and a pure water reflector as illustrated in Figure 5.2 (diffusion parameters and cross sections are shown in Appendix IV). This problem was defined by participants of the 1971 IAEA panel on burn-up physics⁽⁵⁷⁾ and the objective was to provide a convenient common basis for verifying new methods and for comparing the relative merits of various calculational methods of solution.



Upper octant: fuel assembly identification

Lower octant: zone assignments

External boundaries: zero incident current

Symmetry boundaries: zero net current

Fig. 5.2 - 2D-IAEA benchmark problem.(47)

Reference solutions obtained with a fine mesh VENTURE⁽⁵⁸⁾ calculation, which is a mesh-centered finite difference code, and a fine mesh PDQ-7⁽¹⁾ calculation, which is a mesh-cornered finite difference code, agree to within only 2% in assembly-averaged power distribution⁽¹⁸⁾, as illustrated in Figure 5.3. For the evaluation of the present method, however, the VENTURE solution is chosen as reference solution. One reason is that several VENTURE calculations were made and the reference solution was obtained by the Richardson extrapolation method and secondly because the mesh-centered scheme is considered by some investigators to be slightly more accurate than the mesh-cornered schemes.⁽¹⁸⁾ The computational time for the VENTURE calculations is presented in Table 5.3.

Table 5.3 Computational time required for VENTURE calculation⁽¹⁷⁾ (with IBM 360/91) for different mesh sizes. ($\Delta P/P$ is the relative deviation of assembly averaged power distribution.)

| Mesh width (cm) | k_{eff} | maximum $ \Delta P/P $ (%) | CPU (sec) |
|--------------------|-------------------|----------------------------|-----------|
| 5 | 1.02924 .00020 | 13.9 | 19 |
| 2.5 ↓ 1.25 | 1.02944 .00010 | 5.2 | 204 |
| 1.25 ↓ .5833 | 1.02954 .00004 | 2.0 | 930 |
| 2/3 | 1.02958 | 0.32 | 4800 |
| extrapolated | 1.02960 | ref. solution | - |

2D IAEA Benchmark Problem

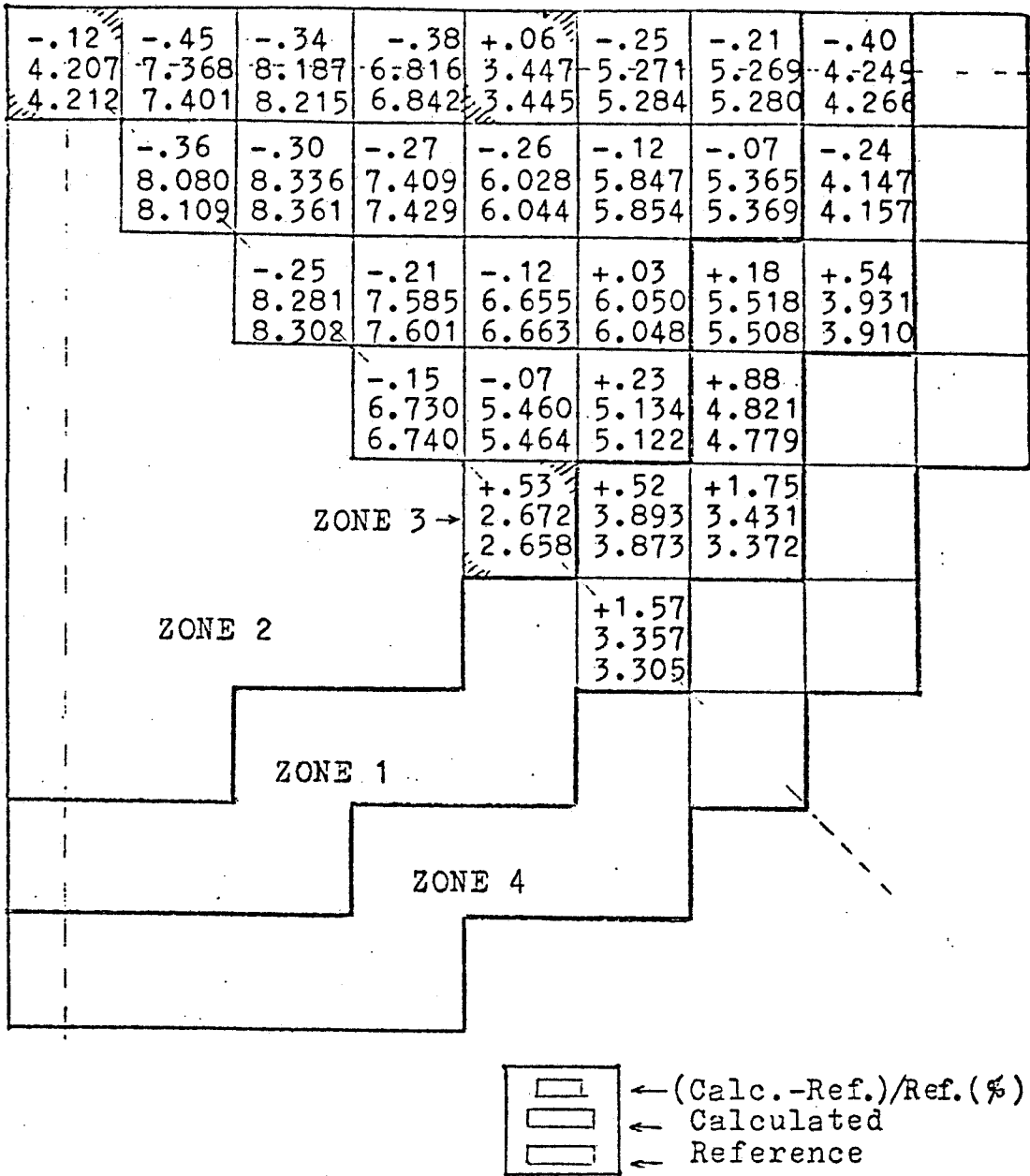





Fig.5.3 -2D-IAEA assembly averaged power distribution calculated with corner mesh fine mesh(1 cm) finite difference scheme(PDQ-7).
Reference:center mesh finite difference scheme(VENTURE) with Richardson extrapolation.

The results of the finite element response matrix method is presented below and for the rest of the presentation an abbreviated expression is used to describe the calculational approximation adopted for each computation. The notation "9/4 quadratic calculation" refers to quadratic approximations for the global flux and partial currents, performed with 4 coarse meshes per fuel assembly (2x2), using response matrices generated (in the local calculation) with 9 subdomains (3x3) for each coarse mesh.

Table 5.4 presents the computational time required to generate the response matrix for one unique assembly and it can be noted that the processing time required for quadratic and cubic calculations is of the same order.

Table 5.4 Computational time required for response matrix generation.

| current and flux approximation (global calculation) | number of subdomains | CPU (sec) |
|--|--|-----------|
| quadratic | 4  | .032 |
| | 9  <i>coarse mesh</i> | .118 |
| | 16  | .356 |
| cubic | 4 | .046 |
| | 9 | .147 |
| | 16 | .411 |

1/4 →

9/4

1 coarse mesh

0 coarse mesh

9/16 subdomains

1 elem. coarse

divided by 4

coarse mesh

coarse mesh

with coarse

9 subdomains

The convergence of the calculational scheme is measured by comparing the nodal values of the neutron fluxes in two successive outer iterations, and from the results shown in Table 5.5 one can expect that the convergence limit, ϵ_ϕ , of about 10^{-5} yields sufficiently converged results. As noted above, the convergence criterion for the partial currents in the global calculation was fixed at $\epsilon_J = .01$.

Table 5.5 Effect of convergence criterion ϵ_ϕ .

| Calculation | no. of outer iterations | ϵ_ϕ | CPU(sec) | k_{eff} | maximum $ \Delta P/P $ (%) |
|---------------|-------------------------|-----------------|----------|------------------|----------------------------|
| 16/1 cubic | 34 | 10^{-3} | 10.5 | 1.0297 | 3.54 |
| | 59 | 10^{-4} | 14.3 | 1.0298 | 1.39 |
| | 83 | 10^{-5} | 18.0 | 1.0298 | 1.16 |
| 4/1 quadratic | 23 | 10^{-3} | 3.5 | 1.0292 | 2.26 |
| | 51 | 10^{-4} | 5.9 | 1.0293 | 4.04 |
| | 64 | 10^{-5} | 7.1 | 1.0293 | 4.25 |

The summary of the 2D-IAEA benchmark calculations with the finite element response matrix method is presented in Table 5.6. One can conclude that with an increase in the number of subdomains for response matrix generation the solution converges faster and the results

Table 5.6 - Summary of 2D-IAEA benchmark calculations.
(Benchmark $k_{\text{eff}}=1.02960$)

| Calculation | No. of outer iterations | ϵ_{ϕ} | CPU (sec) | k_{eff} | maximum $ \Delta P /P(\%)$ |
|----------------|-------------------------------|----------------------|--------------|------------------|-------------------------------|
| 4/1 quadratic | 64 | $1. \times 10^{-5}$ | 7.1 | 1.0293 | 4.25 |
| | 51 | $1. \times 10^{-4}$ | 5.9 | 1.0293 | 4.04 |
| 9/1 quadratic | 66 | $1. \times 10^{-5}$ | 8.2 | 1.0296 | 1.76 |
| | 50 | $1. \times 10^{-4}$ | 6.6 | 1.0296 | 1.52 |
| 16/1 quadratic | 66 | $1. \times 10^{-5}$ | 10.2 | 1.0296 | .83 |
| | 42 | $1. \times 10^{-4}$ | 7.9 | 1.0296 | .54 |
| 9/4 quadratic | 150 | $3. \times 10^{-5}$ | 47.4 | 1.0295 | 1.41 |
| | 106 | $1. \times 10^{-4}$ | 34.8 | 1.0294 | 1.18 |
| 16/4 quadratic | 150 | $2. \times 10^{-5}$ | 49.8 | 1.0294 | .77 |
| | 90 | $1. \times 10^{-4}$ | 32.4 | 1.0293 | .26 |
| 4/1 cubic | 91 | $1. \times 10^{-5}$ | 16.3 | 1.0298 | 2.04 |
| | 72 | $1. \times 10^{-4}$ | 13.1 | 1.0298 | 1.83 |
| 9/1 cubic | 99 | $1. \times 10^{-5}$ | 18.3 | 1.0299 | 1.35 |
| | 64 | $1. \times 10^{-4}$ | 12.8 | 1.0299 | 1.47 |
| 16/1 cubic | 83 | $1. \times 10^{-5}$ | 18.0 | 1.0298 | 1.16 |
| | 59 | $1. \times 10^{-4}$ | 14.3 | 1.0298 | 1.39 |
| 9/4 cubic | 149 | $1. \times 10^{-5}$ | 82.9 | 1.0295 | .64 |
| | 93 | $1. \times 10^{-4}$ | 54.3 | 1.0295 | .65 |
| 16/4 cubic | 150 | 1.3×10^{-5} | 86.4 | 1.0294 | .26 |
| | 85 | $1. \times 10^{-4}$ | 53.9 | 1.0294 | .63 |

are improved. Better results are also obtained by increasing the number of coarse meshes per fuel assembly but with the penalty of increased computational time due to the slower convergence. The decrease in convergence rate with small mesh size is due to the fact that the spectral norm of the response matrix method increases with decreasing size of the coarse mesh (Appendix III). Examples of the assembly averaged power distribution are presented in Figure 5.4 and Figure 5.5, for 9/1 quadratic calculation and 9/1 cubic calculation, respectively.

The thermal neutron flux distribution in the core is illustrated in Figure 5.6 through Figure 5.9 for quadratic and cubic calculations, and compared with the detailed solution obtained with FEMB⁽⁴⁷⁾ (second order Lagrange polynomials in rectangular elements). The results of the quadratic calculation (Figure 5.6) indicate noticeable disagreement in the core-reflector region, due to the poor interpolation properties of the quadratic polynomials in large (20cmx20cm) coarse meshes. The cubic calculation (Figure 5.7) with identical coarse meshes indicates better agreement in the neutron flux distribution in the neighborhood of the reflector. The results of smaller coarse meshes (10cmx10cm) are in much better agreement with the detailed FEMB solutions, and for these smaller coarse meshes, the cubic calculation (Figure 5.9) results in better agreement than the quadratic calculation

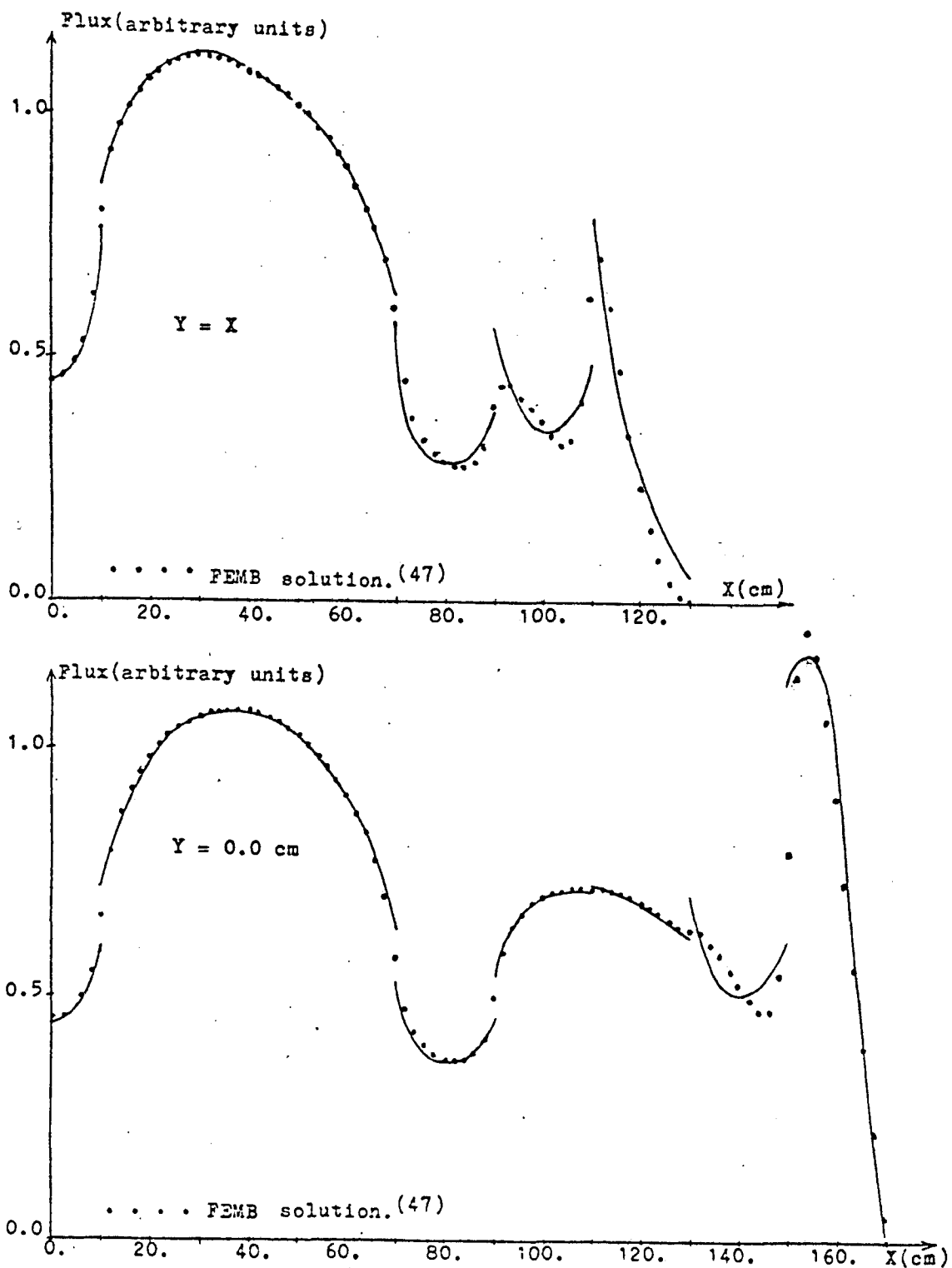


Fig. 5.6 - 2D-IAEA thermal neutron flux distribution obtained with 16/1 quadratic calculation ($\epsilon_{\phi} = 10^{-5}$).

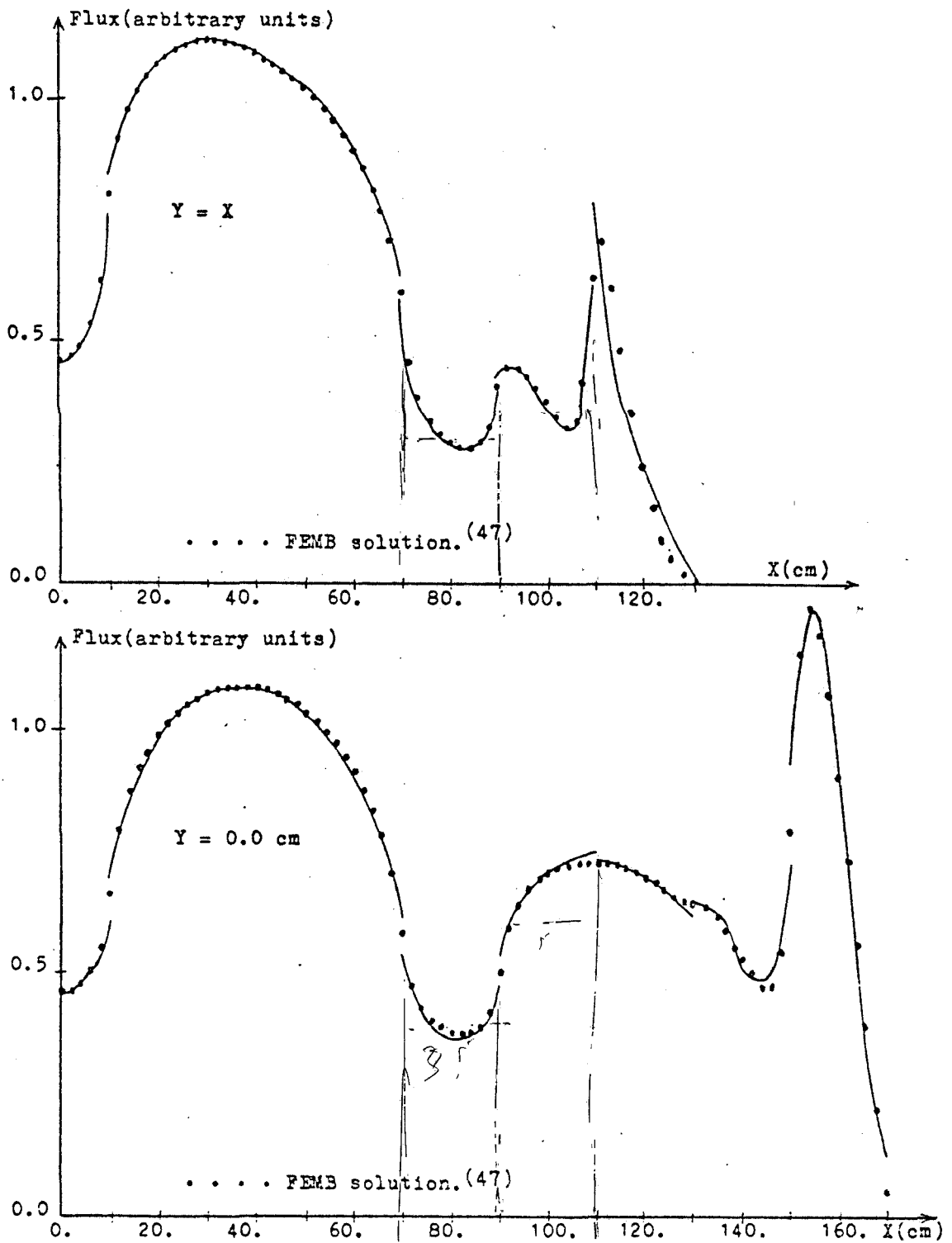


Fig. 5.7 - 2D-IAEA thermal neutron flux distribution obtained with 16/1 cubic calculation ($\epsilon\phi = 10^{-5}$).

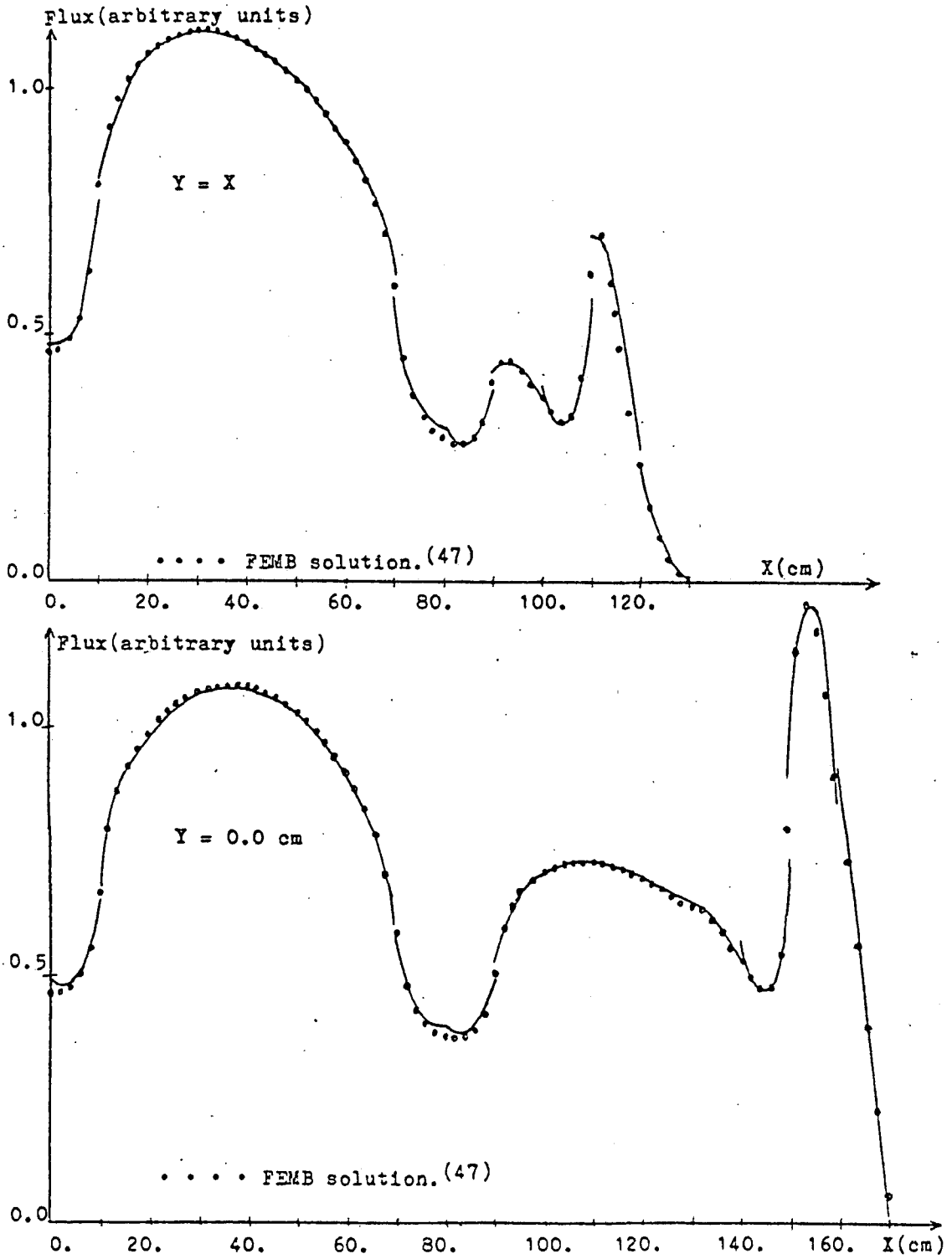


Fig. 5.8 - 2D-IAEA thermal neutron flux distribution obtained with 16/4 quadratic calculation ($\epsilon\phi = 2 \times 10^{-5}$).

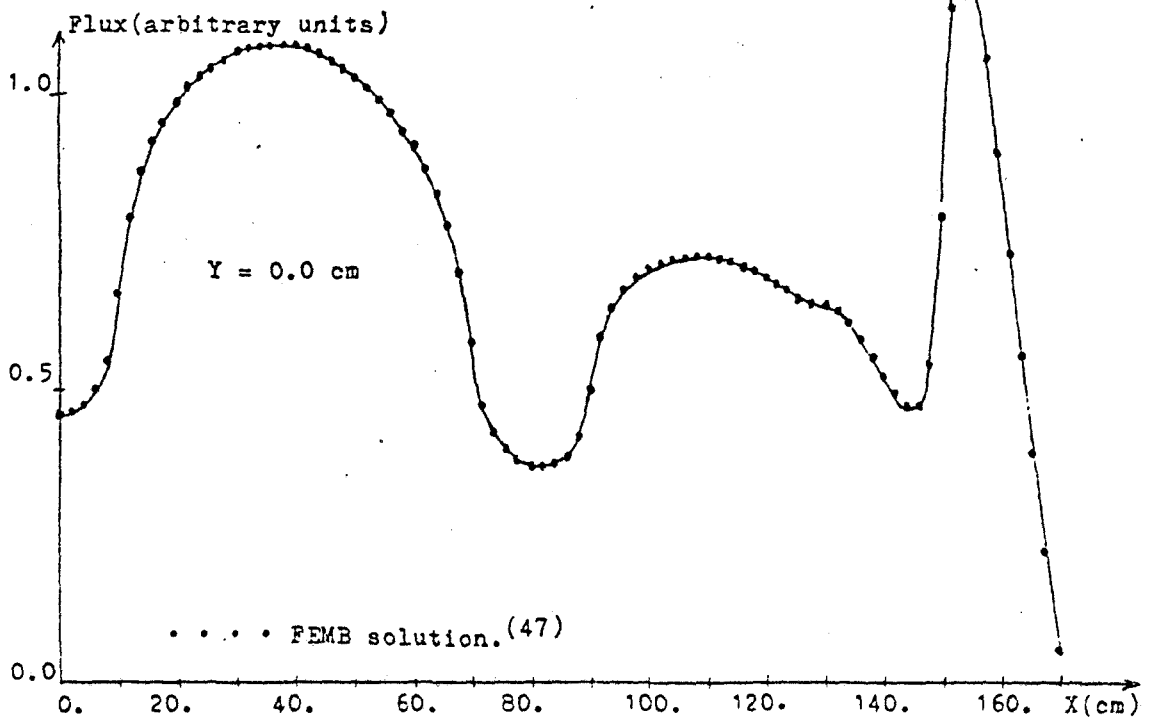
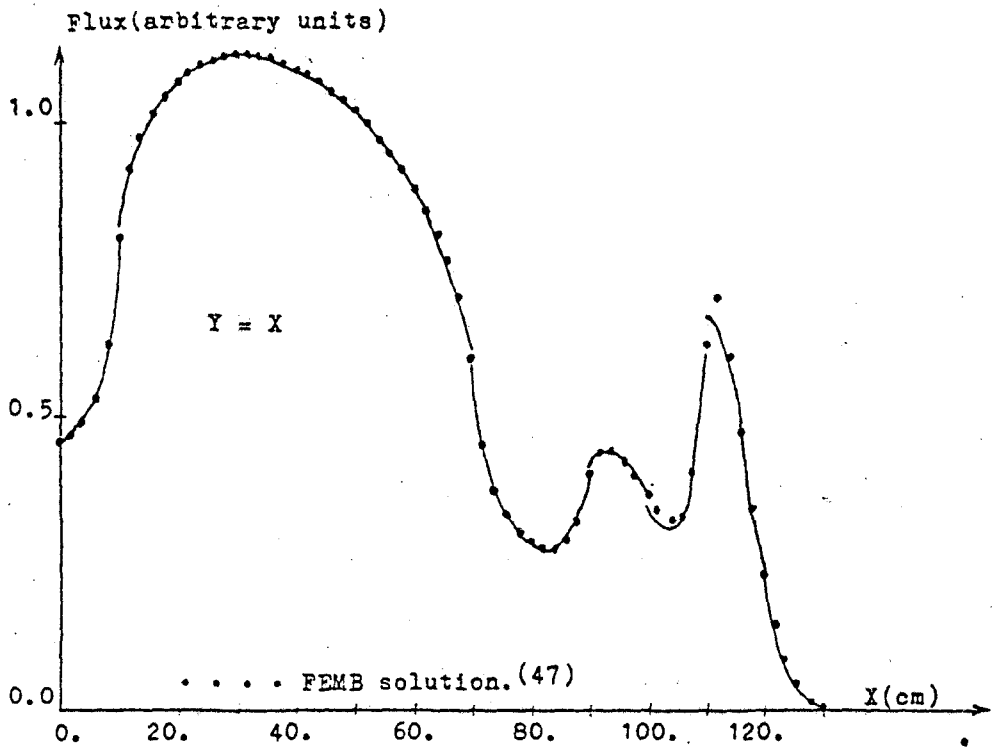


Fig. 5.9 - 2D-IAEA thermal neutron flux distribution obtained with 16/4 cubic calculation ($\bar{\epsilon}\phi = 1.3 \times 10^{-5}$).

(Figure 5.8).

Except for the 4/1 quadratic calculation, the results shown in Table 5.6 are well within the accuracy expected from a coarse mesh method. To illustrate, Table 5.7 contains results obtained with several well-known efficient coarse mesh methods, some of which are routinely used for production level calculations.

The results of 9/1 and 16/1 calculations for both quadratic and cubic approximations shown in Table 5.6 are relatively accurate and at the same time economical in view of the results shown in Table 5.7, taking into account the size of the coarse meshes (20cmx20cm). Moreover, the fact that the spatial neutron flux distribution is available throughout the core for the finite element response matrix method, compensates for some extent the slight disadvantage in computation time. However, the extensive and expensive optimization of various internal parameters and detailed investigation of the acceleration (outer iterations) methods more suitable for the present calculational method should be considered before production level status is achieved.

5.2.2 Biblis Benchmark Calculation

The Biblis benchmark problem⁽⁵⁶⁾ is an idealized PWR with checkerboard loading and reflected by water as illustrated in Figure 5.10 (diffusion parameters and cross

Table 5.7 2D-IAEA benchmark problem solved by coarse mesh methods. (17,18,20,47)

| coarse mesh method | k_{eff} | maximum $ \Delta P /P(\%)$ | coarse mesh size | order | CPU ^(b) (sec) | no. of outer iterations |
|--|-----------|----------------------------|--------------------------|-------|--------------------------|-------------------------|
| NEM(MEDIUM-2 program ⁽¹⁷⁾) | 1.0296 | .05 | 3 1/3 cm | 4 | 15.1 ^(c) | 42 |
| | 1.0298 | 1.67 | 10 cm | 4 | 4.17 | 26 |
| | 1.0300 | 3.67 | 20 cm | 4 | 1.77 | 35 |
| NGFM ⁽²⁰⁾ | 1.0296 | .71 | 20 cm | 2 | 1.8 ^(c) | - |
| FEM(FEM2D program ⁽¹⁸⁾) | 1.0297 | 1.87 | 606 nodes | 2 | 35.8 | 76 |
| | 1.0302 | 14.87 | 182 nodes ^(a) | 2 | 6.8 | 40 |

(a) average of 2 triangular coarse meshes per assembly.

(b) CDC 6600 computer.

(c) CYBER 175 computer.

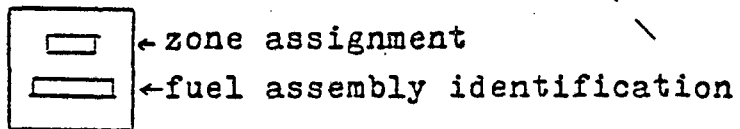
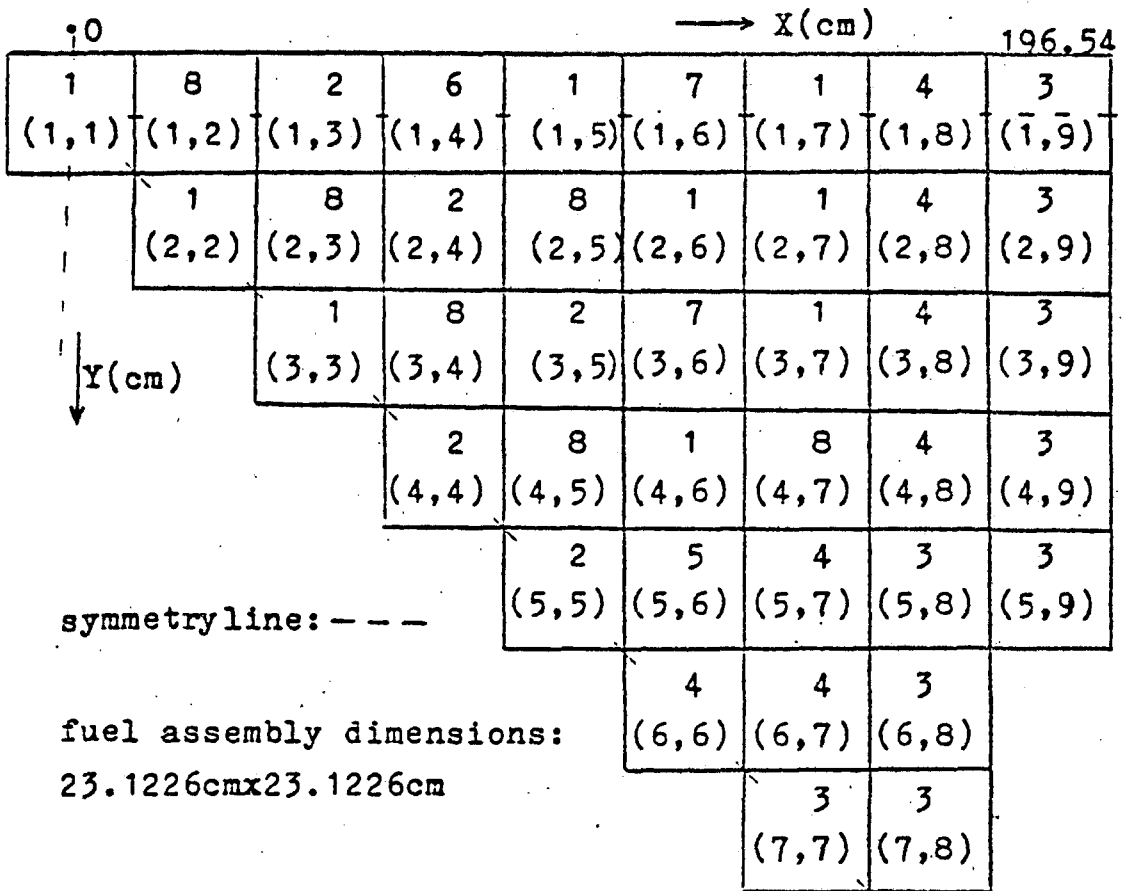


Fig. 5.10 - Biblis benchmark problem.⁽⁵⁶⁾

sections are given in Appendix IV). This problem is highly nonseparable (x-y separability) and thus represents a severe challenge⁽⁵⁶⁾ to the coarse mesh methods. Although there is no accurate fine mesh finite difference results available, two of the coarse mesh methods, NEM and NGFM, have produced results⁽⁵⁶⁾ which agree to within 0.15% in assembly averaged power distribution as shown in Table 5.8. Therefore, the reference solution adopted for the evaluation of present investigation is the NEM solution obtained with 5.781cm x 5.781cm coarse meshes.

Table 5.8 Biblis benchmark problem solved by coarse mesh methods. (19, 20, 56)

| coarse mesh method | k_{eff} | maximum $ \Delta P /P(\%)$ | coarse mesh size | order |
|--------------------|-----------|----------------------------|------------------|-------|
| NEM | 1.02511 | ref. solution | 5.781 cm | 3 |
| | 1.0251 | 1.6 | 23.1226 cm | 3 |
| NGFM | 1.0251 | .15 | 3.854 cm | 2 |
| | 1.0252 | 1.7 | 23.1226 cm | 2 |

From the summary of Biblis benchmark calculations presented in Table 5.9, one concludes that the 11.561cm x 11.561cm coarse mesh calculations, i.e., the 16/4 quadratic and 16/4 cubic calculations, yield essentially the same results as the 5.781cm x 5.781cm NEM coarse mesh calcula-

Table 5.9 Summary of Biblis benchmark calculations.

| calculation | no. of outer iterations | ϵ_{ϕ} | CPU (sec) | k_{eff} | maximum $ \Delta P /P(\%)$ |
|----------------|-------------------------------|--------------------|--------------|------------------|-------------------------------|
| 9/1 quadratic | 73 | 1×10^{-4} | 9.9 | 1.0255 | 2.79 |
| | 99 | 1×10^{-5} | 12.5 | 1.0255 | 2.51 |
| 16/1 quadratic | 66 | 1×10^{-4} | 13.6 | 1.0253 | 1.72 |
| | 99 | 3×10^{-5} | 16.7 | 1.0253 | 1.17 |
| 16/4 quadratic | 101 | 1×10^{-4} | 41.5 | 1.0250 | .90 |
| | 150 | 3×10^{-5} | 55.6 | 1.0250 | .20 |
| 9/1 cubic | 52 | 1×10^{-4} | 13.9 | 1.0255 | 3.67 |
| | 99 | 1×10^{-5} | 21.8 | 1.0255 | 2.96 |
| 16/1 cubic | 54 | 1×10^{-4} | 19.9 | 1.0254 | 2.11 |
| | 99 | 2×10^{-5} | 26.9 | 1.0254 | 1.55 |
| 16/4 cubic | 102 | 1×10^{-4} | 70.5 | 1.0250 | .87 |
| | 150 | 2×10^{-5} | 96.8 | 1.0250 | .23 |

tion. Figures 5.11 and 5.12 illustrate this in more detail by comparing the assembly averaged power distribution for the reference solution (NEM), the nodal Green's function method (NGFM) solution, and 16/4 quadratic and 16/4 cubic calculations, respectively. Computation times for the finite element response matrix solution are given in Table 5.9; however, computation times for the NEM and NGFM solution are not available.

Biblis Benchmark Problem

| | | | | | | | | |
|-------|-------|-------|-------|-------|-------|-------|-------|-----|
| 5.644 | 5.707 | 6.431 | 6.314 | 5.640 | 5.087 | 5.676 | 5.264 | |
| 5.656 | 5.710 | 6.441 | 6.326 | 5.642 | 5.087 | 5.668 | 5.249 | - - |
| 5.652 | 5.708 | 6.438 | 6.323 | 5.640 | 5.089 | 5.672 | 5.256 | |
| | 5.783 | 5.865 | 6.335 | 5.527 | 5.349 | 5.558 | 5.037 | |
| | 5.793 | 5.879 | 6.342 | 5.533 | 5.346 | 5.549 | 5.022 | |
| | 5.790 | 5.877 | 6.339 | 5.533 | 5.346 | 5.553 | 5.028 | |
| | | 5.811 | 5.718 | 5.803 | 4.785 | 4.828 | 4.279 | |
| | | 5.817 | 5.727 | 5.804 | 4.785 | 4.821 | 4.267 | |
| | | 5.814 | 5.726 | 5.803 | 4.786 | 4.823 | 4.272 | |
| | | | 6.013 | 5.379 | 4.926 | 3.966 | 2.831 | |
| | | | 6.017 | 5.383 | 4.923 | 3.964 | 2.824 | |
| | | | 6.014 | 5.382 | 4.922 | 3.965 | 2.827 | |
| | | | | 5.819 | 5.147 | 4.535 | | |
| | | | | 5.818 | 5.147 | 4.533 | | |
| | | | | 5.816 | 5.146 | 4.532 | | |
| | | | | | 6.218 | 3.550 | | |
| | | | | | 6.219 | 3.549 | | |
| | | | | | 6.216 | 3.546 | | |
| | | | | | | | | |



 ← Calculated
 ← NGFM(3.854cm mesh)
 ← NEM (5.781cm mesh)

Fig. 5.11 -Biblis assembly averaged power distribution obtained with 16/4 quadratic calculation. ($\epsilon_\phi = 3 \times 10^{-5}$)

Biblis Benchmark Problem

| | | | | | | | | |
|-------|-------|-------|-------|-------|-------|-------|-------|-----|
| 5.642 | 5.695 | 6.428 | 6.312 | 5.636 | 5.084 | 5.674 | 5.266 | |
| 5.656 | 5.710 | 6.441 | 6.326 | 5.642 | 5.087 | 5.668 | 5.249 | - - |
| 5.652 | 5.708 | 6.438 | 6.323 | 5.640 | 5.089 | 5.672 | 5.256 | |
| | 5.779 | 5.865 | 6.332 | 5.527 | 5.346 | 5.554 | 5.038 | |
| | 5.793 | 5.879 | 6.342 | 5.533 | 5.346 | 5.549 | 5.022 | |
| | 5.790 | 5.877 | 6.339 | 5.533 | 5.346 | 5.553 | 5.028 | |
| | | 5.807 | 5.718 | 5.802 | 4.784 | 4.827 | 4.279 | |
| | | 5.817 | 5.727 | 5.804 | 4.785 | 4.821 | 4.267 | |
| | | 5.814 | 5.726 | 5.803 | 4.786 | 4.823 | 4.272 | |
| | | | 6.012 | 5.379 | 4.926 | 3.969 | 2.832 | |
| | | | 6.017 | 5.383 | 4.923 | 3.964 | 2.824 | |
| | | | 6.014 | 5.382 | 4.922 | 3.965 | 2.827 | |
| | | | | 5.818 | 5.148 | 4.537 | | |
| | | | | 5.818 | 5.147 | 4.533 | | |
| | | | | 5.816 | 5.146 | 4.532 | | |
| | | | | | 6.225 | 3.554 | | |
| | | | | | 6.219 | 3.549 | | |
| | | | | | 6.216 | 3.546 | | |
| | | | | | | | | |

| | |
|--|-----------------------|
| | ← Calculated |
| | ← NGFM (3.854cm mesh) |
| | ← NEM (5.781cm mesh) |

Fig.5.12 -Biblis assembly averaged power distribution
 obtained with 16/4 cubic calculation.
 ($\epsilon\phi = 2 \cdot 10^{-5}$)

Biblis Benchmark Problem

| | | | | | | | | |
|-------|-------|-------|-------|-------|-------|-------|-------|--|
| -0.92 | -0.93 | -0.82 | -0.70 | -0.43 | -0.10 | +0.32 | +1.05 | |
| 5.600 | 5.655 | 6.385 | 6.279 | 5.616 | 5.084 | 5.690 | 5.311 | |
| 5.652 | 5.708 | 6.438 | 6.323 | 5.640 | 5.089 | 5.672 | 5.256 | |
| | -0.86 | -0.82 | -0.65 | -0.45 | -0.04 | +0.32 | +1.05 | |
| | 5.740 | 5.829 | 6.298 | 5.508 | 5.344 | 5.571 | 5.081 | |
| | 5.790 | 5.877 | 6.339 | 5.533 | 5.346 | 5.553 | 5.028 | |
| | | -0.67 | -0.58 | -0.34 | -0.04 | +0.37 | +1.10 | |
| | | 5.775 | 5.693 | 5.783 | 4.784 | 4.841 | 4.319 | |
| | | 5.814 | 5.726 | 5.803 | 4.786 | 4.823 | 4.272 | |
| | | | -0.40 | -0.19 | +0.10 | +0.48 | +1.17 | |
| | | | 5.990 | 5.372 | 4.927 | 3.984 | 2.860 | |
| | | | 6.014 | 5.382 | 4.922 | 3.965 | 2.827 | |
| | | | | .00 | +0.23 | +0.71 | | |
| | | | | 5.816 | 5.158 | 4.564 | | |
| | | | | 5.816 | 5.146 | 4.532 | | |
| | | | | | +0.51 | +1.10 | | |
| | | | | | 6.248 | 3.585 | | |
| | | | | | 6.216 | 3.546 | | |
| | | | | | | | | |

| | |
|---|------------------------|
| ▬ | ← (Calc.-Ref.)/Ref.(%) |
| ▬ | ← Calculated |
| ▬ | ← Reference (NEM) |

Fig. 5.13 -Biblis assembly averaged power distribution obtained with 16/1 quadratic calculation.
($\epsilon_\phi = 3 \times 10^{-5}$)

Biblis Benchmark Problem

| | | | | | | | | |
|-------|-------|-------|-------|-------|-------|-------|-------|-------|
| -1.10 | -1.09 | -.95 | -.82 | -.55 | -.24 | +.25 | +1.03 | |
| 5.590 | 5.646 | 6.377 | 6.271 | 5.609 | 5.077 | 5.686 | 5.310 | - - - |
| 5.652 | 5.708 | 6.438 | 6.323 | 5.640 | 5.089 | 5.672 | 5.256 | |
| | -1.04 | -.95 | -.76 | -.52 | -.19 | +.25 | +1.05 | |
| | 5.730 | 5.821 | 6.291 | 5.504 | 5.336 | 5.567 | 5.081 | |
| | 5.790 | 5.877 | 6.339 | 5.533 | 5.346 | 5.553 | 5.028 | |
| | | -.81 | -.65 | -.38 | -.10 | +.37 | +1.17 | |
| | | 5.767 | 5.689 | 5.781 | 4.781 | 4.841 | 4.322 | |
| | | 5.814 | 5.726 | 5.803 | 4.786 | 4.823 | 4.272 | |
| | | | -.43 | -.20 | +.14 | +.66 | +1.38 | |
| | | | 5.988 | 5.371 | 4.929 | 3.991 | 2.866 | |
| | | | 6.014 | 5.382 | 4.922 | 3.965 | 2.827 | |
| | | | | +.07 | +.47 | +1.06 | | |
| | | | | 5.820 | 5.170 | 4.580 | | |
| | | | | 5.816 | 5.146 | 4.532 | | |
| | | | | | +.92 | +1.55 | | |
| | | | | | 6.273 | 3.601 | | |
| | | | | | 6.216 | 3.546 | | |
| | | | | | | | | |

| | |
|---|-------------------------|
| ▬ | ← (Calc.-Ref.)/Ref. (%) |
| ▬ | ← Calculated |
| ▬ | ← Reference (NEM) |

Fig. 5.14 -Biblis assembly averaged power distribution
 obtained with 16/1 cubic calculation.
 ($\epsilon_{\phi} = 2. \times 10^{-5}$)

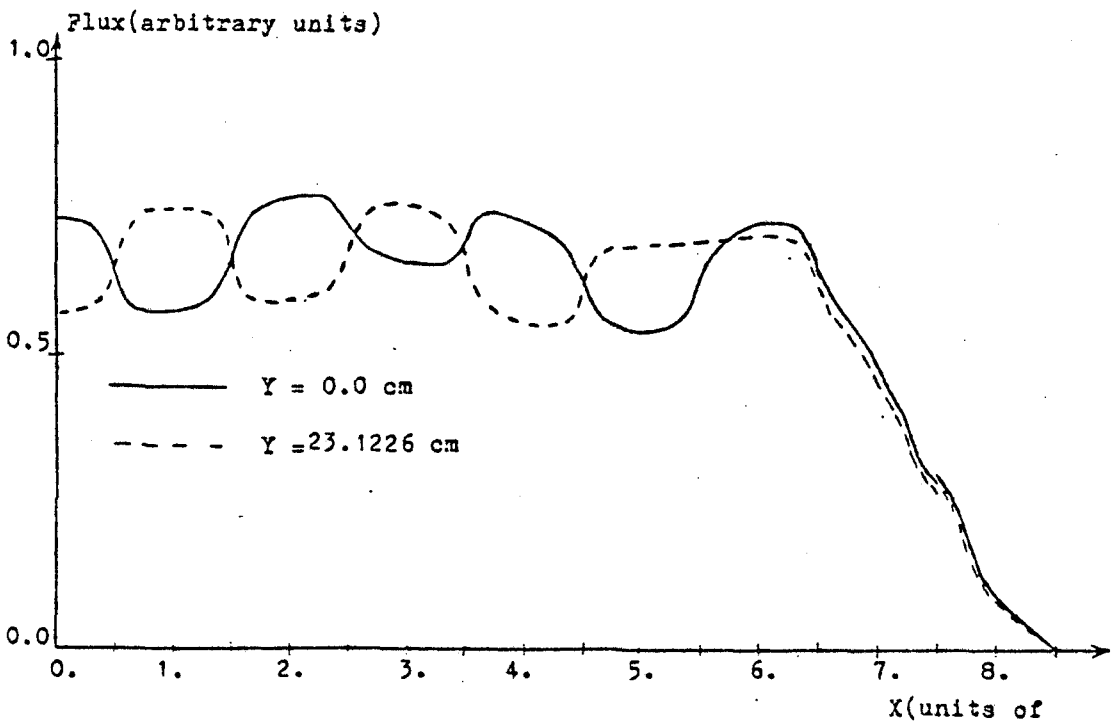
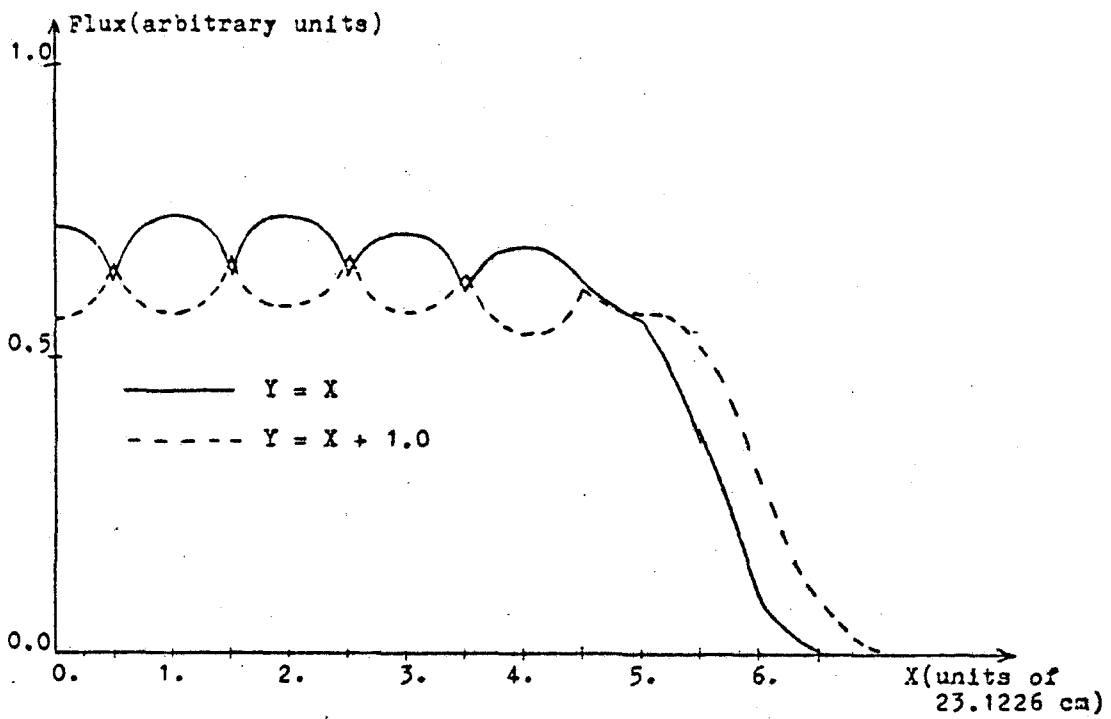


Fig. 5.15 - Biblis thermal neutron distribution obtained with 16/4 cubic calculation ($\epsilon\phi = 2 \times 10^{-5}$).

It is also noted that 16/1 quadratic and 16/1 cubic calculations yielded results acceptable (within 2% for assembly averaged power levels) for coarse mesh methods but with a significant improvement in computational time, compared with the 16/4 quadratic and cubic calculations. Figures 5.13 and 5.14 present the results utilizing the 16/1 quadratic and 16/1 cubic approximations, respectively.

The small relative increase in computational time when compared with 2D-IAEA benchmark calculation is primarily due to two causes: the increase in the number of different loading zones thus requiring generation of a greater number of response matrices and the slower convergence of the outer iterations caused by the highly nonseparable neutron flux distribution, which is illustrated in Figure 5.15.

CHAPTER 6

CONCLUDING REMARKS

6.1 Summary of Investigation

The present investigation examined an alternative formulation of the response matrix method implemented with the finite element method for application to coarse mesh reactor analysis.

The finite element method was applied in a two level scheme. The first level, the local (or assembly-level) calculation, utilized quadratic Serendipity elements to solve the weak form of the inhomogeneous diffusion equation subject to incoming partial current boundary conditions. The results of the local calculations are then used to generate the response matrices. The unique feature of the response matrix formulation is the use of two types of response matrices - one giving the response in the outgoing partial current on the boundary due to incoming neutrons which diffuse to the boundary (without absorption or outscatter) and the second type giving the response in the outgoing partial current due to a source within the node (inscatter or fission or external source). Conventional response matrix methods only utilize the former type of response matrix, which is then generalized to

include the response in the outgoing current due to the incoming neutrons which eventually reach the boundary. The second level of the finite element application is then to utilize the response matrices from the local calculation to solve for the global fluxes and currents. The global fluxes and currents are themselves expanded in either quadratic or cubic Serendipity elements (a user option), which are independent of the finite element basis functions used for the expansion of the local fluxes and currents. The unknown expansion coefficients for the global fluxes and currents are then solved for utilizing a Gauss-Seidel iterative method to sweep through the global mesh, until the partial currents and fluxes converge.

This alternative formulation of the response matrix method (two types of response matrices) has the advantage that it decouples the response matrix generation from the internal neutron multiplication factor, k_{eff} , since the response matrices are not a function of k_{eff} as in the conventional response matrix formulation. Thus the expensive regeneration of response matrices during the global solution is avoided, which is a significant advantage. Secondly, the multigroup diffusion equation can be readily solved by standard source iteration methods (outer iterations). Finally, acceleration of the outer iterations convergence rate was obtained by using the Chebyshev polynomial method.

6.2 Conclusions

Based on the preceding discussion of the investigation into the finite element response matrix method for coarse mesh reactor analysis, the following conclusions are made:

1. The method was applied to the idealized zone loading PWR problem, the 2D-IAEA test problem, with excellent results. The error in the assembly averaged power distribution is within the error observed with fine mesh (about 1 cm) finite difference calculations (VENTURE and PDQ-7) when compared with the reference extrapolated results. The savings in the computational time, therefore, are substantial given the comparable accuracy and the significant increase in the amount of information available, e.g., the detailed spatial neutron flux distribution. The disagreements in the neutron multiplication factor, k_{eff} , are slight and well within the accuracy expected from coarse mesh methods.

2. An accurate comparison in the computational efficiency of the present method with some of the highly efficient production level coarse mesh codes, e.g., NEM and NGFM, is not possible due to the difficulty in comparing relative efficiencies of different computers used with the various methods. However it would appear, using the information available^(59,60) concerning relative speeds for the various computers, that NEM and NGFM programs are

somewhat more efficient than the finite element response matrix method at the present stage. However, the fact that additional information is available with the finite element response matrix method, in particular the detailed neutron flux/power distribution, represents significant advantage for the present method. In addition, the unquestionable potential to incorporate additional capabilities such as treatment of spatially dependent cross sections, triangular geometry, and highly heterogeneous fuel assemblies, also compensate to some extent the relative increase in the computational time when compared with NEM and NGFM.

3. The successful application of the finite element response matrix method to the highly nonseparable problem, the Biblis PWR with checkerboard loading, has shown the capabilities of the present calculational method to solve practical problems with realistic loading configurations. In particular, the assembly averaged power distribution calculated with a relatively coarse mesh yielded essentially the same results as somewhat finer meshes for the NEM and NGFM methods.

4. Concerning the accuracy and efficiency of the finite element response matrix method as a function of polynomial order and mesh spacing, comparable results are obtained for the test problems with 9/1 quadratic or 9/1 cubic calculations, with the cubic elements yielding more accurate results than quadratic elements at the cost of a

slight increase in computational time. The subdivision of the coarse mesh (assembly) into 9 subdomains to generate the response matrix is sufficiently accurate compared with the results with 16 subdivisions, and for smaller coarse mesh size (e.g., 9/4 calculation) the results are better but the convergence rate for the outer iterations decreases substantially due to the larger spectral norm of the iteration matrix for smaller mesh sizes, with consequent increase in computational time (about factor of 4).

5. The alternative formulation of the response matrix method, utilizing two types of response matrices, avoids the expense of recalculating the response matrices (or parameterizing them) as a function of k_{eff} . This is especially significant in fuel management analyses where all of the fuel assemblies (or even portions of them) will have different burnups, hence different response matrices.

6. The present method is readily generalized to treat heterogeneous assemblies (e.g., waterholes or poison pins) or depletion induced spatial variations in the nodal cross sections. This is due to the fact that the use of the finite element method for the generation of the response matrices is not restricted to a homogeneous domain, although the current code does have this restriction. Thus the method is capable of generating detailed within-node neutron flux/power distributions in a heterogeneous assembly with little increase in computational time.

6.3 Recommendations for Further Study

Since the capabilities of the finite element response matrix method have been demonstrated in realistic reactor calculations, future effort should be expended to extend the calculational model and optimize the computational efficiency of the code. In particular, further study should be directed at the following:

1. The convergence of the outer iterations should be improved developing a more effective acceleration scheme than the Chebyshev polynomial method used presently. For example, an examination of the theoretical foundations for the coarse mesh rebalance acceleration method⁽⁵⁴⁾ with respect to the finite element response matrix method could be undertaken in order to develop an equivalent acceleration scheme to improve the convergence of the outer iterations.

2. Extend the present method to take into account the effect of depletion induced spatial cross sections variations, as suggested by Kavenoky and Lautard⁽²³⁾ for the finite element method.

3. Provide a feedback calculational capability by treating separately small regions of the core (coarse mesh) and regenerating the response matrix only for these regions. Also a scheme which would allow inexpensive regeneration of the response matrix should be investigated to allow inclusion of a small spatially dependent perturbation into the inhomogeneous term (source term).

4. Generalize the response matrix generation to heterogeneous assemblies which would allow the treatment of local heterogeneities and would result in the calculation of local pin power peaking within the coarse mesh node.

5. The use of a triangular mesh (with the associated finite element) should be developed in order to extend the calculational capability to hexagonal fuel assemblies of fast reactors.

6. Improve the computational efficiency by optimizing the computational algorithm and the programming. For instance, higher order finite element approximations, e.g., cubic or quartic, should be investigated for the local calculation (generation of the response matrices) in order to improve the accuracy of the global calculations without excessive increase in the computational time.

APPENDICES

APPENDIX I
ACCELERATION SCHEMES

The outer iterations convergence of the finite element response matrix method was accelerated by two acceleration schemes: asymptotic source acceleration method and Chebyshev polynomial method.

In order to apply the asymptotic source acceleration method and the Chebyshev polynomial method to the response matrix method, the solutions given in the equations (2.20) and (2.21) is rewritten for a fixed source problem as
(for group g)

$$j^+ = (I - R^{\sigma} H)^{-1} R^{\xi} S$$

$$\phi = M^{\sigma} j^+ + M^{\xi} S \quad (2.20)$$

$$\underline{\Phi}^g = \underline{K}_g \cdot \underline{S}^g \quad \phi = M^{\sigma} (I - R^{\sigma} H)^{-1} R^{\xi} S + M^{\xi} S$$

where

$$\underline{K}_g = \left[\underline{M}_g^{\sigma} \cdot (\underline{I} - \underline{R}_g^{\sigma} \underline{H}_g)^{-1} \cdot \underline{R}_g^{\xi} + \underline{M}_g^{\xi} \right]$$

Therefore the problem (4.8) can be given as

$$\begin{cases} \underline{\Phi}^1 = \underline{K}_1 \cdot \underline{S}^1 \\ \underline{\Phi}^2 = \underline{K}_2 \cdot \underline{S}^2 \end{cases} \quad (\text{I.1})$$

where

$$\underline{S}^1 = \frac{1}{k_{eff}} \left[\underline{F}_1 \cdot \underline{\Phi}^1 + \underline{F}_2 \cdot \underline{\Phi}^2 \right]$$

$$\underline{S}^2 = \underline{T}_{21} \cdot \underline{\Phi}^1$$

\underline{F}_g , $g=1,2$, is $(L \times N) \times (L \times N)$ diagonal with elements $\nu^g \Sigma_{fi}^g$, $i=1, \dots, (L \times N)$,

\underline{T}_{21} is $(L \times N) \times (L \times N)$ diagonal matrix with elements Σ_{21i} , $i=1, \dots, (L \times N)$,

and $\nu^g \Sigma_f^g(r)$ and $\Sigma_{21}(r)$ were expanded in the same basis functions as $\Phi^g(r)$, with $\nu^g \Sigma_{fi}^g$ and Σ_{21i} as expansion coefficients, respectively.

Defining

$$\underline{Y} = \underline{F}_1 \cdot \underline{\Phi}^1 + \underline{F}_2 \cdot \underline{\Phi}^2 \quad (\text{I.2})$$

the equations (I.1) yield

$$\underline{\Phi}^1 = \frac{1}{k_{eff}} \underline{K}_1 \cdot \underline{Y} \quad (\text{I.3})$$

$$\underline{\Phi}^2 = \frac{1}{k_{eff}} \underline{K}_2 \cdot \underline{T}_{21} \cdot \underline{K}_1 \cdot \underline{Y},$$

and introducing the equation (I.3) into the equation (I.2), one gets

$$\underline{Y} = \frac{1}{k_{eff}} \underline{K} \cdot \underline{Y}$$

where

$$\underline{\underline{K}} = \underline{\underline{T}}_1 \cdot \underline{\underline{K}}_1 + \underline{\underline{T}}_2 \cdot \underline{\underline{K}}_2 \cdot \underline{\underline{T}}_{21} \cdot \underline{\underline{K}}_1,$$

Now the outer iterations can be given by the power method (source iteration method) as

$$\underline{y}^{(t)} = \frac{1}{\text{Reff}} \underline{\underline{K}} \cdot \underline{y}^{(t-1)}, \quad t=1, 2, \dots \quad (\text{I.4})$$

Asymptotic Source Extrapolation

The asymptotic source extrapolation method⁽⁵¹⁾ assumes that some previous outer iterations are performed such that $\underline{y}^{(t)}$ has reached asymptotic convergence behavior where higher eigenmodes are sufficiently damped and the error is dominated by the first eigenmode.

Assume $k_0 > k_1 \gg k_2 \gg \dots \gg k_{L \times N - 1} > 0$, where k_i is the eigenvalue of $\underline{\underline{K}}$,

$$\underline{\underline{K}} \cdot \underline{\underline{\phi}}_i = k_i \underline{\underline{\phi}}_i$$

and $\underline{\underline{\phi}}_i$, $i=0, 1, \dots, L \times N - 1$, are the eigenvectors of $\underline{\underline{K}}$.

For finite difference equations this assumption has been proven to be valid⁽⁵⁴⁾ but for the response matrix method one has to assume its validity because the proof is not available. The positivity⁽³⁾ of $\underline{\underline{K}}_1$ and $\underline{\underline{K}}_2$ cannot be proven for the response matrix method, because the elements of the response matrices $\underline{\underline{R}}_i^J$ are not strictly positive.

Expand

$$\underline{y}^{(0)} = \sum_{i=1}^{L \times N} a_i \underline{\varphi}_i$$

and assume that convergence has reached an asymptotic behavior such that $k_{eff}^{(t)} = k_0$, then for iteration t ,

$$\underline{y}^{(t)} = \underline{y}_0 + a_1 \left(\frac{k_1}{k_0} \right)^t \underline{\varphi}_1 \left\{ 1 + O \left[\left(\frac{k_2}{k_1} \right)^t \right] \right\}$$

$$\underline{y}^{(t)} = \underline{y}^{(\infty)} + \underline{y}^{\perp} \sigma^t$$

where $\sigma = k_1/k_0$ is the dominance ratio, and

$\underline{y}^{(\infty)}$ is the fundamental mode to be determined.

The eigenvector \underline{y}^{\perp} can be estimated by two successive iterations as

$$\underline{y}^{\perp} = \frac{\underline{y}^{(t)} - \underline{y}^{(t-1)}}{\sigma^{(t-1)}(\sigma - 1)}$$

such that the estimate of the fundamental mode is given by

$$\underline{y}^{(\infty)} = \underline{y}^{(t)} + \frac{\bar{\sigma}}{1 - \bar{\sigma}} \left(\underline{y}^{(t)} - \underline{y}^{(t-1)} \right)$$

where $\bar{\sigma}$ is the estimate of dominance ratio obtained by a procedure based on the error decay rate as described in Ref. 51.

Chebyshev Polynomial Method

The convenient form of the response matrix method in order to apply the Chebyshev polynomial method can be obtained by rewriting the equations (I.1) as

$$\begin{bmatrix} \underline{\underline{I}} & \underline{\underline{O}} \\ -\underline{\underline{K}}_2 \underline{\underline{T}}_{21} & \underline{\underline{I}} \end{bmatrix} \cdot \begin{bmatrix} \underline{\underline{\Phi}}^1 \\ \underline{\underline{\Phi}}^2 \end{bmatrix} = \frac{1}{k_{eff}} \begin{bmatrix} \underline{\underline{K}}_1 \underline{\underline{F}}_1 & \underline{\underline{K}}_1 \underline{\underline{F}}_2 \\ \underline{\underline{O}} & \underline{\underline{O}} \end{bmatrix} \cdot \begin{bmatrix} \underline{\underline{\Phi}}^1 \\ \underline{\underline{\Phi}}^2 \end{bmatrix}$$

or succinctly

$$\underline{\underline{\Phi}}^{12} = \frac{1}{k_{eff}} \underline{\underline{P}} \cdot \underline{\underline{\Phi}}^{12}$$

where

$$\underline{\underline{P}} = \begin{bmatrix} \underline{\underline{I}} & \underline{\underline{O}} \\ -\underline{\underline{K}}_2 \underline{\underline{T}}_{21} & \underline{\underline{I}} \end{bmatrix}^{-1} \cdot \begin{bmatrix} \underline{\underline{K}}_1 \underline{\underline{F}}_1 & \underline{\underline{K}}_1 \underline{\underline{F}}_2 \\ \underline{\underline{O}} & \underline{\underline{O}} \end{bmatrix}, \quad \underline{\underline{\Phi}}^{12} = \begin{bmatrix} \underline{\underline{\Phi}}^1 \\ \underline{\underline{\Phi}}^2 \end{bmatrix},$$

assuming that the inverse exists.

Then the outer iterations can be given by the power method as

$$\underline{\underline{\Phi}}^{12(t)} = \frac{1}{k_{eff}^{(t-1)}} \underline{\underline{P}} \cdot \underline{\underline{\Phi}}^{12(t-1)}, \quad t=1,2,\dots$$

The eigenvalues of P are again assumed

$k_0 > k_1 \gg k_2 \gg \dots \gg k_{L \times N - 1} > 0$ and the corresponding eigenvectors are $\underline{X}_i, i=0, \dots, L \times N - 1$, that is

$$\underline{P} \underline{X}_i = k_i \underline{X}_i .$$

Assume a sufficiently converged eigenvalue is available, $k_{\#}^{(t)} \simeq k_0$, after t iterations.

The Chebyshev polynomial method as shown by Hageman and Pfeifer⁽⁵³⁾ can be derived by choosing the accelerated solutions as a linear combination of eigenvector iterates $\underline{\Phi}^{12(t)}$ such that

$$\underline{\Phi}^{*12(t+p)} = a_{0p} \underline{\Phi}^{12(t)} + a_{1p} \underline{\Phi}^{12(t+1)} + \dots + a_{pp} \underline{\Phi}^{12(t+p)} . \quad (\text{I.5})$$

Expanding

$$\underline{\Phi}^{12(t)} = \sum_{i=1}^I c_i \underline{X}_i ,$$

normalized such that $c_1=1$, the equation (I.5) becomes

$$\underline{\Phi}^{*12(t+p)} = \sum_{i=1}^I c_i \sum_{j=0}^p a_{jp} \left(\frac{k_{i-1}}{k_0} \right)^j \underline{X}_i , \quad (\text{I.6})$$

and if one defines $P_p(y) = \sum_{j=0}^p a_{jP} y^j$, equation (I.6) becomes

$$\underline{\Phi}^{*12(x+p)} = P_p(1) \underline{X}_1 + \sum_{i=2}^I c_i P_p\left(\frac{k_{i-1}}{k_0}\right) \underline{X}_i \quad (I.7)$$

The accelerated solution is obtained by choosing $P_p(y)$ such that $P_p(1)=1$ and $\max_{0 \leq y \leq \sigma} |P_p(y)|$ is minimized, which is the classical Chebyshev minimax property. The polynomials $P_p(y)$ are therefore Chebyshev polynomials given by

$$P_p(y) = C_p\left(\frac{2y}{\sigma} - 1\right) / C_p\left(\frac{2}{\sigma} - 1\right)$$

where

$$C_p(y) = \begin{cases} \cosh(p \cosh^{-1} y) & , y \geq 1 \\ \cos(p \cos^{-1} y) & , -1 \leq y \leq 1 \end{cases}$$

Using the recursion relationship for Chebyshev polynomials, the acceleration scheme can be given by the algorithm

$$\underline{\Phi}^{12(x+p)} = \frac{1}{k_{x+1}} \underline{P} \cdot \underline{\Phi}^{12(x+p-1)}$$

$$\begin{aligned} \underline{\Phi}^{*12}(t+p) &= \underline{\Phi}^{*12}(t+p-1) + \alpha_p \left[\underline{\Phi}^{12}(t+p) - \underline{\Phi}^{12}(t+p-1) \right] \\ &\quad + \beta_p \left[\underline{\Phi}^{*12}(t+p-1) - \underline{\Phi}^{*12}(t+p-2) \right], \end{aligned}$$

$$\frac{\|\underline{\Phi}^{*12}(t+p)\|}{\|\underline{\Phi}^{*12}(t+p-1)\|} = \frac{\|\underline{\Phi}^{*12}(t+p)\|}{\|\underline{\Phi}^{*12}(t+p-1)\|},$$

$$p=1, 2, \dots,$$

where $\alpha_1 = 2/(2 - \bar{\sigma})$, $\beta_1 = 0$,

$$\alpha_p = \frac{4}{\bar{\sigma}} \left\{ \frac{\cosh[(p-1)\delta]}{\cosh[p\delta]} \right\},$$

$$\beta_p = (1 - \bar{\sigma}/2) \alpha_{p-1},$$

$$\delta = \cosh^{-1}(2/\bar{\sigma} - 1),$$

$\bar{\sigma}$ is the estimate of dominance ratio obtained from the decay rate of the error

$$\bar{\sigma} = \lim_{t \rightarrow \infty} \left(\frac{\underline{E}^{(t)T} \cdot \underline{E}^{(t)}}{\underline{E}^{(t-1)T} \cdot \underline{E}^{(t)}} \right)^{1/2}$$

where

$$\underline{E}^{(t)} = \underline{\Phi}^{12}(t) - \underline{\Phi}^{12}(t-1)$$

APPENDIX II

VARIATIONAL FORMULATION OF DIFFUSION EQUATION

The quadratic functional (the definition of each term is given in Chapter 3) for the coarse mesh Ω_m

$$F(\psi_m) = \int_{\Omega_m} [D_m(\underline{x}) \nabla \psi_m(\underline{x}) \nabla \psi_m(\underline{x}) + \sum_{a_m}(\underline{x}) \psi_m(\underline{x}) \psi_m(\underline{x}) - 2s_m(\underline{x}) \psi_m(\underline{x})] d\underline{x} + \frac{1}{2} \oint_{\partial\Omega_m} [4j_m^-(\pi_s) - \psi_m(\underline{x})]^2 d\pi_s, \quad (\text{II.1})$$

$$\psi_m(\underline{x}) \in H_2^1,$$

has a minimum for $\psi_m = \phi_m$, where ϕ_m is the solution of the diffusion equation (assembly level calculations)

$$-\nabla D_m(\underline{x}) \nabla \phi_m(\underline{x}) + \sum_{a_m}(\underline{x}) \phi_m(\underline{x}) = s_m(\underline{x}), \quad \underline{x} \in \Omega_m, \quad (\text{II.2})$$

subject to the boundary condition

$$j_m^-(\pi_s) = \frac{1}{4} \phi_m(\pi_s) + \frac{1}{2} D_m(\pi_s) \nabla \phi_m(\underline{x}) \Big|_{\underline{x}=\pi_s} \cdot \underline{m}(\pi_s), \quad \pi_s \in \partial\Omega_m,$$

and the interface conditions of continuity of current and flux.

PROOF: Define the bilinear functional

$$b(\phi_m, \psi_m) = \int_{\Omega_m} \left[D_m(\underline{r}) \nabla \phi_m(\underline{r}) \nabla \psi_m(\underline{r}) + \sum_{a_m}(\underline{r}) \phi_m(\underline{r}) \psi_m(\underline{r}) \right] d\underline{r}$$

and use the definitions in Chapter 3 for the volume and boundary inner products to express $F(\psi_m)$ as follows

$$F(\psi_m) = b(\psi_m, \psi_m) - 2(s_m, \psi_m) \tag{II.3}$$

$$+ \frac{1}{2} \langle 4j_m^- - \psi_m, 4j_m^- - \psi_m \rangle, \quad \psi_m \in H_2^1.$$

Now multiply equation (II.2) by $\psi_m(\underline{r})$ and integrate over Ω_m ,

$$\int_{\Omega_m} \psi_m(\underline{r}) \left[-\nabla \cdot D_m(\underline{r}) \nabla \phi_m(\underline{r}) \right] d\underline{r} + \int_{\Omega_m} \psi_m(\underline{r}) \sum_{a_m}(\underline{r}) \phi_m(\underline{r}) d\underline{r} = \int_{\Omega_m} \psi_m(\underline{r}) s_m(\underline{r}) d\underline{r}. \tag{II.4}$$

The objective is to include the boundary condition on $\partial\Omega_m$ by an integration by parts; however, $\psi_m(\underline{r})$ ($\in H_2^1$) is a continuous function with discontinuous first derivatives within Ω_m and one cannot directly integrate equation (II.4) by parts. But if the domain is partitioned in M subdomains Ω_{mm} , $m=1, \dots, M$, such that $\psi_m(\underline{r})$ has continuous first derivatives within each Ω_{mm} , the integral involving the derivative can be expressed as a summation of integrals yielding

$$\sum_{m=1}^M \int_{\Omega_{mm}} \Psi_m(\underline{r}) \left[-\nabla \cdot \underline{D}_m(\underline{r}) \nabla \phi_m(\underline{r}) \right] d\underline{r} + \quad (\text{II.5})$$

$$\int_{\Omega_m} \Psi_m(\underline{r}) \sum_{a_m}(\underline{r}) \phi_m(\underline{r}) d\underline{r} = \int_{\Omega_m} \Psi_m(\underline{r}) s_m(\underline{r}) d\underline{r} .$$

Denoting the summation term as Σ , each integral in the summation can be integrated by parts to yield

$$\begin{aligned} \Sigma &= \sum_{m=1}^M \left\{ \int_{\Omega_{mm}} \underline{D}_m(\underline{r}) \nabla \phi_m(\underline{r}) \nabla \Psi_m(\underline{r}) d\underline{r} - \int_{\Omega_{mm}} \nabla \cdot \left[\Psi_m(\underline{r}) \underline{D}_m(\underline{r}) \nabla \phi_m(\underline{r}) \right] d\underline{r} \right\} \\ &= \int_{\Omega_m} \underline{D}_m(\underline{r}) \nabla \phi_m(\underline{r}) \nabla \Psi_m(\underline{r}) d\underline{r} - \sum_{m=1}^M \oint_{\partial \Omega_{mm}} \Psi_m(\underline{r}_s) \underline{D}_m(\underline{r}_s) \nabla \phi_m(\underline{r}) \cdot \underline{n}_m(\underline{r}_s) d\underline{r}_s \end{aligned}$$

where $\underline{n}_m(\underline{r}_s)$ is the vector normal to the boundary $\partial \Omega_{mm}$

But the interface condition of continuity of current, $-\underline{D}_m(\underline{r}) \nabla \phi_m(\underline{r})$, eliminates all of the interior surface integrals, and the boundary condition on the outer boundary $\partial \Omega_m$ can be applied to yield

$$\Sigma = \int_{\Omega_m} \underline{D}_m(\underline{r}) \nabla \phi_m(\underline{r}) \nabla \Psi_m(\underline{r}) d\underline{r} - \oint_{\partial \Omega_m} \Psi_m(\underline{r}_s) \left[2\underline{j}_m^-(\underline{r}_s) - \frac{1}{2} \phi_m(\underline{r}_s) \right] d\underline{r}_s .$$

Inserting Σ into equation (II.5) yields

$$\begin{aligned} & \int_{\Omega_m} D_m(\underline{r}) \nabla \phi_m(\underline{r}) \nabla \psi_m(\underline{r}) d\underline{r} - 2 \oint_{\partial\Omega_m} j_m^-(\underline{r}_s) \psi_m(\underline{r}_s) d\underline{r}_s \\ & + \frac{1}{2} \oint_{\partial\Omega_m} \phi_m(\underline{r}_s) \psi_m(\underline{r}_s) d\underline{r}_s + \int_{\Omega_m} \Sigma_m(\underline{r}) \phi_m(\underline{r}) \psi_m(\underline{r}) d\underline{r} \\ & = \int_{\Omega_m} s_m(\underline{r}) \psi_m(\underline{r}) d\underline{r} , \end{aligned}$$

which in terms of $b(\phi_m, \psi_m)$ and the volume and boundary inner products can be written as

$$\begin{aligned} b(\phi_m, \psi_m) + \frac{1}{2} \langle \phi_m, \psi_m \rangle = \\ (s_m, \psi_m) + 2 \langle j_m^-, \psi_m \rangle \end{aligned} \tag{II.6}$$

or rearranging

$$(s_m, \psi_m) = b(\phi_m, \psi_m) - \frac{1}{2} \langle 4j_m^- - \phi_m, \psi_m \rangle . \tag{II.7}$$

Inserting equation (II.7) into equation (II.3),

$$\begin{aligned} F(\psi_m) = b(\psi_m, \psi_m) - 2b(\phi_m, \psi_m) + \langle 4j_m^- - \phi_m, \psi_m \rangle \\ + \frac{1}{2} \langle 4j_m^- - \psi_m, 4j_m^- - \psi_m \rangle . \end{aligned} \tag{II.8}$$

But since

$$b(\psi_m - \phi_m, \psi_m - \phi_m) = b(\psi_m, \psi_m) - 2b(\phi_m, \psi_m) + b(\phi_m, \phi_m)$$

and

$$\langle 4j_m^- - \psi_m, 4j_m^- - \psi_m \rangle = \langle 4j_m^-, 4j_m^- \rangle - 2\langle 4j_m^-, \psi_m \rangle + \langle \psi_m, \psi_m \rangle$$

the equation (II.8) can be rewritten as

$$\begin{aligned} F(\psi_m) &= b(\psi_m - \phi_m, \psi_m - \phi_m) - b(\phi_m, \phi_m) - \langle \phi_m, \psi_m \rangle \\ &+ \frac{1}{2} \langle 4j_m^-, 4j_m^- \rangle + \frac{1}{2} \langle \psi_m, \psi_m \rangle. \end{aligned} \quad (\text{II.9})$$

The value of the functional at ϕ_m is

$$\begin{aligned} F(\phi_m) &= -b(\phi_m, \phi_m) - \frac{1}{2} \langle \phi_m, \phi_m \rangle \\ &+ \frac{1}{2} \langle 4j_m^-, 4j_m^- \rangle. \end{aligned} \quad (\text{II.10})$$

Subtracting equation (II.10) from equation (II.9) one gets

$$\begin{aligned} F(\psi_m) - F(\phi_m) &= b(\psi_m - \phi_m, \psi_m - \phi_m) + \frac{1}{2} \langle \phi_m, \phi_m \rangle \\ &- \langle \phi_m, \psi_m \rangle + \frac{1}{2} \langle \psi_m, \psi_m \rangle \end{aligned}$$

or

$$F(\psi_m) = F(\phi_m) + b(\psi_m - \phi_m, \psi_m - \phi_m) + \frac{1}{2} \langle \phi_m - \psi_m, \phi_m - \psi_m \rangle$$

and for $\phi_m \neq \psi_m$, $\phi_m \in H_2^1$,

$$F(\psi_m) > F(\phi_m) \quad , \text{ for all } \psi_m \in H_2^1.$$

where ϕ_m is the solution of the diffusion equation (II.2) subject to the irradiation of $\bar{j}_n(r_s)$.

Therefore, $F(\psi_m)$ is minimized by ϕ_m , as was to be proven.

Galerkin Approximation

The Galerkin approximation for variational problem (II.1), can be derived assuming that $F(\psi_m)$ has a minimum at $\phi_m \in H_2^1$, which implies that $F(\phi_m + t\psi_m)$ has a minimum at $t=0$ for arbitrary $\psi_m \in H_2^1$, or

$$\left. \frac{\partial}{\partial t} F(\phi_m + t\psi_m) \right|_{t=0} = 0, \text{ for all } \psi_m \in H_2^1.$$

Then, $F(\phi_m + t\psi_m) = b(\phi_m + t\psi_m, \phi_m + t\psi_m) -$

$$2(s_m, \phi_m + t\psi_m) + \frac{1}{2} \langle 4j_m^- - \phi_m - t\psi_m, 4j_m^- - \phi_m - t\psi_m \rangle$$

or $F(\phi_m + t\psi_m) = F(\phi_m) + 2t [b(\phi_m, \psi_m) -$

$$(s_m, \psi_m) - \frac{1}{2} \langle 4j_m^- - \phi_m, \psi_m \rangle] + \frac{t^2}{2} \langle \psi_m, \psi_m \rangle.$$

But

$$\left. \frac{\partial}{\partial t} F(\phi_m + t\psi_m) \right|_{t=0} = 0, \text{ for all } \psi_m \in H_2^1,$$

results in

$$b(\phi_m, \psi_m) = (s_m, \psi_m) + \frac{1}{2} \langle 4j_m^- - \phi_m, \psi_m \rangle.$$

Then using the definition of a (ϕ_m, ψ_m) in Chapter 3, one obtains

$$a(\phi_m, \psi_m) = (s_m, \psi_m) + \frac{1}{2} \langle 4j_m^-, \psi_m \rangle, \text{ for all } \psi_m \in H_2^1,$$

which is the Galerkin approximation derived in Chapter 3.

Ritz-Galerkin Approximation

The Ritz-Galerkin approximation can be obtained by admitting the solution defined by equation (3.8) in Chapter 3, in order to minimize the functional $F(\psi_m)$.

Rewriting the functional (II.3) as

$$F(\psi_m) = b(\psi_m, \psi_m) - 2(s_m, \psi_m) + \frac{1}{2} \langle 4j_m^-, 4j_m^- \rangle - \langle 4j_m^-, \psi_m \rangle + \frac{1}{2} \langle \psi_m, \psi_m \rangle$$

and inserting the approximation (3.8) of Chapter 3,

$$F(\psi_m^h) = \sum_{i=1}^{Ne} \sum_{j=1}^{Ne} \phi_{mi} \phi_{mj} b(\psi_{mi}^h, \psi_{mj}^h) - 2 \sum_{j=1}^{Ne} \phi_{mj} (s_m, \psi_{mj}^h) + \frac{1}{2} \langle 4j_m^-, 4j_m^- \rangle - \sum_{j=1}^{Ne} \phi_{mj} \langle 4j_m^-, \psi_{mj}^h \rangle + \frac{1}{2} \sum_{i=1}^{Ne} \sum_{j=1}^{Ne} \phi_{mi} \phi_{mj} \langle \psi_{mi}^h, \psi_{mj}^h \rangle.$$

By imposing $\frac{\partial}{\partial \phi_{mk}} F(\phi_m^h) = 0$ for all $k=1, \dots, N_e$, the stationary point which coincides with the minimum of $F(\phi_m^h)$ is obtained,

$$\frac{\partial}{\partial \phi_{mk}} F(\phi_m^h) = 0 = 2 \sum_{i=1}^{N_e} \phi_{mi} b(\psi_{mi}^h, \psi_{mk}^h) - 2(s_{m, \psi_{mk}^h}) \quad (\text{II.11})$$

$$-\frac{1}{2} \langle 4j^-, \psi_{mk}^h \rangle + \sum_{i=1}^{N_e} \phi_{mi} \langle \psi_{mi}^h, \psi_{mk}^h \rangle .$$

Then from the definition of a (ψ_{mi}, ψ_m) from Chapter 3, equation (II.11) can be rewritten as

$$\sum_{i=1}^{N_e} \phi_{mi} a(\psi_{mi}^h, \psi_{mk}^h) = (s_{m, \psi_{mk}^h}) + 2 \langle j^-, \psi_{mk}^h \rangle \quad (\text{II.12})$$

which is the Ritz-Galerkin approximation.

APPENDIX III

INTERPRETATION OF THE BLOCK-JACOBI SPECTRAL NORM

The spectral norm of the block-Jacobi matrix shown in Fig. 4.5 can be given by the largest absolute row sum. (2) From the definition of the matrices $\underline{T}_k(i,j)$, $k=1,\dots,4$, given in Sec. 4.2 and observing the block-row (i,j) , the block-Jacobi row sum is given by the row sum of the response matrix $\underline{R}^{J^-}(i,j)$. Therefore the spectral norm can be given by the largest absolute row sum of all response matrices $\underline{R}^{J^-}(i,j)$, $i=1,\dots,i_{\max}$; $j=1,\dots,j_{\max}$.

A physical interpretation of the spectral norm can be obtained by assuming a simpler situation, where the partial currents on each face of the coarse mesh are assumed spatially constant. In this case no negative element is possible (Table 4.1 and 4.2) in the response matrix $\underline{R}^{J^-}(i,j)$ because a positive inward partial current on any face of the coarse mesh must yield positive outward partial currents from each face of the coarse mesh.

If an inward partial current of constant magnitude is considered,

$$\underline{J}^-(i,j) = \omega (1, 1, 1, 1),$$

the outward partial current is given, in the absence of internal sources, by

$$\underline{J}^+(i,j) = \begin{pmatrix} \text{1st row sum of } \underline{\underline{R}}^J(i,j) \\ \text{2nd row sum of } \underline{\underline{R}}^J(i,j) \\ \text{3rd row sum of } \underline{\underline{R}}^J(i,j) \\ \text{4th row sum of } \underline{\underline{R}}^J(i,j) \end{pmatrix}$$

Since the magnitude of the outward partial current must be less than the magnitude of the inward partial current, every element of $\underline{J}^+(i,j)$ must be less than unity, and it can be interpreted as the probability of an incident neutron to emerge from a boundary of the coarse mesh without being absorbed or outscattered.

Because every element of $\underline{\underline{R}}^J(i,j)$ is positive, each element of $\underline{J}^+(i,j)$ coincides with the absolute row sum of $\underline{\underline{R}}^{J-}(i,j)$. Therefore the spectral norm of the block-Jacobi matrix may be interpreted as the largest probability of an incident neutron to emerge from some side of any coarse mesh. Equivalently, the spectral norm is the largest transmission or reflection probability in the system.

Therefore the block-Jacobi matrix will have a larger spectral norm for coarse meshes with smaller dimensions or decreased absorption+removal cross section, since the transmission probability in each case will increase.

APPENDIX IV
DIFFUSION GROUP CONSTANTS

The one-group diffusion constants for the simplified 200cm x 200cm bare reactor used for fixed source calculations are given in Table IV.1.

Table IV.1 One-group diffusion constants for bare homogeneous reactor.
(Source = 1.0/s/cm³).

| D (cm) | Σ_a (/cm/b) | $\nu \Sigma_f$ (/cm/b) | B_z^2 (/cm ²) |
|--------|--------------------|------------------------|-----------------------------|
| .90 | .10 | .09 | 0.0 |

The two-group diffusion constants for 2D-IAEA benchmark problem⁽⁴⁷⁾ and Biblis benchmark problem⁽⁵⁶⁾ are given in Tables IV.3 and IV.2, respectively.

Table IV.2 - Two-group diffusion constants for
 Biblis benchmark problem. (56)
 ($B_z^2 = 0.0$, $\chi^1=1.0$, $\chi^2=0.0$)

| ZONE | GROUP | D^g | Σ_a^g | Σ_f^g | $\nu \Sigma_f^g$ | Σ_{L2} |
|------|-------|--------|--------------|--------------|------------------|---------------|
| 1 | 1 | 1.4360 | .0095042 | .0023768 | .0058708 | .017754 |
| | 2 | .3635 | .0750058 | .0388940 | .0960670 | |
| 2 | 1 | 1.4366 | .0096785 | .0025064 | .0061908 | .017621 |
| | 2 | .3636 | .0784360 | .0419350 | .1035800 | |
| 3 | 1 | 1.3200 | .0026562 | .0 | .0 | .023106 |
| | 2 | .2772 | .0715960 | .0 | .0 | |
| 4 | 1 | 1.4389 | .0103630 | .0030173 | .0074527 | .017101 |
| | 2 | .3638 | .0914080 | .0535870 | .1323600 | |
| 5 | 1 | 1.4381 | .0100030 | .0025064 | .0061908 | .017290 |
| | 2 | .3665 | .0848280 | .0419350 | .1035800 | |
| 6 | 1 | 1.4385 | .0101320 | .0026026 | .0064285 | .017192 |
| | 2 | .3665 | .0873140 | .0441740 | .1091100 | |
| 7 | 1 | 1.4389 | .0101650 | .0025064 | .0061908 | .017125 |
| | 2 | .3679 | .0880240 | .0419350 | .1035800 | |
| 8 | 1 | 1.4393 | .0102940 | .0026026 | .0064285 | .017027 |
| | 2 | .3680 | .0905100 | .0441740 | .1091100 | |

Table IV.3 Two-group diffusion constants for
 2D-IAEA benchmark problem.
 ($B_z^2 = .8 \times 10^{-4} \text{cm}^{-2}$).

| Zone | D^1 | D^2 | Σ_{21} | Σ_a^1 | Σ_a^2 | $\nu \Sigma_f^2$ | χ^1 | χ^2 | material |
|------|-------|-------|---------------|--------------|--------------|------------------|----------|----------|-----------|
| 1 | 1.5 | .4 | .02 | .01 | .08 | .135 | 1. | .0 | fuel 1 |
| 2 | 1.5 | .4 | .02 | .01 | .085 | .135 | 1. | .0 | fuel 2 |
| 3 | 1.5 | .4 | .02 | .01 | .13 | .135 | 1. | .0 | fuel2+rod |
| 4 | 2.0 | .3 | .04 | .0 | .01 | .0 | 0. | .0 | reflector |

REFERENCES

REFERENCES

1. W. R. Cadwell, "PDQ-7 Reference Manual", WAPD-TM-678, Bettis Atomic Power Laboratory, Pittsburgh, PA (1969).
2. R. Varga, Matrix Iterative Analysis, Prentice-Hall, N.J. (1962).
3. E. L. Wachspress, Iterative Solution of Elliptic Systems, Prentice-Hall, N.J. (1966).
4. S. Nakamura, Computational Methods in Engineering and Science, John Wiley, N.Y. (1977).
5. R. Froehlich, "Summary Discussion and State of the Art Review for Coarse-Mesh Computational Methods", Atomkernenergie, 30, 152 (1977).
6. A. F. Henry, "Refinements in Accuracy of Coarse-Mesh Finite-Difference Solution of the Group-Diffusion Equations", Proc. Conf. Num. Reactor Calculations, IAEA-SM-154/21, p.447, IAEA (1972).
7. A. Birkhofer, S. Langenbuch, W. Werner, "Coarse Mesh Method for Space-Time Kinetics", Trans. Am. Nucl. Soc., 18, 153 (1974).
8. C. P. Robinson, J. D. Eckard, Jr., "A Higher Order Difference Method for Diffusion Theory", Trans. Am. Nucl. Soc., 15, 297 (1972).
9. S. Kaplan, "Some New Methods of Flux Synthesis", Nucl. Sci. Eng., 13, 22 (1962).
10. E. L. Wachspress, M. Becker, "Variational Synthesis with Discontinuous Trial Functions", Proc. Conf. Appl. OF Comp. Methods, ANL-7050, p. 191, ANL (1965).
11. J. B. Yasinsky, S. Kaplan, "Synthesis of Three-Dimensional Flux Chapes Using Discontinuous Sets of Trial Functions", Nucl. Sci. Eng., 28, 426 (1967).

12. W. M. Stacey, Jr., "Variational Flux Synthesis Methods for Multigroup Neutron Diffusion Theory", *Nuc. Sci. Eng.*, 47, 449 (1972).
13. R. A. Shober, R. N. Sims, A. F. Henry, "Two Nodal Methods for Solving Time-Dependent Group Diffusion Equations", *Nuc. Sci. Eng.*, 64, 582 (1977).
14. K. Koebke, M. R. Wagner, "The Determination of the Pin Power Distribution in a Reactor Core on the Basis of Nodal Coarse Mesh Calculations", *Atomkernenergie*, 30, 136 (1977).
15. M. R. Wagner, "Nodal Synthesis Method and Imbedded Flux Calculations", *Trans. Am. Nucl. Soc.*, 18, 152 (1974).
16. M. R. Wagner, H. Finneman, R. R. Lee, D. A. Meneley, B. Micheelsen, I. Misfeldt, D. R. Vondy, W. Werner, "Multidimensional LWR Benchmark Problem", *Trans. Am. Nuc. Soc.*, 23, 211 (1976).
17. M. R. Wagner, H. Finneman, K. Koebke, H. J. Winter, "Validation of the Nodal Expansion Method and the Depletion Program MEDIUM-2 by Benchmark Calculation and Direct Comparison with Experiment", *Atomkernenergie*, 30, 129 (1977).
18. M. R. Wagner, "Current Trends in Multidimensional Static Reactor Calculations", Proc. Conf. Computational Methods in Nuclear Energy, CONF 750413-V.II, p. I-1, U.S. ERDA (1975).
19. H. Finneman, F. Bennewitz, M. R. Wagner, "Interface Current Techniques for Multidimensional Reactor Calculations", *Atomkernenergie*, 30, 123 (1977).
20. R. D. Lawrence, J. J. Dorning, "A Nodal Green's Function Method for Multidimensional Neutron Diffusion Calculations", *Nuc. Sci. Eng.*, 76, 219 (1980).
21. G. Strang, J. Fix, An Analysis of the Finite Element Method, Prentice-Hall, N.J. (1973).
22. O. C. Zienkiewicz, The Finite Element Method in Engineering Science, McGraw-Hill, London (1971). 5171266f(3)
23. A. Kavenoky, J. J. Lautard, "A Finite Element Depletion Diffusion Calculation Method with Space-Dependent Cross Sections", *Nuc. Sci. Eng.*, 64, 563 (1977).

24. T. Ohnishi, "Application of Finite Element Solution Technique to Neutron Diffusion and Transport Equations", Conf. on New Developments in Reactor Math. and Appl., Idaho Falls, CONF 710302-V.II, p. 723 (1971).
25. L. A. Semenza, E. E. Lewis, E. C. Rossow, "The Application of The Finite Element Method to the Multigroup Neutron Diffusion Equation", Nuc. Sci. Eng., 47, 302 (1972).
26. H. G. Kaper, G. K. Leaf, A. J. Lindeman, "A Timing Comparison Study for Some High Order Finite Element Approximation Procedures and A Low Order Finite Difference Approximation Procedure for the Numerical Solution of the Multigroup Neutron Diffusion Equation", Nuc. Sci. Eng., 49, 27 (1972).
27. C. M. Kang, K. F. Hansen, "Finite Element Methods for Reactor Analysis", Nuc. Sci. Eng., 51, 456 (1973).
28. W. F. Walters, G. D. Miller, "Quadratic Finite Elements for X-Y and R-Z Geometries", Proc. Conf. Computational Methods in Nuclear Energy, Charleston, South Carolina, CONF 750413-V.I, p. I-39, U.S. ERDA (1975).
29. F. A. R. Schmidt, H. Ambrosius, H. P. Franke, E. Sapper, M. R. Wagner, "Experiences with the Finite Element Method for Standard Reactor Calculations", Proc. Conf. Computational Methods in Nuclear Energy, Charleston, South Carolina, CONF 750413-V.I, p. I-53, U.S. ERDA (1975).
30. V. Jagannathan, "Axial Continuous Synthesis Model with Finite Element Trial Functions", Tans. Am. Nucl. Soc., 31, 253 (1979).
31. Y. Abushady, "A Synthesis Finite Element Method for Three-Dimensional Reactor Calculations", Trans. Am. Nucl. Soc., 32, 304 (1979).
32. G. G. Stokes, "On the Intensity of the Light Reflected From or Transmitted Through a Pile of Plates", Proc. Roy. Soc., London, 11, 545 (1862).
33. W. Pfeiffer, J. L. Shapiro, "Reflection and Transmission Functions in Reactor Physics", Nuc. Sci. Eng., 38, 253 (1969).

34. R. Bellman, R. Kalaba, "On the Principle of Invariant Imbedding and Propagation Through Inhomogeneous Media", Proc. Nat. Acad. Sci., 42, 629 (1956).
35. K. Aoki, A. Shimizu, "Application of the Response Matrix Method to Criticality Calculations of Two-Dimensional Reactors", J. Nuc. Sci. Tech., 2, 149 (1965).
36. A. Shimizu, "Response Matrix Method", J. At. Energy Soc. Japan, 5, 359 (1963).
37. A. Leonard, C. T. McDaniel, "Multigroup Two Dimensional Collision Probability Techniques for Non-Uniform Lattices", Trans. Am. Nucl. Soc., 14, No. 1, 222 (1971).
38. R. J. Pryor, W. E. Graves, "Response Matrix Method for Treating Reactor Calculations", Mathematical Models and Computational Techniques for Analysis of Nuclear Systems, CONF 730414-P.2, p. VII-179, U.S. AEC (1973).
39. H. S. Bailey, "Response Matrix Analysis for Fast Reactors", Mathematical Models and Computational Techniques for Analysis of Nuclear Systems, CONF 730414-P.2, p. VII-187, U.S. AEC (1973).
40. C. T. McDaniel, "A Two Dimensional Few Group Response Matrix Calculation Method for Flux and Reactivity", Proc. Conf. Computational Methods in Nuclear Energy, Charleston, South Carolina, CONF 750413-V.II, p.V-111, U.S. ERDA (1975).
41. M. M. Anderson, Sr., H. C. Honeck, "An Interface Current Technique for Two Dimensional Cell Calculations", Mathematical Models and Computational Techniques for Analysis of Nuclear Systems, CONF 730414-P.1, p. I-53, U.S. AEC (1973).
42. A. Leonard, "Collision Probability and Response Matrices: An Overview", Proc. Conf. Computational Methods in Nuclear Energy, CONF 750413-V.II, p. III-5. U.S. ERDA (1975).
43. Z. Weiss, S. O. Lindahl, "High-Order Response Matrix Equation in Two-Dimensional Geometry", Nuc. Sci. Eng., 58, 166 (1975).

44. Z. Weiss, "Some Basic Properties of the Response Matrix Equations", *Nuc. Sci. Eng.*, 63, 457 (1977).
45. T. J. Burns, J. J. Dorning, "Multidimensional Applications of an Integral Balance Technique for Neutron Diffusion Computation", Proc. Conf. Computational Methods in Nuclear Energy, Charleston, South Carolina, CONF 750413-V.II, p. V-57, U.S. ERDA (1975).
46. T. J. Burns, "The Partial Current Balance Method: A Local Green's Function Technique for the Numerical Solution of Multidimensional Neutron", Ph.D. Thesis, Univ. of Illinois, Urbana, Illinois (1975).
47. "Argonne Code Center: Benchmark Problem Book", ANL 7416-Supp. 2, Argonne National Laboratory (1977).
48. I. Ergatoudis, B. M. Irons, O. C. Zienkiewicz, "Curved, Isoparametric, 'Quadrilateral' Elements for Finite Element Analysis", *Int. J. Solids Structures*, 4, 31 (1968).
49. B. M. Irons, S. Ahmad, Techniques of Finite Elements, Chapter 26, John Wiley (1980).
50. J. J. Duderstadt, L. J. Hamilton, Nuclear Reactor Analysis, John Wiley (1976).
51. M. R. Wagner, "GAUGE- A Two-Dimensional Few Group Neutron Diffusion-Depletion Program for a Uniform Triangular Mesh", GA-8307, Gulf General Atomic, San Diego, CA (1968).
52. D. A. Flanders, G. Shortley, "Numerical Determination of Fundamental Modes", *J. Appl. Physics*, 21, 1326 (1950).
53. L. A. Hageman, C. J. Pfeifer, "The Utilization of the Neutron Diffusion Program PDQ-5", WAPD-TM-395, Bettis Atomic Power Laboratory, Pittsburgh, PA (1965).
54. R. Froehlich, "A Theoretical Foundation for Coarse Mesh Variational Techniques", GA-7870, General Dynamics, San Diego, CA (1967).
55. Z. Weiss, "Nodal Equations Derived from Invariant Imbedding Theory", *Nuc. Sci. Eng.* 48, 235 (1972).

56. M. R. Wagner, Kraftwerk Union AG, Erlangen, Fed. Rep. Germany, Personal communication, June (1981).
57. Proc. of a Panel on Reactor Burn-up Physics, IAEA, Vienna, July 12-16, 1971, STI/PUB/336.
58. D. R. Vondy, T. B. Fowler, G. W. Cunningham, "VENTURE: A Code Block for Solving Multigroup Neutronics Problems Applying the Finite-Difference Diffusion Theory Approximation to Neutron Transport", ORNL-5062, Oak Ridge National Laboratory, (1975).
59. W. A. Rhodes, D. B. Simpson, R. L. Childs, W. W. Engle, Jr., "The DOT-IV Two-Dimensional Discrete Ordinates Transport Code with Space-Dependent Mesh and Quadrature", ORNL/TM-6529, Oak Ridge National Laboratory (1978).
60. C. Maeder, K. Foskolos, H. C. Honeck, J. M. Paratte, G. Varadi, "Calculations with the EIR Light Water Reactor Code System", Proc. of a Specialists' Meeting on Calculation of 3-Dimensional Rating Distributions in Operating Reactors, Paris, NEA (1979).